UNIVERSITY OF CALIFORNIA

Los Angeles

Population dynamics of sensory adaptation in cortical circuits

A dissertation submitted in partial satisfaction of the requirements for the degree Doctor of Philosophy in Neuroscience

by

Zoe Anne Dobler

2024

ABSTRACT OF THE DISSERTATION

Population dynamics of sensory adaptation

in cortical circuits

by

Zoe Anne Dobler

Doctor of Philosophy in Neuroscience

University of California, Los Angeles, 2024

Professor Carlos Portera-Cailliau, Chair

Our sensory systems are remarkably flexible, able to adjust and recalibrate as we move through environments composed of drastically different stimuli. This flexibility is achieved in part through sensory adaptation (SA), a process whereby brain circuits adjust neuronal activity based on the spatiotemporal context in which stimuli are encountered. Several functions have been proposed for SA, including the improvement of discrimination between stimuli, maximizing information transmission in the current sensory environment, and the reduction of metabolic costs. While SA has been extensively studied at the level of individual neurons on timescales of tens of milliseconds to a few seconds, little is known about SA over longer timescales or at the population level. Here, we investigate population-level SA in the barrel field of the mouse somatosensory cortex (S1BF), which processes whisker inputs, using in vivo 2-photon calcium imaging and Neuropixels

recordings of excitatory neurons in awake mice. Amongst stimulus responsive (SR) neurons we found both adapting and facilitating neurons that decreased or increased their firing with repetitive whisker stimulation, respectively. We also discovered that population SA to one stimulus frequency does not necessarily generalize to a different frequency. Moreover, responses of individual neurons to repeated rounds of stimulation were strikingly heterogeneous and stochastic, such that their adapting or facilitating response profile to the same stimulus was not stable across tens of minutes. Such representational drift was particularly striking when recording longitudinally across several days, as SA response profiles of most SR neurons changed drastically from one day to the next. Remarkably, repeated exposure to a familiar stimulus paradoxically shifted the population away from strong adaptation and toward facilitation. Finally, we investigated SST interneurons as a candidate network mechanism underlying population SA, and our preliminary results suggest they may modulate the balance between adaptation and facilitation in S1BF. Together, our studies indicate that the SA profile of S1BF neurons is not a fixed property of neurons, but rather highly a dynamic feature that is shaped by sensory experience across days. These findings provide valuable insight into the complex dynamics of population SA in S1BF and will serve as an important reference for future mechanistic studies of population SA as well as interrogations of its potential alteration in neurological and psychiatric conditions.

The dissertation of Zoe Anne Dobler is approved.

Dean Buonomano

Maria Neimark Geffen

Dario L Ringach

Ladan Shams

Carlos Portera-Cailliau, Committee Chair

University of California, Los Angeles

2024

Table of Contents

Abstract	*ii-iii*
Committee Page	*iv*
List of Figures	*vi-vii*
Acknowledgments	*viii-xiii*
Vita	*xiv-xv*
Introduction	*1-13*
Chapter 1: Response dynamics of L2/3 excitatory neurons in awake head-fixed mice vary across whisker stimulus parameters	*14-29*
Chapter 2: Flexibility in SA dynamics in L2/3 after a switch in stimulus frequency	*30-61*
Chapter 3: Instability and drift in SA profiles of S1BF populations across multiple timescales	*62-82*
Chapter 4: SST interneurons may modulate sensory adaptation at the population level in S1BF	*83-94*
Discussion	*95-108*
Appendix: Statistical Methods	*109*
References	*110-130*

List of Figures

Figure 1: Setup for 2-photon calcium imaging in awake, head-fixed mice.

Figure 2: Response dynamics of L2/3 excitatory neurons across different whisker stimulation parameters.

Figure 3: Automated vs. manual methods of classifying S1BF neurons as stimulus responsive.

Figure 4: Impact of stimulus duration and i.s.i. on neuronal responsiveness.

Figure 5: The mean response of SR neurons to 5 Hz whisker stimulation is mildly adapting.

Figure 6: Diverse and stochastic responses of L2/3 excitatory neurons to bouts of repetitive 5 Hz whisker stimulation.

Figure 7: Calculation of adaptation index.

Figure 8: Adapting neurons outnumber facilitating neurons in L2/3 of S1BF.

Figure 9: Two different methods for quantifying the adaptation index (AI) of SR neurons.

Figure 10: Spatial distribution of and correlations between adapting and facilitating neurons.

Figure 11: Comparison of SA response dynamics between 5 Hz and 12.5 Hz whisker stimulation protocols.

Figure 12: Neuropixels recordings of regular-spiking neurons in S1BF confirm preponderance of adapting over facilitating neurons after repetitive whisker stimulation.

Figure 13: Adapting neurons transiently facilitate after an upward switch in stimulus frequency.

Figure 14: Responses of L2/3 neurons to a downward frequency switch, and control analyses to determine which neurons dynamically change their SA profile to an upward frequency switch.

Figure 15: Instability of response profiles of neurons after control stimulation protocols.

Figure 16: The SA profile of individual L2/3 neurons is highly dynamic across different rounds of 20 whisker stimulations over tens of minutes.

Figure 17: Stochasticity of L2/3 neurons during a single imaging session.

Figure 18: Experience-dependent decrease in L2/3 population adaptation across days.

Figure 19: Major and mild changes in response profiles of L2/3 neurons across days.

Figure 20: SA response dynamics to repetitive whisker stimulation across days in L4 resemble those in L2/3.

Figure 21: Response dynamics of L4 during 5 Hz whisker stimulation.

Figure 22: FOVs above the C2 barrel of S1BF exhibiting viral GCaMP6s and ChRmine expression.

Figure 23: Stimulation protocols used and example responses to optogenetic stimulation.

Figure 24: Percentage of neurons responding to different stimulation protocols at different cortical depths.

Figure 25: Percentage of SR neurons after exclusion of neurons driven by optogenetic stimulation.

Figure 26: Activation of SST neurons impacts the relative abundance of adapting and facilitating neurons in superficial S1BF.

Acknowledgments

I would first like to thank my advisor, Dr. Carlos Portera-Cailliau, for his active support, mentorship, and reliability over the course of my doctoral training. My rotation in the Portera-Cailliau Lab began in March 2020, mere days into the COVID-19 pandemic. Despite the obstacles posed by such an uncertain time, Carlos was always there, ready to hop on a Zoom call and discuss any questions, problems, or ideas I had as I started to think about the work I wanted to do for my PhD. Even over Zoom, his dedication to his trainees was clear. Throughout my years in the lab, he has remained steadfast in his commitment to my scientific development and success. From the early days of my project to the final stages of the PhD, he regularly expressed excitement about my work, and this enthusiasm has fueled my progress throughout my training. Even in the busiest of moments, he has always made time for his trainees, and has always been happy to provide thoughtful and valuable feedback on my manuscript drafts, grant proposals, application statements, and the like throughout the years. I have benefitted immeasurably from his constant encouragement and have grown extensively as a scientist as a result of his mentorship.

I would like to thank members of the Portera-Cailliau Lab, past and present, for their camaraderie and scientific expertise. Thank you to Dr. Nazim Kourdougli for his thoughtful answers to the countless questions I have asked him over these years, whether they were about experiments, the scientific literature, or French vocabulary. Thank you to Dr. Anand Suresh for his help with experiments, insights regarding data analysis and experimental design, and for his collaboration on lab equipment projects, whether it be assembling a new 2-photon microscope or updating the intrinsic signal imaging rig. I would also like to extend a big thank you to Sunny Mula, a former undergraduate in the lab, who worked with me from 2021-2023; with her perseverance and

curiosity, I'm confident she will find success in any path she takes in life. I thank Trishala Chari for the Neuropixels recordings and analysis that she contributed to my project, and for our conversations about navigating grad school over the years. I thank Michelle Wu, Dr. Carlos Sanchez-León, and Dr. Irma Tello-García for their helpfulness in the lab, and for our innumerable office conversations and shared laughs.

I would also like to thank Dr. William Zeiger and members of the Zeiger Lab, with whom we share weekly joint lab meetings. Will, thank you for your constructive feedback on my data and your willingness to always lend a hand when I was troubleshooting experiments or analysis approaches. Thank you also to Zeiger Lab members Dr. Baruc Campos, Brenda Vasquez, Dr. Aye Theint Theint, and Sravya Gadepalli.

Thank you to the CHS 7th floor neuroscience community for fostering a collaborative and good-natured atmosphere. Thank you to Dr. João Couto for his assistance with code for our intrinsic signal imaging rig.

Components of the Introduction, Discussion, and introductory paragraphs of Chapter 4, as well as substantial components of Chapter 2 and Chapter 3, and Appendix are included in a manuscript that was submitted to *Current Biology* in 2023, titled "Adapting and facilitating responses of neuron populations in mouse somatosensory cortex are dynamic and shaped by experience across days". The manuscript is currently under revision, and the results from Chapter 4 will also be included in the revised manuscript. I am the first author on this manuscript, and my coauthors are Trishala Chari, Supriya Mula, Dr. Dean Buonomano, and Dr. Carlos Portera-Cailliau, who is the

corresponding author. Dr. Anand Suresh will be added as an author to the revised version of this manuscript, making the author list as follows: Zoe Dobler, Trishala Chari, Dr. Anand Suresh, Supriya Mula, Dr. Dean Buonomano, and Dr. Carlos Portera-Cailliau. Carlos and I conceived the project and designed the experiments. Trishala performed experiments and analyzed data for the Neuropixels figures, which appear in Chapter 2 (**Figs. 12 & 13g-h**). Anand wrote MATLAB code for the whisker and optogenetic stimulation protocols used in this study, implanted cranial windows in the Scnn1a-Cre;Ai162 mice used for layer 4 experiments in Chapter 3, and wrote MATLAB code for an early part of the analysis pipeline for the layer 4 data from Chapter 3. Supriya Mula wrote MATLAB code for the correlation analysis performed in Chapter 2 (**Fig. 10b-c**). Dean wrote MATLAB code for the linear regression approach to quantifying adaptation. I performed the experiments and analyzed the data in all other cases. Carlos, Dean and I interpreted the data. Carlos and I wrote the manuscript (with the exception of the Methods for the Neuropixels recordings, which were written by Trishala Chari), with input from the other authors.

This work was supported by a Jessamine Hilliard Neurobiology Graduate Student Grant, which I was awarded in 2023, and a BRI/Semel Institute Graduate Travel Award that I received the same year. This work was also supported by the following grants and fellowships: R01NS117597 (NIHNINDS), R01HD108370 and R01HD054453 (NIH-NICHD), and Department of Defense (DOD, 13196175) awarded to Dr. Carlos Portera-Cailliau, Training in Neurotechnology Translation T32NS115753 (NIH) and F31HD108043 (NIH/NICHD) awarded to Trishala Chari, a graduate student fellowship from the Achievement Rewards for College Scientists Foundation awarded to Trishala Chari, a Bennett and Jeanelle Duval Undergraduate Scholarship awarded to Supriya Mula, and a Whitcome Fellowship awarded to Supriya Mula.

I would like to thank my committee for their suggestions, questions, and feedback as I embarked on this project. I thank Dr. Dean Buonomano for his suggestions regarding approaches to quantifying adaptation, as well as valuable discussions and feedback at all stages of my research and while preparing the manuscript. I thank Dr. Maria Neimark Geffen for her willingness to join this committee from an outside institution, for her positivity, and for her helpful feedback. I thank Dr. Dario Ringach for his insightful ideas about how best to analyze the data for my project, and for his willingness to break down those ideas further when I had questions. I thank Dr. Ladan Shams for her questions and valuable perspective as someone with expertise in human psychophysics and sensory perception.

I thank Dr. Felix Schweizer, Jenny Lee, Aftin Whitten, and all NSIDP administrative staff. As a PhD student passionate about science communication, I have always been heartened by Felix's enthusiastic support of new science communication initiatives within the BRI and NSIDP, as well as his openness in general to input from students. Jenny— it's safe to say we NSIDP students would be lost without your incredible wealth of knowledge and ability to answer every single one of our questions. I would also like to thank the faculty both within and outside of the NSIDP who have taught the courses that I have taken throughout my PhD training.

I thank current and former members of the Neurology staff, including Margot Chang, George W. Luker III, Krystal Paulino, Genea Taylor, Roberto Martinez, and Anna Mokraiy, for their assistance with orders, reimbursements, and answering any other questions I have had during my time here.

I would also like to thank Tensie Palmer, as well as all DLAM technicians and staff who have helped me and the lab over the years.

During graduate school, I have had the pleasure of being involved with science communication initiatives at Knowing Neurons, an award-winning neuroscience education website, and the Science Policy Group at UCLA. I would like to thank all the wonderful, passionate young scientists I have gotten the chance to know and work with at both of these organizations.

I thank previous mentors and friends at IST Austria, NYU, and WVU, who have been instrumental in my training and scientific development. I would also like to thank the organizers, instructors, and teaching assistants at the Allen Institute's Summer Workshop on the Dynamic Brain, which I had the pleasure of attending in 2022. The supportive environment they fostered during the workshop made it possible for me to learn valuable skills for analyzing my data.

Thank you to my friends for all the dinners, brunches, FaceTime chats, hikes, and movie nights over these years. Marisa, Lauren, Tanisha, Candice, Allison, Matt, Payton, Blair— our conversations, jokes over text, and time spent together always leave me feeling recharged, and your friendship is invaluable to me. Thank you to the friends I made at the Summer Workshop on the Dynamic Brain—Tanisha, Christine, Kayla, and James—meeting you all was a special bonus I did not expect from that experience, and I'm extremely grateful for it. I would also like to thank my NSIDP cohort, as well as students from other years, for all of the fun adventures, hangouts, and laughs as we've navigated graduate school together.

I thank my family for their love and support. Thank you for being there for me and always checking in on me, even from thousands of miles away. Thank you to my parents for your unconditional love and for encouraging my curiosity even from an early age. Thank you to my siblings for our conversations and adventures together—I'm so grateful to be able to navigate life alongside you. Thank you to our family dogs, who, even in their old age, always lift my spirits whenever I come to visit.

Speaking of dogs— I would also like to thank Jones, who came into my life during graduate school and has been an unexpected blessing. I am grateful for his comforting presence, companionship, and endearing personality.

Finally, I thank my partner, for her unwavering love, support, and encouragement. Lex— your companionship, patience, humor, and understanding have sustained me throughout this process, and you believed in me even in the moments where I struggled to believe in myself. In many ways, this has been as much a journey for you as it has been for me, and you have navigated it while radiating kindness and support every step of the way. The way you show up for me each day means more than I can say, and I could not have done this without you.

Vita

EDUCATION

UCLA Neuroscience Interdepartmental Ph.D. Program 2019 –

West Virginia University 2014 – 2018
Bachelor of Arts, Magna Cum Laude, with University Honors
Major: Biology, Area of Emphasis in Genomics

RESEARCH EXPERIENCE

PhD Student, UCLA Interdepartmental PhD Program in Neuroscience 2019 – Current
- PhD thesis research on the population dynamics of sensory adaptation in mouse barrel cortex

Fulbright Grantee, Institute of Science and Technology Austria 2018 – 2019
- Full-time neuroscience research in Austria for 1 year, characterizing synaptic changes within specific brain regions in a mouse model of intellectual disability and ASD

Student Intern, New York University Langone Medical Center 2018
- Postbaccalaureate summer internship laying groundwork for a new project focused on a zebrafish model of progressive supranuclear palsy

Undergraduate Researcher, West Virginia University Department of Biology 2017 – 2018
- Undergraduate thesis research investigating genetic mechanisms of neural development in zebrafish

PUBLICATIONS

- **Dobler Z.,** Chari T., Mula S., Buonomano D.V., Portera-Cailliau C. Adapting and facilitating responses of neuron populations in mouse somatosensory cortex are dynamic and shaped by experience across days. (*Manuscript under revision*)
- Kourdougli, N., Nomura, T., Wu, M.W., Heuvelmans, A., **Dobler, Z.,** Contractor, A., Portera-Cailliau, C. The NKCC1 inhibitor bumetanide restores cortical feedforward inhibition and lessens sensory hypersensitivity in early postnatal fragile X mice. (*Manuscript under review*)
- Coltogirone, R.A., Sherfinski, E.I., **Dobler, Z.A.,** Peterson, S.N., Andlinger, A.R., Fadel, L.C., Patrick, R.L., Bergeron, S.A. (2022). Gsx2 but not Gsx1 is necessary for early forebrain patterning and long-term survival in zebrafish. *Dev Dyn*. doi: 10.1002/dvdy.542
- Hamling K.R., Harmon K., Greaney M., **Dobler Z.,** Kimura Y., Higashijima S., Schoppik D. (2021). Synaptic encoding of vestibular sensation regulates movement and coordination. Pre-print on bioRxiv. doi: 10.1101/2021.07.05.451142
- Morandell J., Schwarz L.A., Basilico B., Tasciyan S., Dimchev G., Nicolas A., Sommer C., Kreuzinger C., Dotter C.P., Knaus L.S., **Dobler Z.,** Cacci E., Schur F.K.M., Danzl J.G., Novarino G. (2021). *Cul3* regulates cytoskeleton protein homeostasis and cell migration

during a critical window of brain development. *Nat Commun.* doi: 10.1038/s41467-021-23123-x

SELECTED PRESENTATIONS

Neuroscience 2023 – Washington, DC (Poster) Nov 2023

Dobler Z., Chari T., Mula S., Portera-Cailliau C. Adapting and facilitating responses of excitatory neuron populations in mouse somatosensory cortex are dynamic and shaped by experience across days.

Structure, Function, and Development of Neural Circuits – Irvine, CA (Poster) Aug 2023

Dobler Z., Mula S., Portera-Cailliau C. Adapting and facilitating responses of excitatory neuron populations in mouse somatosensory cortex are dynamic and shaped by experience across days.

Neuroscience 2022 and Barrels 2022 Meetings – San Diego, CA (Poster) Nov 2022

Dobler Z., Mula S., Portera-Cailliau C. The remarkably dynamic identity of adapting and facilitating neurons in mouse somatosensory cortex.

CSHL Neuronal Circuits 2022 Meeting – Cold Spring Harbor, NY (Poster). Mar 2022

Dobler Z., Portera-Cailliau C. Sensory adaptation over behaviorally relevant timescales in mouse barrel cortex.

Neuroscience 2021 – Chicago, IL (Virtual Poster) Nov 2021

Dobler Z., Portera-Cailliau C. Mechanisms of sensory adaptation over behaviorally relevant time scales in mouse barrel cortex.

SELECTED HONORS & AWARDS

UCLA Brain Research Institute/Semel Institute Graduate Travel Award 2023
Jessamine Hilliard Neurobiology Graduate Student Grant 2023
Science Communication Training Award, UCLA BRI NeuroComm Affinity Group 2021
Honorable Mention, National Science Foundation Graduate Research Fellowship Program 2021
Eberly College Outstanding Senior for Biology, West Virginia University 2018
Fulbright Austrian-Marshall Plan Foundation Award in Science and Technology 2018

TEACHING EXPERIENCE

Teaching Assistant, Graduate Systems Neuroscience Course (NEURO 205) 2023

- Supported systems neuroscience course, a required core course for UCLA NSIDP students

Student Tutor, MindFit, West Virginia University 2018
Student-Athlete Tutor, West Virginia University 2017-2018
Teaching Assistant for Introductory Biology Courses, West Virginia University 2015-2016

INTRODUCTION

Adaptation and its function in sensory circuits

To construct a stable and coherent representation of the external world, sensory circuits must adapt their activity based on the statistics of the surrounding environment. Sensory adaptation (SA) is a ubiquitous phenomenon across species and sensory modalities, in which the responsiveness of neurons to sensory stimuli is repeatedly adjusted based on the spatiotemporal context in which such stimuli are encountered (Adibi & Lampl, 2021; Whitmire & Stanley, 2016). Through SA, the brain can maintain remarkable flexibility in what aspects of the environment it most robustly encodes at a given moment, depending on the salience of those environmental stimuli and their relevance to behavior.

In 1961, Horace Barlow hypothesized that "sensory relays recode sensory messages so that their redundancy is reduced but comparatively little information is lost" (Barlow, 1961). Many studies since his proposition support the notion that SA promotes the efficient encoding of stimuli in dynamic sensory environments (Adibi et al., 2013; Maravall et al., 2007) by constantly recalibrating neuronal output to maximize the information encoded about external stimuli (Brenner et al., 2000). In sensory cortex, neurons encode stimuli in the environment through their response dynamics; given a certain distribution of sensory stimuli, neurons can encode a range of sensory inputs using the range of their firing rates—this is often referred to as the input-output relation (Brenner et al., 2000; Laughlin, 1981). However, this range of firing rates is finite, and without adaptation, neurons would only be able to encode a certain number of inputs (Whitmire & Stanley, 2016). Through adaptation, neurons constantly adjust this input-output relation for the output to best represent the statistics of incoming stimuli, allowing for flexible, context-dependent rescaling

of neuronal responsiveness (Adibi et al., 2013; Adibi & Lampl, 2021; Brenner et al., 2000; Weber et al., 2019; Whitmire & Stanley, 2016).

Several functions for SA have been proposed. In addition to improving coding efficiency (and, in turn, reducing redundancy) (Barlow, 1961; Laughlin, 1981), SA has been implicated in noise reduction, reducing neuronal responsiveness to—and perception of—repetitive stimulation (Adibi et al., 2013; Adibi & Lampl, 2021; Berglund & Berglund, 1970). By reducing net neuronal activity in response to repetitive stimuli, SA is also thought to conserve metabolic resources (Adibi et al., 2013; Benucci et al., 2013), which can instead be used to amplify signals from other, more behaviorally relevant stimuli (Weber et al., 2019). Studies in humans and animal models have demonstrated that SA also enhances the ability to discriminate between stimuli that resemble the adapting stimulus (Goble & Hollins, 1993, 1994; Tannan et al., 2006), though at the expense of stimulus detection (Ollerenshaw et al., 2014).

SA that is specific to frequently encountered stimuli—often referred to as stimulus-specific adaptation— may aid in deviance detection, by adjusting the input-output curve such that neurons respond most robustly to rarely encountered stimuli that do not resemble the adapting stimulus (Musall et al., 2014; Natan et al., 2015; Ulanovsky et al., 2003). Several of these proposed functions involve a net reduction in response to predictable stimuli and thus also align with the idea of SA as a form of predictive coding (Keller & Mrsic-Flogel, 2018; Weber et al., 2019). The predictive coding framework asserts that the brain continually compares incoming sensory input to higher-order predictions about that input, which originate from an internal model of the external world (Rao & Ballard, 1999). Discrepancies between these bottom-up and top-down signals

produce prediction errors, which can then be used to update the internal model (Keller & Mrsic-Flogel, 2018). This framework, which focuses specifically on encoding deviations from internal predictions to reduce coding redundancy, is highly compatible with the functions of SA described above, and could conceivably be instantiated in sensory cortex through top-down projections to primary sensory areas, which modulate responses dynamics based on stimulus predictability (Bastos et al., 2023; Hamm et al., 2021; Han & Helmchen, 2024).

Alterations in SA have been proposed to underlie sensory hypersensitivity symptoms observed in neurodevelopmental conditions, including autism (He et al., 2017; Puts et al., 2014; Tommerdahl et al., 2007). Indeed, children and adolescents with autism spectrum disorders exhibit greater activation and less adaptation in primary sensory cortices in response to mildly aversive auditory and tactile stimuli (Green et al., 2015). In humans with Fragile X Syndrome (FXS), SA to auditory and tactile stimuli is significantly reduced (Ethridge et al., 2016; Miller et al., 1999), and this is observed for tactile stimuli in the *Fmr1* knockout mouse model of FXS as well (He et al., 2017; Kourdougli et al., 2023). Tactile defensiveness is a prominent feature of autism spectrum disorders (Baranek et al., 1997; Marco et al., 2011; Wiggins et al., 2009). Accordingly, interrogating the mechanisms modulating SA to tactile stimuli is particularly clinically relevant, as it will provide insight into the specific circuits that may be altered in neurodevelopmental conditions, which could serve as targets for future therapeutic approaches.

Rodent barrel cortex as a model system for understanding SA to tactile stimuli

In rodents, the barrel field of the primary somatosensory cortex (S1BF) is the primary sensory area for processing tactile stimuli sensed through the whiskers (Petersen, 2007), which possess discriminatory capabilities comparable to those of primate fingertips (Carvell & Simons, 1990). In 1970, Woosley and Van der Loos discovered that each whisker is represented by a barrel-like structure in layer (L) 4 of rodent somatosensory cortex, and that these "barrels" are somatotopically organized in a manner strikingly similar to the arrangement of the whiskers themselves (Woolsey & Van Der Loos, 1970). Since this discovery over half a century ago, S1BF has been characterized in detail, and its distinct somatotopic organization and well defined circuitry make it an ideal model system for interrogating the neural underpinnings of tactile processing (Feldmeyer, 2012; Feldmeyer et al., 2013; Petersen, 2007).

In the rodent somatosensory system, two main parallel pathways convey information from whisker to cortex: the lemniscal pathway and the paralemniscal pathway (Staiger & Petersen, 2021). As we move from periphery to cortex in the lemniscal pathway, trigeminal ganglion neurons innervate the principal trigeminal nucleus (PrV) of the brainstem, which provides input to the ventral posteromedial nucleus (VPM) of the thalamus, which in turn targets L4 of S1BF (Deschênes et al., 2005; Diamond et al., 2008). Spiny stellate neurons in L4 proceed to innervate pyramidal neurons in L2/3 (Staiger & Petersen, 2021). In contrast, the paralemniscal pathway proceeds from the trigeminal ganglion to the nucleus interpolaris (SpVi) of the brainstem, followed by the thalamic posterior medial nucleus (POm) of the thalamus, and then L1 and L5a of S1BF (Adibi, 2019; Petersen, 2007). While the lemniscal pathway conveys touch and whisker position information to its targets (Staiger & Petersen, 2021), the paralemniscal pathway carries whisking information pertaining to sensorimotor coordination, and may thus play an important role during active

exploration (Adibi, 2019; Petersen, 2007). In contrast with the paralemniscal pathway, the lemniscal pathway exhibits the well-known somatotopic organization at all relays from the brainstem to S1BF (Staiger & Petersen, 2021). The lemniscal pathway also comprises several components of the "canonical" circuitry proposed to exist throughout the neocortex (Douglas & Martin, 1991; Feldmeyer et al., 2013), such as the progression from the thalamus to L4 followed by L2/3. These highly conserved circuit motifs, coupled with well-defined somatotopy, make the lemniscal pathway uniquely well positioned for investigations of sensory processing across multiple levels of the somatosensory hierarchy.

L2/3 of S1BF is subject to bottom-up modulation through excitatory projections from L4 while simultaneously receiving long-range inputs from other cortical regions, including other sensory cortices and higher-order brain regions. For example, S1 exhibits reciprocal connectivity with secondary somatosensory cortex (Aronoff et al., 2010), a higher-order region in rodent somatosensory system. Furthermore, several major subclasses of GABAergic interneurons exist within the superficial layers of S1BF and modulate the firing of L2/3 pyramidal neurons through distinct circuit motifs, such as vasoactive intestinal peptide (VIP) interneuron-mediated disinhibition (S. Lee et al., 2013). These local interneuron subclasses receive distinct long-range inputs from other cortical areas—secondary somatosensory inputs to superficial S1BF preferentially target parvalbumin-positive interneurons, while whisker-related primary motor cortex inputs target vasoactive intestinal peptide-positive interneurons. Thus, within L2/3 of S1BF, we are able to study the impact of disparate influences (bottom-up modulation, top-down modulation, modulation of the network by local interneurons) on the local population. Furthermore, S1BF as a whole is an ideal model system for sensory processing studies, as it

possesses the canonical microcircuitry present across neocortex, includes all three major GABAergic interneuron subtypes, and exhibits elegant somatotopy allowing for precise interrogations and manipulations of sensory circuitry.

Limitations of prior studies on SA in the rodent somatosensory system and other regions

Prior studies in different sensory areas and animal species have provided detailed characterizations of SA, but with certain limitations. SA has largely been studied in individual neurons or small groups of neurons (i.e., not across a large population) using electrophysiological techniques (Kheradpezhouh et al., 2017). This effort has provided vital insight into intrinsic forms of SA at the single-cell level, such as spike frequency adaptation (Azouz & Gray, 2000; Benda & Herz, 2003; Bhattacharjee & Kaczmarek, 2005; Pozzorini et al., 2013; Sanchez-Vives et al., 2000; Wilent & Contreras, 2005), a ubiquitous phenomenon in which a single neuron's firing reduces with continuous synaptic input. In the rodent whisker system, electrophysiological studies in small groups of neurons have identified the depression of thalamocortical synapses as an important bottom-up component of adaptation in S1BF (Castro-Alamancos, 2004; Chung et al., 2002; Khatri et al., 2004).

In the tactile modality specifically, the degree of SA to repetitive whisker stimuli generally increases as one ascends the relays of the lemniscal pathway (Ganmor et al., 2010; Yang et al., 2016). However, SA within a given relay of this pathway also depends on stimulus parameters; for example, increasing stimulus intensity (i.e., amplitude and velocity) tends to decrease adaptation

in neurons in PrV, VPM, and S1BF (Ganmor et al., 2010; Mohar et al., 2013), while increasing stimulation frequency elicits stronger adaptation in thalamus and cortex (Ahissar et al., 2000; Khatri et al., 2004; Kheradpezhouh et al., 2017). These findings suggest that the specific dynamics of SA to tactile stimuli depend on the parameters of the stimulus as well as the location within the somatosensory hierarchy.

Many of the studies characterizing SA in S1BF have been carried out under anesthesia (Chung et al., 2002; Khatri et al., 2004; Kheradpezhouh et al., 2017). Across sensory modalities, anesthesia decreases spontaneous activity (Syka et al., 2005)—which is coupled with an increase in population synchrony (Erchova et al., 2002; H. Lee et al., 2021)— and alters inhibitory and cortical dynamics (Adesnik et al., 2012; Constantinople & Bruno, 2011; Haider et al., 2013; K. D. Harris & Thiele, 2011). Several of the basic effects of SA seen in the anesthetized rodent somatosensory system have also been observed in an awake context, such as reduced firing and spike timing precision (Ollerenshaw et al., 2014; Whitmire et al., 2016). However, whether additional SA effects emerge in an awake context that are not present under anesthesia remains an unresolved question. One study suggests the degree of SA in S1BF of the awake animal may be reduced relative to anesthesia conditions due to thalamocortical synapses already being in a depressed state (Castro-Alamancos, 2004). Furthermore, while excitatory and inhibitory neurons in S1BF show comparable levels of rapid SA under anesthesia, recordings in awake mice reveal that excitatory neurons exhibit a significantly greater degree of SA compared to putative inhibitory interneurons, suggesting distinct circuit dynamics across these two states (Wright et al., 2021).

In the awake animal, behavioral state is likely to play a role in SA. For example, in L4 of S1BF, passive whisker deflection recruits different degrees of neuronal responsiveness depending on whether the animal is in a state of quiet wakefulness or actively whisking (Crochet & Petersen, 2006). Neuromodulators that regulate arousal, such as acetylcholine and norepinephrine, are also known to impact cortical and thalamic state in the rodent whisker system (Castro-Alamancos & Gulati, 2014). Given the known impact of anesthesia on various aspects of neuronal activity, a detailed characterization of SA in the awake animal would improve our understanding of what SA looks like in naturalistic settings. While several studies have begun to investigate adaptation to tactile stimuli in the awake animal (Alisha et al., 2023; Castro-Alamancos, 2004; Colins Rodriguez et al., 2022; Crochet & Petersen, 2006; Musall et al., 2014), an extensive, population-level characterization is still needed.

Finally, studies characterizing SA in the rodent whisker system have also largely focused on rapid timescales of less than 5 s (Castro-Alamancos, 2004; Chung et al., 2002; Khatri et al., 2004; Kheradpezhouh et al., 2017; Musall et al., 2014). Kheradpezhouh and colleagues provide a detailed characterization of SA over frequencies spanning 2-32 Hz, however their timescale of investigation did not extend past 3 s (Kheradpezhouh et al., 2017). One study examining SA across auditory, tactile, and visual cortices demonstrated the existence of SA in S1BF on timescales spanning hundreds of milliseconds to 4 seconds (Latimer et al., 2019). Thus, while it has been demonstrated that timescales of SA can range from milliseconds to several seconds, SA dynamics have not been well characterized past this timescale. Several publications in other model systems have demonstrated the existence of SA across longer timescales, ranging from tens of seconds (La Camera et al., 2006; Lundstrom et al., 2008; Ulanovsky et al., 2003) to several minutes (Fairhall

et al., 2001). In the visual system, retinal ganglion cells are known to exhibit SA over tens of seconds (Chander & Chichilnisky, 2001; Kim & Rieke, 2001; Smirnakis et al., 1997), and a recent pre-print demonstrates that some auditory cortex neurons can even show adaptation on timescales of up to 20 minutes (Gill & Francis, 2023). Thus, SA over tens of seconds to minutes is a legitimate phenomenon present in several sensory systems but relatively uncharacterized in S1BF.

Diversity of SA responses

Typically, repeated presentation of the same stimulus results in a progressive decrease in neuronal activity. However, facilitating neurons that progressively increase their response magnitude with repetitive stimulation have also been identified in the visual (Dhruv et al., 2011; Kastner & Baccus, 2011), auditory (Phillips et al., 2017), and somatosensory (Kheradpezhouh et al., 2017) cortical regions. In S1BF, a small proportion of neurons facilitate to repeated whisker stimulation on timescales of a couple of seconds and generally at frequencies < 10 Hz (Adibi & Lampl, 2021; Garabedian et al., 2003; Kheradpezhouh et al., 2017). Another study in S1BF found that upon artificial induction of active whisking, L4 neurons tend to facilitate, while L2/3 neurons adapt. This diversity of responses merits further exploration, as it implies that complex SA population dynamics could occur beyond a net reduction in neuronal response magnitude to a familiar stimulus. It also remains unclear what the purpose is of these seemingly contradictory response profiles; in the visual system, adaptation and facilitation in retinal ganglion cells is thought to increase information transmission, with facilitating cells encoding weaker stimuli and adapting cells encoding stronger stimuli (Kastner & Baccus, 2011). In the context of behavior, one could

surmise that S1BF circuits could modulate the relative abundance of these two profiles to tune out irrelevant stimuli (adaptation) or amplify salient or threatening stimuli (facilitation) to enable their detection by the animal.

SA of neuronal populations

How these distinct neuronal responses (adaptation and facilitation) are coordinated to achieve a coherent representation of stimuli, at the network level, is not clear. Though prior studies on adaptation have provided valuable descriptions of how SA affects individual neurons, it remains unclear how SA shapes the activity of neuronal populations and influences the network-level representation of sensory stimuli in S1. Several studies outside of the tactile modality demonstrate the ability of SA to sculpt population dynamics: The activity of a neuron can, for example, also be modulated by the activity of its local population (Carandini & Heeger, 2011), as in the visual system, where adaptation can alter these population signals depending on the temporal context of incoming stimuli (Aschner et al., 2018). Intrinsic adaptation present at the level of individual neurons can compound to impact to information processing at the network level (Gjorgjieva et al., 2014). In the visual system, adaptation also functions to sustain homeostasis at the population level by maintaining mean firing levels in the network (Benucci et al., 2013).

These kinds of dynamics suggest that adaptation impacts neuronal population activity in complex ways that cannot be understood or inferred by studying single neurons. Thus, a detailed characterization of how adaptation and facilitation of individual neurons ultimately affect the

output of the entire population is needed and would require simultaneous observation of a large number of neurons within the local network during sensory stimulation. Moreover, though it may be reasonable to assume that the SA profile of individual neurons is stable over time, whether population drift (Rule et al., 2019) applies to SA is not known. In L2/3, almost half of pyramidal neurons exhibit drift in the specific whiskers to which they are tuned over the course of several days to weeks (Wang et al., 2022). Similarly, a recent longitudinal study of neuronal responses in superficial S1BF to whisker touch showed that while the proportion of touch responsive neurons was stable over days, the individual neurons that comprised that proportion changed across time (Alisha et al., 2023). The results imply that response properties of S1BF neurons can change over days, but the stability of SA in S1BF across time has not yet been examined.

Rationale for research

SA to tactile stimuli has been well characterized at the level of individual neurons, largely on the timescales of < 5 seconds and often under anesthesia. However, it remains unclear how SA is encoded across populations of neurons that work collectively to achieve complex representations of stimuli. Furthermore, whether these SA dynamics are stable across extended periods of time (i.e., days) has not yet been explored. With the advent of 2-photon calcium imaging techniques and transgenic reporter and Cre-driver mouse lines, we can now record the responses of hundreds of neurons in a single brain area simultaneously, and stable transgenic expression of calcium indicators makes it possible to record the same neurons across multiple days. Using these techniques, I have investigated the population dynamics of SA to repetitive whisker stimuli in the

mouse barrel cortex. I focus in particular on the superficial layers of S1BF, a point in the rodent somatosensory system at which bottom-up and top-down modulation converge.

With the experiments described in the chapters of this dissertation, I aim to answer the following questions: 1) Do excitatory neurons in S1BF adapt and facilitate at timescales of tens of seconds? 2) Is the population SA response to one stimulus maintained for a different stimulus? 3) Are SA response dynamics stable across tens of minutes and/or across days? 4) Does SA differ between L2/3 and L4? 5) Do inhibitory interneurons shape SA dynamics in superficial S1BF?

In Chapter 1, I summarize a set of homework experiments investigating how whisker stimuli of varying durations and intervals differentially recruit neurons in L2/3 of S1BF, which informs our selection of stimulus parameters for use in subsequent experiments. In Chapter 2, I characterize the diversity of adaptive response profiles in L2/3 during repetitive whisker stimulation and examine how those dynamics shift after an abrupt change in stimulus parameters. Chapter 3 comprises our investigation of the stability of these dynamics across time—first over tens of minutes, and then over several days. Finally, Chapter 4 details preliminary experiments investigating the role of somatostatin-positive interneurons in modulating SA in the superficial layers of S1BF.

CHAPTER 1:

Response dynamics of L2/3 excitatory neurons in awake head-fixed mice vary across whisker stimulus parameters

Are there features of sensory stimuli that influence the magnitude of SA, like the amplitude, frequency, or duration of the stimulation? SA in the rodent somatosensory system is known to be influenced by the parameters of the whisker stimulus. With higher whisker stimulation frequencies, S1BF neurons exhibit increased adaptation (Khatri et al., 2004; Kheradpezhouh et al., 2017; Martin-Cortecero & Nuñez, 2014), while increasing the amplitude and velocity of whisker stimulation tends to decrease adaptation (Ganmor et al., 2010). In a paradigm where neurons adapt to a repetitive whisker stimulus before being presented with a "test" stimulus, the amplitude of the adapting stimulus substantially affects the magnitude of the test response (Adibi et al., 2013).

While these studies provide valuable descriptions of the dependence of SA in S1BF on stimulus parameters, they overwhelmingly characterize these dynamics on rapid timescales of 3-4 s or less. Whether S1BF neurons exhibit SA to stimuli on prolonged timescales of tens of seconds to minutes thus remains an outstanding question. In the primary visual cortex, repetitive stimulation can alter the response properties of neurons—such as orientation tuning— for several minutes (Dragoi et al., 2000). A hallmark study by Berglund & Berglund on tactile adaptation in humans indicated a period of 2-3 minutes was required to recover from the perceptual effects of repetitive tactile stimulation (Berglund & Berglund, 1970), suggesting that SA effects persist past the frequently studied timescale of hundreds of milliseconds to a few seconds. Furthermore, seminal work from Fairhall and colleagues has demonstrated the existence of multiple timescales of SA in the blow fly visual system and the dependence of this adaptation on stimulus duration (Fairhall et al., 2001). This finding is supported by in vitro studies in rodent cortical slices (La Camera et al., 2006; Lundstrom et al., 2008), with neurons in somatosensory cortex slices showing SA ranging from milliseconds to ~15 s (La Camera et al., 2006).

2-photon calcium imaging (2PCI) is a popular technique for recording neuronal activity in vivo with high resolution and limited bleaching and out-of-focus excitation (Grienberger et al., 2022). 2PCI takes advantage of the influx of intracellular calcium that takes place when neurons fire action potentials and relies on calcium indicators to capture signals of neuronal activity. Genetically encoded calcium indicators (GECIs) like GCaMP (Chen et al., 2013; Tian et al., 2009) consist of a calcium-binding protein and fluorescent protein, and upon binding to calcium ions, the fluorescent component of the GECI undergoes a conformational change and fluoresces when excited at specific wavelengths (Grienberger et al., 2022). Using a 2-photon microscope with a laser whose wavelength aligns with the excitation wavelength of the GECI, these fluctuations in fluorescence can then be recorded as a proxy for neuronal activity. Generally, a portion of the skull is removed and replaced with a cranial window (see Methods) (Holtmaat et al., 2009; Mostany & Portera-Cailliau, 2008) to allow access to the brain for 2PCI. 2PCI is an ideally suited approach for our overarching goal of characterizing the population dynamics of SA in specific layers of S1BF for several reasons: 1) It allows us to record from large populations of neurons in a single layer; 2) Cranial window implantation methods are less invasive than electrodes for electrophysiology, which penetrate the brain tissue; and 3) 2PCI can be combined with Cre-Lox genetics to achieve calcium indicator expression in specific genetically defined neuronal subpopulations, allowing us to record the activity of specific cell types. This can also be combined with optogenetics to record and manipulate the activity of multiple neuronal subtypes at once (see Chapter 4). We thus employ a 2PCI approach in the majority of the experiments described in this dissertation.

In pilot experiments, we examined how whisker stimulation protocols spanning a wide range of timescales (12 s to 1.5 min) impacts the recruitment of neuronal responses, and whether stimulus responsive (SR) neurons exhibit adaptation across these timescales. In alignment with human perceptual research and prior animal model studies, we hypothesized that S1BF neurons exhibit SA at timescales of tens of seconds and that their response dynamics depend on whisker stimulus parameters.

RESULTS

Responsiveness of L2/3 excitatory neurons varies depending on whisker stimulation parameters

We performed in vivo 2-photon calcium imaging (2PCI) to record responses of L2/3 excitatory neurons in S1BF to several stimulation paradigms in an initial cohort (n = 5) of adult Slc17a7-Cre;GCaMP6s$^{fl/fl}$ (Ai162) mice, in which transgenic GCaMP6s expression is restricted to excitatory neurons (Daigle et al., 2018; J. A. Harris et al., 2014) (see Methods for details pertaining to these transgenic lines). Awake 2PCI was performed while mice were head-fixed and their bodies gently restrained in a plexiglass tube (**Fig. 1a**). We used a comb of thin Nylon filaments coupled to a piezo-actuator to deflect most whiskers on one side of the snout in the anterior-posterior axis (see Methods).

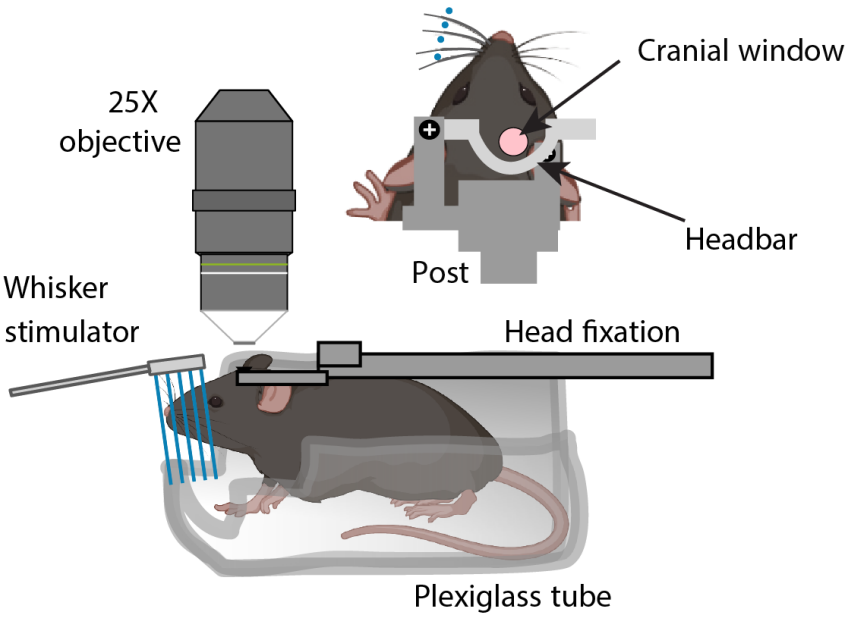

Figure 1. Setup for 2-photon calcium imaging in awake, head-fixed mice. Mouse in figure created with Biorender.com.

Before 2PCI, intrinsic signal imaging was performed while stimulating the C2 whisker to identify the C2 barrel in each mouse (**Fig. 2a**, top), which was where calcium imaging was performed. On average, we captured the activity of 128.6 ± 20.2 neuronal somata in a single field of view (FOV) (**Fig. 2a,** bottom; example traces in **Fig. 2b**).

We first delivered whisker stimuli at 5 Hz across a range of durations and interstimulus intervals (i.s.i.) (**Fig. 2c**). Mice typically whisk spontaneously at frequencies of 5-15 Hz, and with intermittent bouts lasting 1-4 s (Mégevand et al., 2009). To assess the population response, we plotted the mean activity of all SR neurons from each mouse, and subsequently computed a mean

of these mean traces, achieving a "mean of means" (MoM) trace. At the population level, the mean response showed clear adaptation, that is a gradual decrease in response magnitude with progressive stimulation, regardless of stimulation parameters (**Fig. 2e)**. This adapting trajectory of the population MoM trace was not driven by any single mouse, as mean population traces from individual mice behaved similarly (**Fig. 2f**). Of note, in the protocol with the shortest duration and i.s.i. (200 ms/1 s), the mean response showed a slight initial facilitation, likely because calcium transients never returned to baseline between stimulations (**Fig. 2e**, purple trace).

We also examined response reliability to a sequence of whisker stimulations and observed that neuronal responses were variable across the population, with some neurons responding to most bouts of whisker stimulation, while others responded to only a subset of stimulations **(Fig. 2f).** Quantifying the response reliability showed that across mice, most neurons respond to all 10 whisker stimulation bouts, while a minority responded to ≤ half of the stimulation bouts.

Figure 2. Response dynamics of L2/3 excitatory neurons across different whisker stimulation parameters.

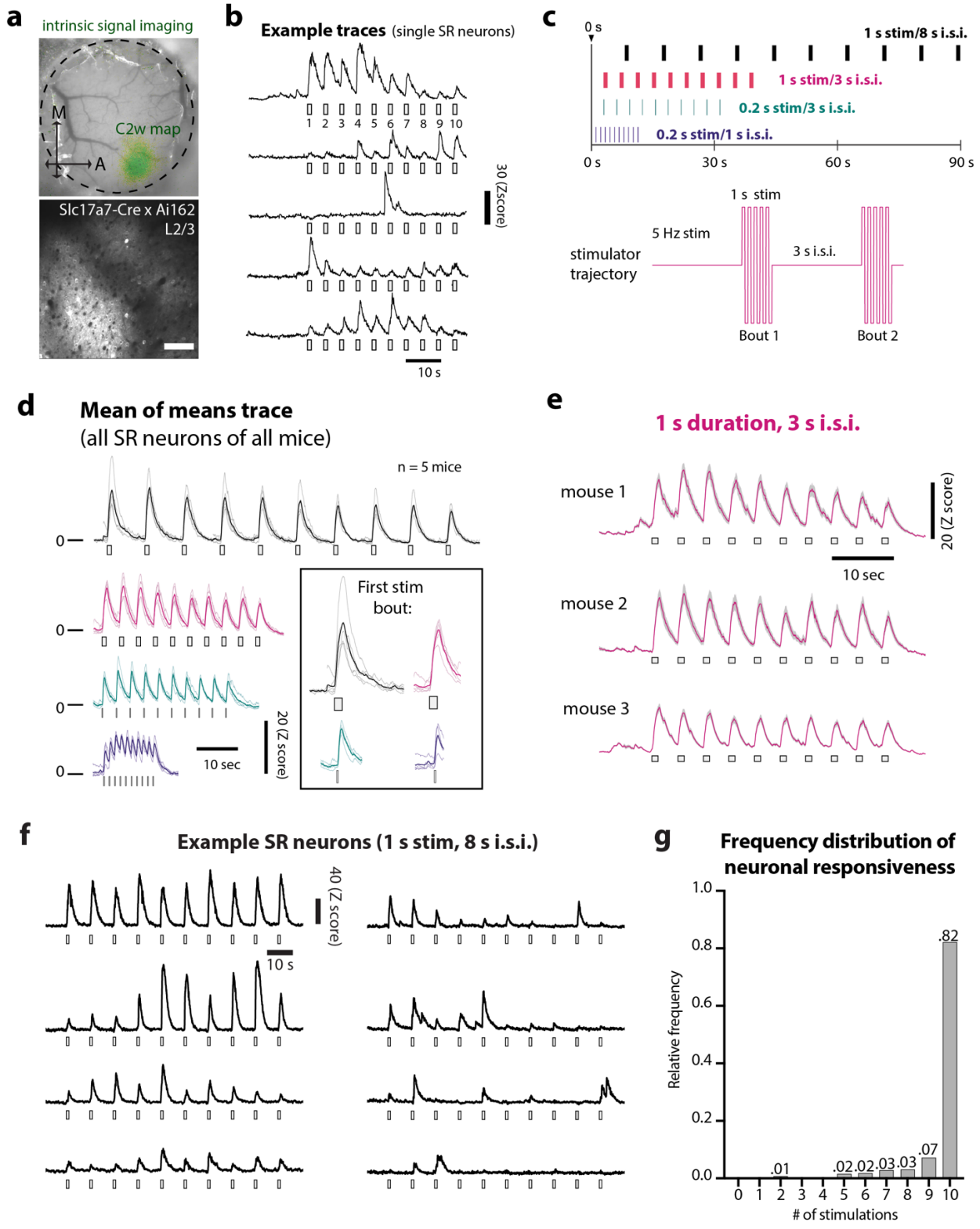

Figure 2. Response dynamics of L2/3 excitatory neurons across different whisker stimulation parameters.

a) Top, cranial window and superimposed intrinsic signal imaging map (green) corresponding to the C2 barrel in S1BF. Bottom, representative FOV from 2PCI in L2/3 above the C2 barrel (scale bar: 100 μm). M, medial. A, anterior.

b) Example traces of SR neurons during 5 Hz whisker stimulation (1 s duration, 3 s i.s.i.).

c) Top, schematic of whisker stimulation paradigms of various durations and intervals. Bottom, trajectory of piezoactuator deflections for the 1 s stim duration, 3 s i.s.i. stimulation paradigm during the first two stimulation bouts. Frequency is 5 Hz.

d) MoM traces for all 4 whisker stimulation paradigms (n = 5 mice for 1 s stim/8 s i.s.i. and 1 s stim/3 s i.s.i., n = 4 mice for 0.2. s stim/3 s i.s.i. ad 0.2 s stim/1 s i.s.i.) Inset, responses to the first stimulation bout for each paradigm.

e) Mean traces of all SR neurons to the 1 s stim/3 s i.s.i. paradigm for 3 different mice.

f) Example traces responding to the 1 s stim/8 s i.s.i. stimulation paradigm. Note the heterogeneity of individual neuronal responses, with some SR neurons responding to all 10 stimulation bouts (top left), while others respond to a couple of stimulation bouts (bottom right).

g) Distribution of cells according to what fraction of stimulation bouts they respond to. Stimulation paradigm is 1 s stim/8 s i.s.i.

Testing two methods of identifying stimulus responsive (SR) neurons

To determine whether neurons responded to bouts of whisker stimulation, we used either visual inspection of all the traces aligned to the bouts of stimulation, or an automated bootstrapping algorithm we used previously (He et al., 2017) (See Methods). Both approaches present potential advantages and disadvantages: the automated bootstrapping approach allows for unbiased, faster identification of SR neurons but may be prone to misclassifying some neurons, while visual inspection ensures that neurons categorized as SR show true responses to the stimulus but proceeds more slowly and could invite more bias than an automated approach. In a separate cohort of mice (n = 7), we compared these two approaches for the 1 s duration/3 s i.s.i. whisker stimulation protocol (with 20 stimulation bouts instead of 10). Visual inspection and classification proved to be more accurate and reliable than our automated approach, and it identified many more SR neurons (**Fig. 3a-b)**. For these reasons, we opted for the former for all analyses of 2PCI data. Results pertaining to SR neurons in the previous figure (**Fig. 2d-g**) use the visual inspection approach.

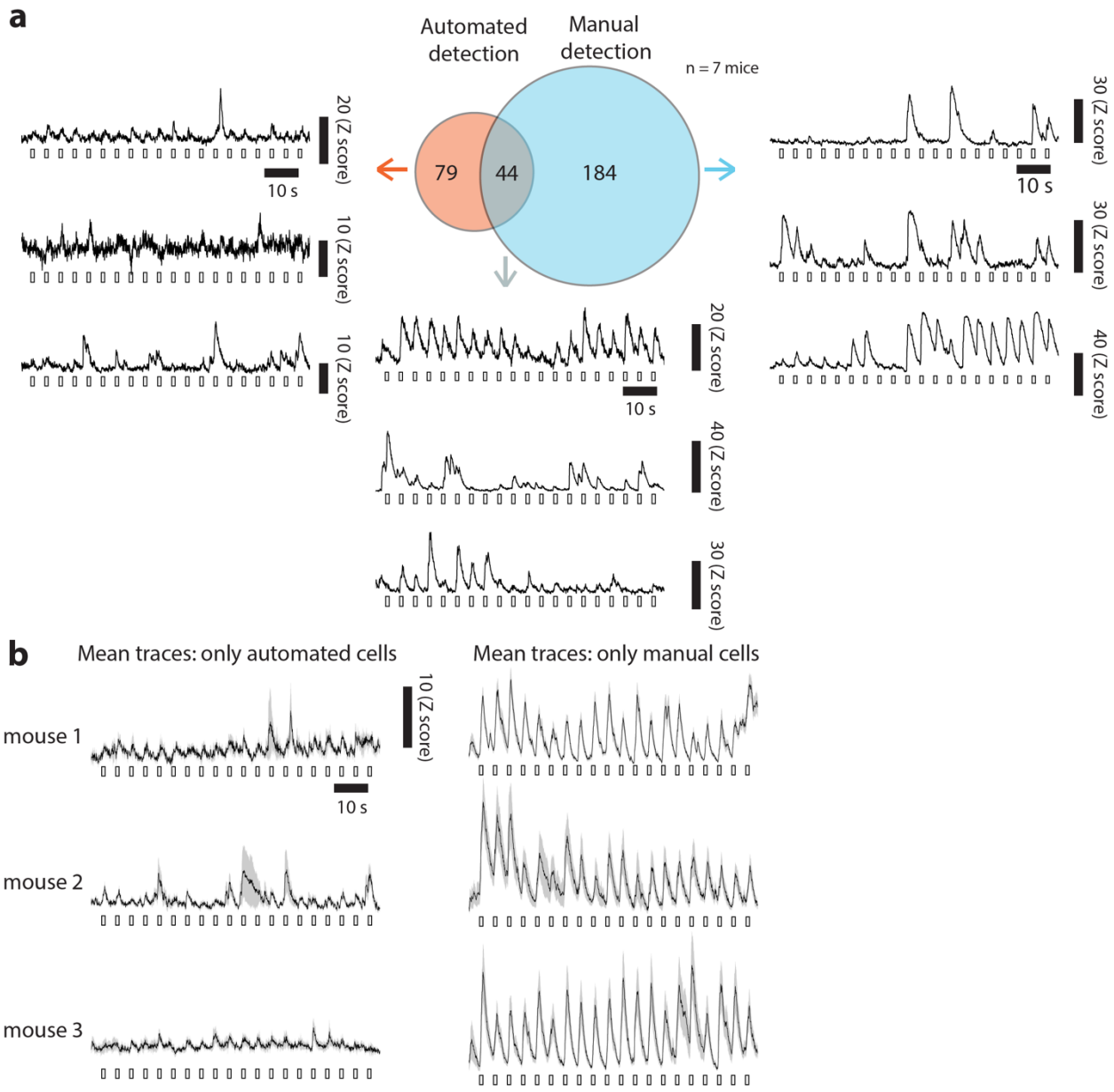

Figure 3. Automated vs. manual methods of classifying S1BF neurons as stimulus responsive.

a) Venn diagram showing how more neurons were categorized as stimulus responsive (SR) by manual approach than by automated approach (see Methods) in a separate cohort of 7 mice. Also shown are traces during whisker stimulation of 3 example SR cells detected solely by either method or detected by both (middle).

b) Mean traces of SR neurons as classified by automated and manual approaches. Note that the traces for neurons selected by manual approach show larger and more distinct calcium transients.

The proportion of SR neurons varied depending on the stimulation protocol but was highest for protocols with the longer stimulus durations (**Fig. 4a**). The magnitude of the response to the first stimulation (mean Z-score) was also slightly higher for protocols with longer stimulus duration (**Fig. 4b**). Together, these data indicate that longer stimuli recruit more neurons in S1BF and that the mean response of the population in S1 is mildly adapting, consistent with previous reports (He et al., 2017).

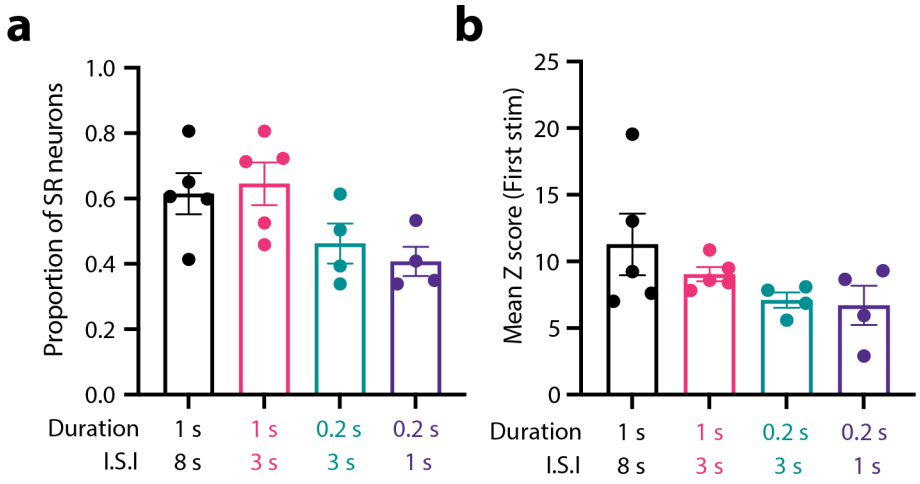

Figure 4. Impact of stimulus duration and i.s.i. on neuronal responsiveness.

a) Proportion of SR neurons for each stimulation paradigm (n = 5 mice).

b) Mean Z score during the first stimulation in each paradigm.

METHODS

Experimental animals

All experiments followed the U.S. National Institutes of Health guidelines for animal research, under an animal use protocol (ARC #2007-035) approved by the Chancellor's Animal Research Committee at the University of California, Los Angeles. Experiments used male and female C57BL/6J mice. We crossed Slc17a7-Cre mice (JAX strain # 023527) to the Ai162 (GCaMP6s) reporter line (JAX strain # 031562) resulting in Cre-dependent expression of GCaMP6s in Vglut1-positive excitatory neurons. The Slc17a7-Cre line is a pan-glutamatergic Cre-driver line which directs reporter expression to Vglut1-positive cells (J. A. Harris et al., 2014), while Ai162 is a Cre-dependent GCaMP6s reporter line (Daigle et al., 2018). All mice were housed in a vivarium with a reverse 12/12 h light/dark cycle and experiments were performed during the dark cycle. Animals were weaned from their dam at postnatal (P) day 21-22 and then group housed with up to five mice per cage.

Cranial window surgery

Cranial window surgery was performed on mice at P45-P90, as described previously (Holtmaat et al., 2009; Mostany & Portera-Cailliau, 2008). Mice were anesthetized with isoflurane (5% induction, 1.5-2% maintenance via a nose cone) and placed in a stereotaxic frame (Kopf). A 4 mm diameter craniotomy was performed over the right S1BF and covered with a 4 mm glass coverslip. A custom horseshoe-shaped titanium head bar (3.15 mm wide x 10 mm long) was affixed to the skull with dental cement to secure the animal to the microscope stage. Animals recovered from the procedure and were fully ambulatory within 1 h after the surgery. Carprofen (5 mg/kg, s.c., once daily) was used for analgesia for 3 d post-op.

Intrinsic signal imaging

Intrinsic signal imaging allows for localization of the barrel cortex by identifying hemodynamic changes related to neuronal activity (Grinvald et al., 1986) during whisker stimulation. Approximately 1 week after cranial window surgery (and at least 3 d before beginning calcium imaging), intrinsic signal imaging was used to map the location of the C2 barrel within barrel cortex, as described previously (Zeiger et al., 2021). The contralateral C2 whisker was gently attached with bone wax to a glass capillary that was coupled to a piezoactuator (Physik Instrumente). Each stimulation trial consisted of a 100 Hz sawtooth stimulation lasting 1.5 s. Thirty stimulation trials were run, with 20 s interstimulus intervals (i.s.i.). The response signal during the whisker stimulations divided by the averaged baseline signal, summed for all trials, was used to generate the C2 barrel map.

2-photon calcium imaging

2PCI was performed in awake mice. We used a commercial 2-photon microscope (DIY Bergamo, ThorLabs) equipped with galvo-resonant scanning mirrors, amplified non-cooled GaAsP photomultiplier tubes (Hamamatsu), a 25X objective (1.05 NA, Olympus), and ThorImage software. The microscope was coupled to a Chameleon Ultra II Ti:sapphire laser (Coherent) tuned to 930 nm, and the average power at the sample was kept <150 mW.

We recorded both spontaneous activity and whisker-evoked activity in S1BF. Mice (n = 5) were first habituated to the microscope setup prior to 2PCI. This process lasted ~10 d and involved a gradual progression from basic daily handling (5 min/d) until mice were comfortable with head fixation and body restraint in a plexiglass tube for periods up to 30 min. Mice were considered ready for imaging when they could remain still during sham whisker stimulation, in which the whisker stimulator is placed in front of the mouse but out of reach of its whiskers. The whisker stimulator consisted of a "comb" of von Frey Nylon filaments intercalated between whiskers. This comb was coupled to a piezoactuator (controlled by MATLAB), which delivered repetitive deflections of the whiskers in the antero-posterior direction at pre-specified frequencies, durations, and intervals (see below). Calcium imaging was performed at a framerate of 15.1 Hz, and we recorded responses of ~120-140 neuronal somata in layer (L) 2/3 neurons (at 200-220 μm depth) above the C2 barrel within a single field of view (FOV) per animal (measuring 512 x 512 pixels, 533.7 x 533.7 μm).

During imaging, we first recorded 3 min of spontaneous activity, and then we delivered various whisker stimulation paradigms (**Fig. 1**), in separate movies (with 4-5 min breaks in between each movie), as follows:

- 10 x 5 Hz: stimulus duration 1 s, interstimulus interval (i.s.i.) 8 s
- 10 x 5 Hz: stimulus duration 1 s, i.s.i. 3 s
- 10 x 5 Hz: stimulus duration 0.2 s, i.s.i. 3 s
- 10 x 5 Hz: stimulus duration 0.2 s, i.s.i. 1 s

We chose 5 Hz because it falls within the range of frequencies at which rodents whisk when exploring their surroundings (Mégevand et al., 2009). A 20 s baseline period was included in each whisker stimulation movie before initiating whisker deflections. Mice were given 4–5-minute breaks between each stimulation paradigm.

Analysis

Motion correction and segmentation: Using a custom MATLAB pipeline already established in the lab (EZcalcium; (Cantu et al., 2020)), calcium movies were motion corrected and semi-automatically segmented. Rigid motion correction was performed in EZcalcium using the following parameters: upsampling factor = 50; max shift = 50 pixels; initial batch size = 200 frames; bin width = 200 frames. Next, we used segmentation in EZcalcium with the following parameters: Initialization = greedy; Search method = ellipse; Deconvolution = constrained FOOPSI CVX; Autoregression = decay; Estimated regions of interest (ROI) = 140; Estimated ROI

width = 15 pixels; Merge threshold = 0.95; Fudge factor = 0.98; Spatial downsampling = 2; Temporal downsampling = 10; Temporal iterations = 3. Following this initial detection of regions of interest (ROIs) we used an initial manual refinement step (also in EZcalcium) to include ROIs that had been missed by the automated segmentation process (typically ~20-30% of final ROIs were added by this manual step). We then proceeded to a ROI refinement step, in which we manually excluded ROIs that had been automatically detected but were considered to have either spatial contours that were atypical of neurons or because their calcium traces did not show dynamics typical of neurons.

Stimulus responsiveness: Following segmentation, changes in raw fluorescence signal intensity ($\Delta F/F$) were quantified for each ROI using a modified Z score ([F(t) – mean(quietest period)]/SD(quietest period)) as previously described (He et al., 2017). ROIs exhibiting calcium transients that were time-locked to bouts of whisker stimulation were identified using either visual inspection (**Figs. 1, 2, & 4**) or a probabilistic bootstrapping method (He et al., 2017) (**Fig. 3**). These ROIs were deemed stimulus responsive (SR).

Response reliability: The peak Z score value for each SR neuron during each stimulation bout (i.e., a response peak) was calculated. In our quantification of response reliability (**Fig. 1f-g**) a neuron was considered responsive during a stimulation bout if it had a response peak with a Z score > 3.

CHAPTER 2: Flexibility in SA dynamics in L2/3 after a switch in stimulus frequency

If the population response in L2/3 of S1 to repetitive whisker stimulation is adapting, does that mean that individual SR neurons across the population respond similarly to these stimuli (i.e., do they all adapt)? Results in Chapter 1 demonstrated that neuronal responses to whisker stimulation varied substantially, and not all neurons showed adaptation (**Fig. 2b**). Previous studies have identified that a minority of cortical sensory neurons can show facilitation, in which response magnitudes progressively increase with ongoing stimulation, typically when the i.s.i. is short (seconds) (Dhruv et al., 2011; Kastner & Baccus, 2011; Kheradpezhouh et al., 2017; Phillips et al., 2017; Seay et al., 2020). However, whether S1BF neurons can show facilitating responses to repetitive stimulation over tens of seconds remains relatively unexplored.

In a naturalistic setting, animals are likely to encounter changes in the stimulus statistics of their environments, which they must detect if they are behaviorally relevant or threatening. We thus also wondered how S1BF neurons respond to a change in stimulus parameters after they have already adapted to one whisker stimulus. Work in early stages of the visual system finds that the dynamics of SA of retinal ganglion cells after a switch in stimulus parameters depends on how much time was spent exposed to the initial adapting stimulus; the more time spent exposed to the adapting stimulus, the longer cells need to adapt (Wark et al., 2009). SA in this system also depends on the discriminability of the change in stimulus parameters; the milder (i.e., less discriminable) the change in stimulus parameters is, the longer it takes cells to adapt. Thus, SA may depend on how different the new stimulus is to the adapting stimulus, as well as how long the animal has been exposed to the adapting stimulus.

In the experiments described in this chapter, we employed in vivo 2-photon calcium imaging (2PCI) and Neuropixels recordings in awake adult mice to characterize the diversity of SA profiles in L2/3 of S1BF. In addition to characterizing the population response to repetitive whisker stimulation, we also explored how neurons responded to a change in whisker stimulus parameters (frequency) after having already been exposed to a previous stimulus.

RESULTS

Individual responses of L2/3 excitatory neurons to repetitive whisker stimulation are stochastic, but the population SA response is adapting.

We first performed in vivo 2PCI to record responses of L2/3 excitatory neurons in S1BF to whisker stimulation in a cohort of young adult (2-3 months) (n = 8). As in Chapter 1, we used Slc17a7 (vGlut1)-Cre;GCaMP6s$^{fl/fl}$ (Ai162) mice, in which GCaMP6s expression is restricted to excitatory neurons (Daigle et al., 2018; J. A. Harris et al., 2014). Intrinsic signal imaging and 2PCI with simultaneous whisker stimulation were performed as in Chapter 1 (**Fig. 5a,** top), but with different whisker stimulation protocols (see Methods). Based on the results of Chapter 1 and whisker stimulation protocols we have used in prior studies (He et al., 2017; Kourdougli et al., 2023), we proceeded with the 1 s duration/3 s i.s.i. whisker stimulation protocol, using a stimulus frequency of either 5 Hz or 12.5 Hz (**Fig. 5a**, bottom), as the latter produced more than twice the number of whisker deflections than the former, and both frequencies fall within the range at which rodents

whisk naturally when exploring (Mégevand et al., 2009). On average, we captured the activity of 158.6 neuronal somata (range: 67-226 somata) in a single field of view (FOV).

At the population level, the mean response in each mouse tended to show adaptation— that is, a gradual decrease in response magnitude with ongoing bouts of whisker stimulation (**Fig. 5d)**. As previously reported (Clancy et al., 2015; He et al., 2017) most L2/3 neurons in S1BF did not respond to whisker stimulation (**Fig. 5c**). A slightly smaller percentage of stimulus responsive (SR) neurons responded to 5 Hz whisker stimulation than to 12.5 Hz stimulation (19.2 ± 10.0% for 5 Hz vs. 24.5 ± 6.3% for 12.5 Hz, p= 0.133, paired t-test; **Fig. 5c**). Amongst SR neurons, we observed that individual responses to a sequence of 20 bouts of whisker stimulations at 5 Hz were variable across the population, with some neurons responding to most bouts of whisker stimulation, while others responded to only a subset of stimulations **(Fig. 6a)**. The majority of SR neurons (82%) responded to more than half of the bouts (**Fig. 6b**). We observed similar proportions for 12.5 Hz whisker stimulation (86% of SR neurons responded to more than half of the bouts; not shown). Example traces of non-SR neurons and mean traces of non-SR neurons can be found in **Fig. 6c-d**.

Together, these data indicate that, despite the stochasticity of individual neuronal responses, the mean response of the L2/3 population in S1BF is adapting, consistent with previous reports in S1 (He et al., 2017) and auditory cortex (Natan et al., 2015, 2017).

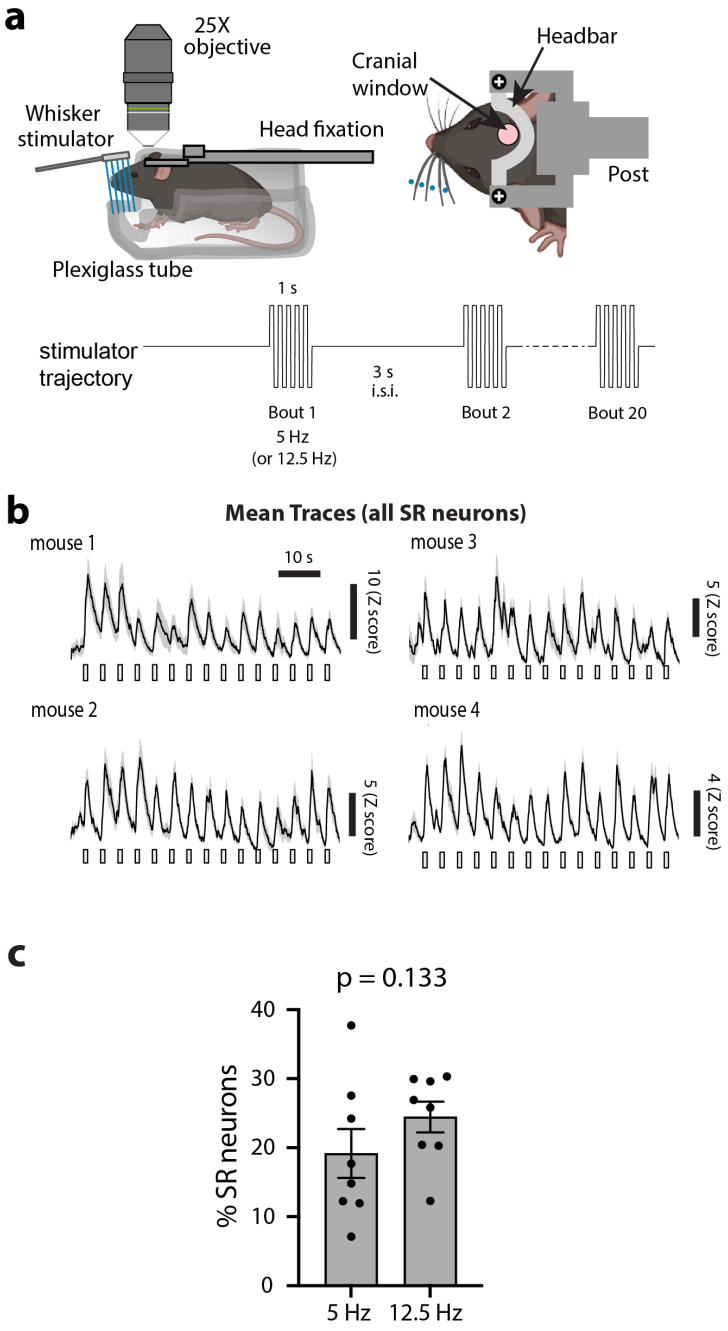

Figure 5. The mean response of SR neurons to 5 Hz whisker stimulation is mildly adapting.

a) Top, cartoon of 2PCI and whisker stimulation setup. Bottom, trajectory of piezoactuator deflections for the 1 s stim duration, 3 s i.s.i. stimulation paradigm. Frequency is 5 or 12.5 Hz. Mouse in figure created with Biorender.com.

b) Mean traces of all stimulus responsive (SR) neurons from 4 representative mice during whisker stimulation at 5 Hz. Note that the mean population response is mildly adapting.

c) The percent of SR neurons was not significantly different between 5 Hz and 12.5 Hz stimulation protocols. Paired t-test.

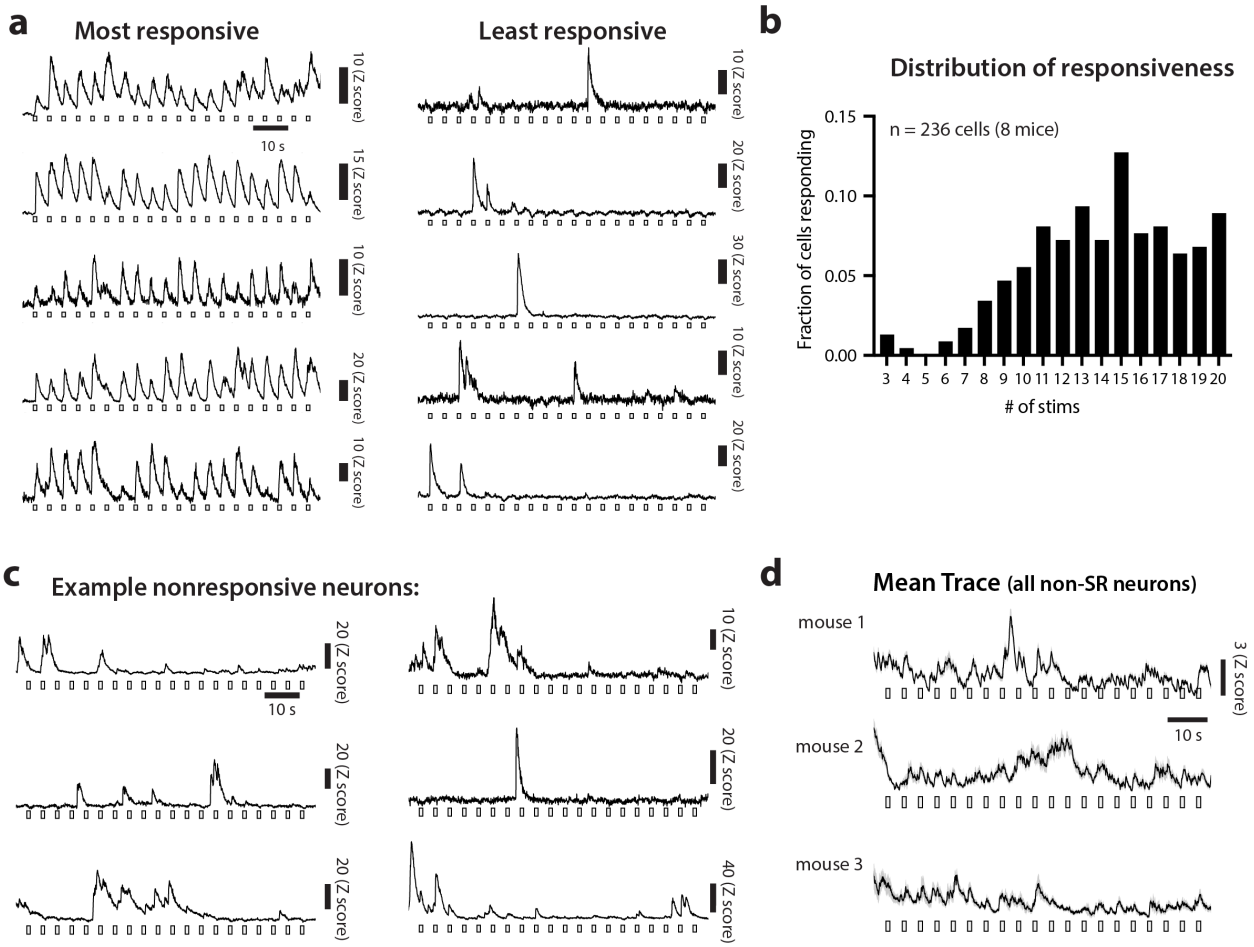

Figure 6. Diverse and stochastic responses of L2/3 excitatory neurons to bouts of repetitive 5 Hz whisker stimulation.

a) Example traces of SR neurons to whisker stimulation. Note the heterogeneity of individual neuronal responses, with some SR neurons responding to all stimulation bouts (top left), while others respond to a couple of bouts (bottom right).

b) Distribution of cells according to what fraction of stimuli they respond to.

c) Example nonresponsive neurons during whisker stimulation. Note how activity of these cells does not track bouts of whisker stimulation.

d) Mean trace of all nonresponsive neurons for 3 example animals.

Individual L2/3 neurons exhibit adapting and facilitating responses to repetitive whisker stimulation.

Given previous literature demonstrating the existence of adapting and facilitating response profiles on more rapid timescales in S1BF (Derdikman, 2006; Garabedian et al., 2003; Kheradpezhouh et al., 2017), we wondered whether this diversity in response profiles was present in S1BF during repetitive whisker stimulation over tens of seconds. To categorize SR neurons as either adapting or facilitating (or neither), we calculated a stringent adaptation index (AI) based on whether the slope of the peak responses of individual neurons to the first 15 bouts significantly differed from zero (**Fig. 7**; see Methods).

A negative AI value indicates an adapting response profile, while a positive AI value denotes facilitation (see examples in **Fig. 8a**). Together, facilitating (7.2%) and adapting neurons (18.6%) comprised roughly a quarter of all SR neurons (**Fig. 8b**). The remaining SR neurons showed non-significant AI slope values. Within this non-significant category, some cells could show adaptation or facilitation, but due to variable responses across the 15 stimulations, our strict AI criteria did not assign them to the facilitating or adapting groups. To assess the population response of adapting and facilitating neurons, we plotted the mean activity of all adapting or facilitating neurons from each mouse, and then computed a "mean of means" (MoM) trace. The MoM trace for all adapting and facilitating neurons across all mice showed the expected trajectories (**Fig. 8c**).

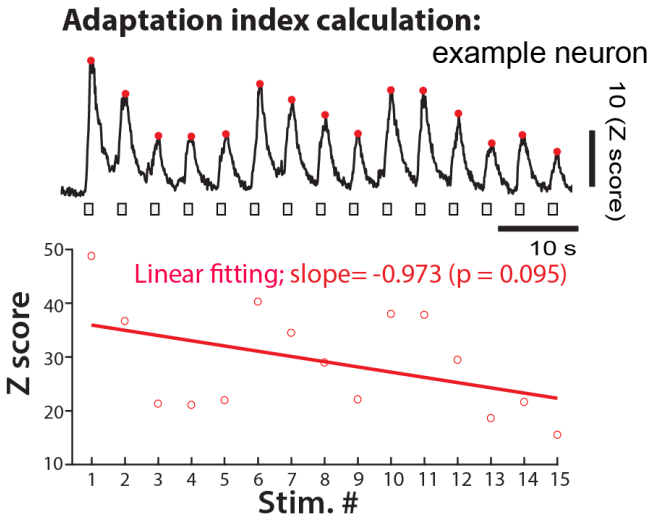

Figure 7. Calculation of adaptation index. Top, example neuron with response peaks labeled in red. Bottom, linear regression-based calculation of adaptation index in the same example neuron.

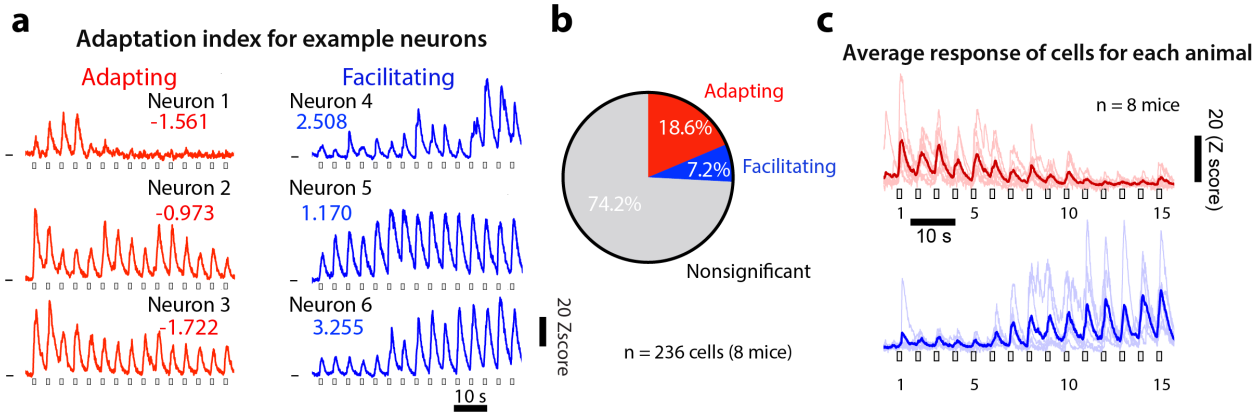

Figure 8. Adapting neurons outnumber facilitating neurons in L2/3 of S1BF.

a) Traces of 6 example L2/3 neurons from the same movie, showing adapting or facilitating responses to whisker stimulation (5 Hz, 1 s stim, 3 s i.s.i.), with corresponding adaptation index values.

b) Relative proportion of adapting, facilitating, and nonsignificant neurons.

c) MoM traces of all adapting (red) and facilitating (blue) neurons responding to whisker stimulation.

We also used a different approach to classify L2/3 neurons as adapting or facilitating based on the change in magnitude of the response peaks from stimulations 1-5 to stimulations 11-15 (**Fig. 9a-b**) (see Methods). This alternate approach identified comparable proportions of adapting (25.4%) vs. facilitating neurons (12.7%) in L2/3 (**Fig. 9c**), and adapting and facilitating MoM traces resembled those using our more stringent statistical method (**Fig. 9d**). Thus, regardless of the method we used to quantify the AI, neurons with adapting responses outnumbered those showing facilitation by at least 2:1.

Figure 9: Two different methods for quantifying the adaptation index (AI) of SR neurons.

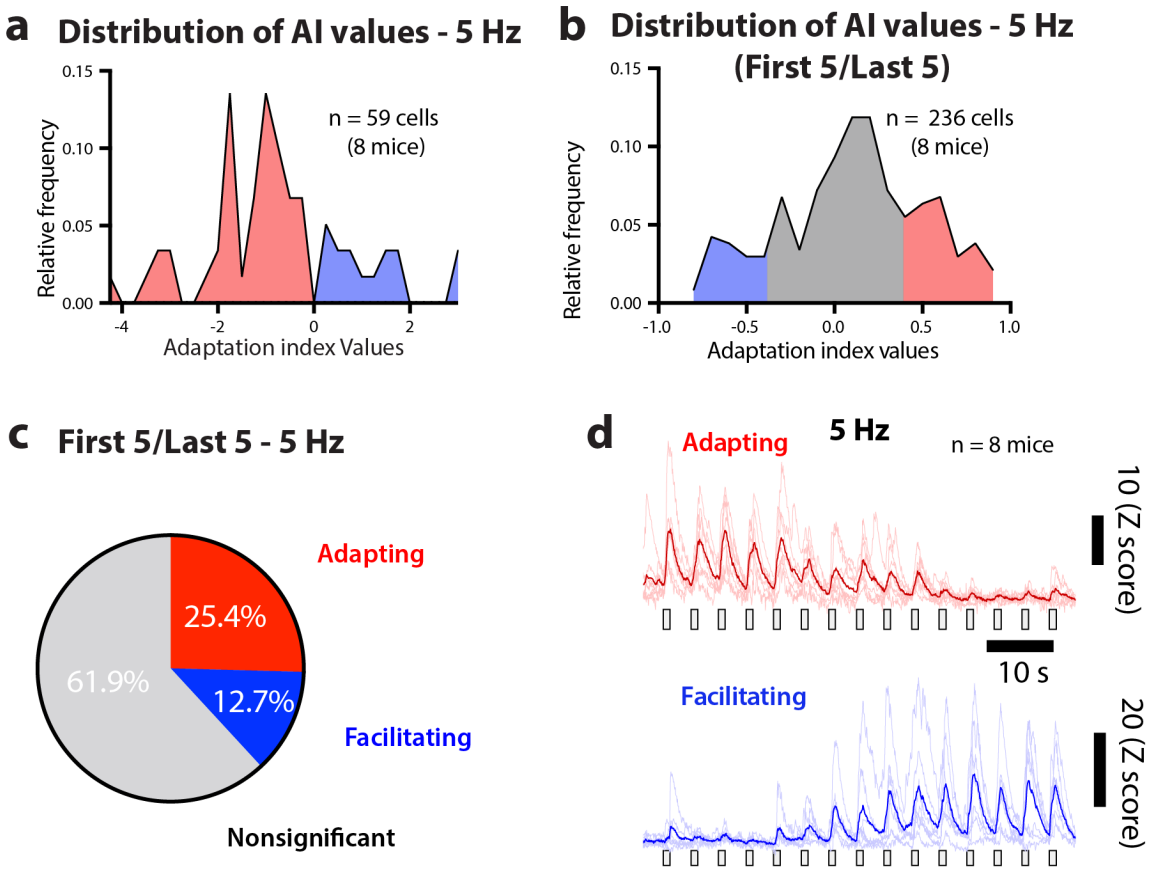

Figure 9. Two different methods for quantifying the adaptation index (AI) of SR neurons.

a) Distribution of AI values for 5 Hz whisker stimulation paradigm using the significant slope method (see *Methods*).

b) Distribution of AI values using an alternate method that compares the mean response peak amplitude during stimulations 1-5 vs. 11-15.

c) Percent of SR neurons in each response profile category using the First 5/Last 5 method.

d) MoM traces of neurons classified as adapting and facilitating by the First 5/Last 5 method

We then asked whether adapting and facilitating neurons are homogenously distributed in S1BF or whether instead they form clusters and are preferentially coupled to other neurons of the same SA profile. When we superimposed all FOVs (each approximately centered above the C2 barrel), we found a salt-and-pepper distribution of adapting and facilitating neurons, and no evidence of spatial segregation (**Fig. 10a**). During the pre-stimulus baseline, adapting neurons were more correlated to each other than to facilitating neurons. During stimulation, correlation coefficients were significantly higher for adapting-adapting and facilitating-facilitating pairs than for adapting-facilitating pairs (**Fig. 10b,** right), but this was likely due to their preferential firing during early or late bouts of stimulation, respectively (**Fig. 10c**).

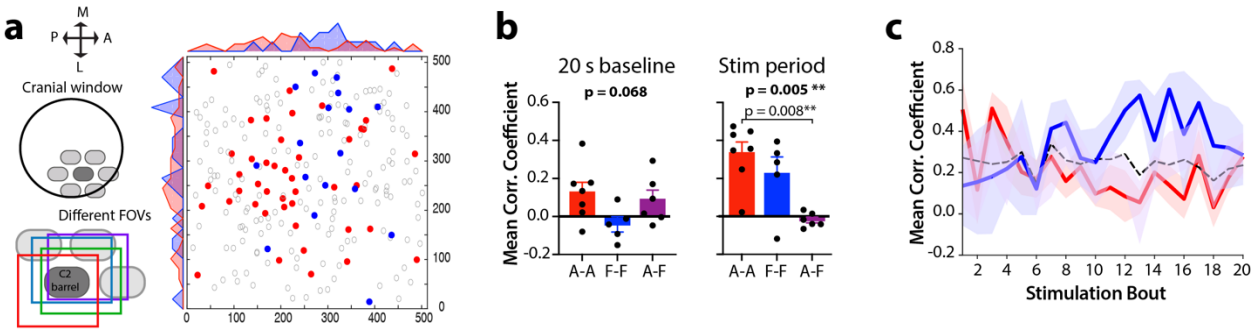

Figure 10. Spatial distribution of and correlations between adapting and facilitating neurons.

a) Spatial distribution of adapting and facilitating neurons within all FOVs (n = 236 cells from 8 mice), approximately aligned to each other with respect to the C2 barrel. M, medial. L, lateral. A, anterior. P, posterior.

b) Left: Mean correlation coefficient for neuron pairs during the 20 s baseline period preceding the first whisker stimulation. Right: Same, but for the stimulation bouts. Kruskal-Wallis test with post-hoc Dunn's test. A: adapting; F: facilitating

c) Mean correlation coefficient of neuron pairs with distinct response profiles during each stimulation bout. Blue: facilitating-facilitating pairs; Red: adapting-adapting pairs; Dashed line: all SR neurons. Solid lines are means, shaded regions are s.e.m.

We also analyzed neuronal responses and SA profiles to 12.5 Hz whisker stimulation in the same animals (**Fig. 11a-d**). The relative proportion of adapting and facilitating neurons were similar (14.4% vs. 12.0 %, respectively; **Fig. 11b)**. Although the percentage of adapting neurons was similar between 5 Hz and 12.5 Hz stimulation, the percentage of facilitating neurons was significantly higher with 12.5 Hz stimulation (**Fig. 11c**). As a result, the mean significant slope of all SR neurons was significantly less negative (less adapting) for 12.5 Hz compared to 5 Hz stimulation (**Fig. 11d**). This was the first hint that SA is dynamic at the population level.

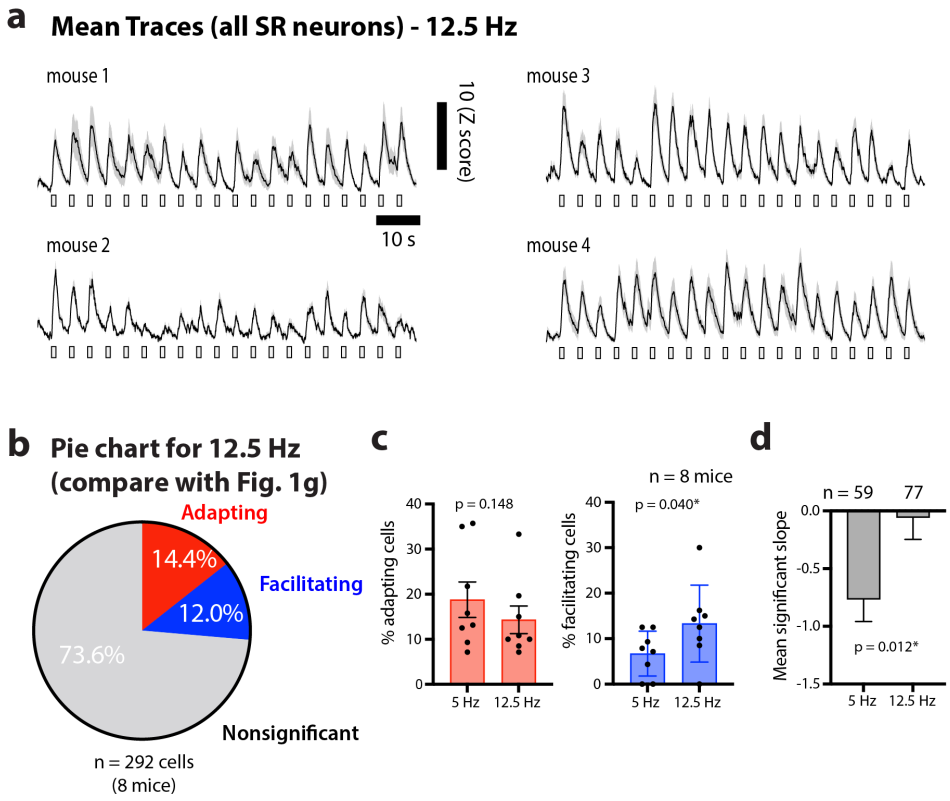

Figure 11. Comparison of SA response dynamics between 5 Hz and 12.5 Hz whisker stimulation protocols.

a) Mean traces of all SR neurons during 12.5 Hz whisker stimulation in 4 example mice.

b) Similar proportions of SR neurons showed adapting vs. facilitating responses to 12.5 Hz whisker stimulation.

c) The proportion of adapting neurons (left) was similar between 5 Hz and 12.5 Hz stimulation protocols, but there was a significantly higher proportion of facilitating neurons with 12.5 Hz stimulation (right). Adapting: Wilcoxon test (non-normal). Facilitating: paired t-test.

d) The mean significant slope for the AI was significantly less negative (less adapting) for 12.5 Hz than for 5 Hz stimulation. Mann-Whitney test.

Neuropixels recordings confirm the presence of adapting and facilitating neurons in L2/3 of S1BF.

Although in vivo 2PCI offers several advantages over electrophysiology, it suffers from poor temporal resolution due to the slow kinetics of the calcium indicator (Grienberger et al., 2022). These slow kinetics could contribute to an overestimation of facilitating responses if the fluorescence intensity did not fully return to baseline prior to the next stimulation (particularly in highly active cells). Although we have observed this phenomenon when using bouts of whisker stimulation with a shorter i.s.i. of 1 s (**Fig. 2d**, purple trace), we did not observe a significant additive response of calcium transients for our stimulation protocols with a 3 s i.s.i. Calcium imaging might also have missed neurons that responded with few action potentials. Thus, we performed in vivo electrophysiological recordings in S1BF with Neuropixels probes (Jun et al., 2017) (see Methods; **Fig. 12a,b**) while mice (n= 9) were exposed to 20 bouts of whisker stimulation at 10 Hz. Our analysis focused on regular-spiking (excitatory) neurons across all cortical layers (a total of 579 single units). Again, we calculated an AI for SR neurons based on whether the slope of the fit peak firing rate for each bout of stimulation was significantly different from zero (**Fig. 12c**). Neuropixels recordings revealed the presence of both adapting and facilitating neurons in S1BF, and these showed stochastic response profiles to individual bouts of stimulation, just as we had observed with 2PCI (**Fig. 12d**). The relative proportions of adapting (25.0%) and facilitating neurons (6.3%), as well as the mean traces of adapting and facilitating neurons, were similar between Neuropixels recordings and 2PCI (**Fig. 12e-f**). Thus, in vivo electrophysiological recordings confirmed our results about SA obtained with 2PCI.

Figure 12: Neuropixels recordings of regular-spiking neurons in S1BF confirm preponderance of adapting over facilitating neurons after repetitive whisker stimulation.

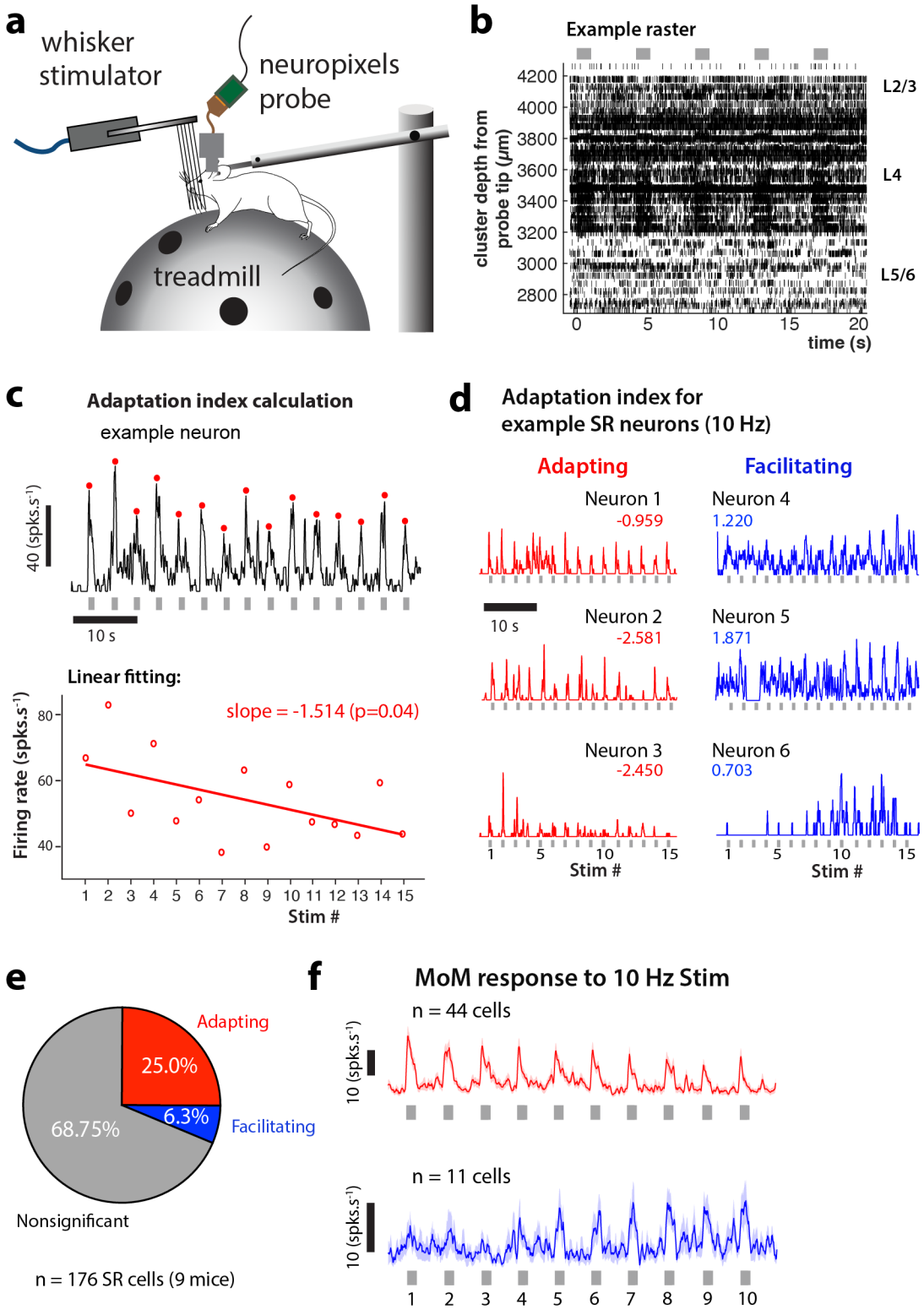

Figure 12. Neuropixels recordings of regular-spiking neurons in S1BF confirm preponderance of adapting over facilitating neurons after repetitive whisker stimulation.

a) Schematic of Neuropixels recording setup.

b) Example raster plot from one animal during the first 5 whisker stimulations at 5 Hz. Approximate boundaries of cortical layers are noted.

c) Adaptation index calculation in an example regular-spiking (RS) unit.

d) Example adapting and facilitating neurons during 10 Hz whisker stimulation.

e) Relative proportion of adapting, facilitating, and non-significant RS neurons in S1BF.

f) Mean trace of all adapting (red) and facilitating (blue) neurons responding to 10 Hz whisker stimulation.

Adapting neurons transiently facilitate after a switch to whisker stimulation at a higher frequency.

Are SA response profiles of individual neurons fixed? In other words, is the adapting or facilitating identity of a neuron in S1BF maintained across time? And, at the population level, can the overall response in S1BF change with experience or with different stimulation parameters? To begin to answer these questions we first considered whether cortical neurons maintain the same SA identity after a switch in stimulation parameters and tested if S1BF neurons that adapt to repetitive whisker stimulation at one frequency also adapt to a different frequency. We performed frequency switch experiments, in which we delivered 10 stimulation bouts (1 s duration, 3 s i.s.i.) at one frequency (5 or 12.5 Hz) and then abruptly switched to the alternate frequency for the next 10 stimulation

bouts (**Fig. 13a**). As a control, the same mice were stimulated at the same frequency for all 20 stimulation bouts. During the control paradigms, the mean population response of all SR neurons progressively decreased, as expected, regardless of frequency, though slightly more so with the higher frequency (**Fig. 13b**).

We then classified SR neurons as adapting or facilitating by calculating the AI based on the slope of peak responses to the first 9 stimulations. When we compared the responses of adapting vs. facilitating neurons, we found that facilitating neurons did not exhibit any substantial change in response peak amplitudes after the frequency switch compared to the control stimulation (**Fig. 13c-f,** bottom). In contrast, adapting neurons exhibited a noticeable increase in their response peak amplitudes after a switch to the higher frequency (**Fig. 13c-f**, top). Of note, the increase in response peak amplitude of adapting neurons was not due to an 'oddball' phenomenon, as it did not occur immediately after the switch (**Fig. 13c**), but rather emerged gradually as a result of facilitation (**Fig. 13d**). When we quantified the difference in mean peak z-score before and after the switch, we found that adapting neurons exhibited a significant change, which was not seen in the control protocol (**Fig. 13e-f, top**). In contrast, facilitating neurons did not manifest a significant change in the mean peak z-score (**Fig. 13e-f**, bottom), and neither did SR neurons with non-significant AI (neither adapting nor facilitating; (**Fig. 14a-b**). Moreover, a change in response peak amplitudes was not observed for adapting or facilitating neurons when switching to a lower frequency (**Fig. 14c-d**). Normalizing peak Z scores to the first response peak showed similar results for the upward frequency switch (not shown).

We also used Neuropixels probes to record responses during the same frequency switch experiment. These recordings confirmed that adapting neurons significantly increase their firing (i.e., they become facilitating) in response to a switch to a higher frequency, whereas facilitating neurons do not (**Fig. 13g-h**). Altogether, frequency-switch experiments revealed that, although most SR L2/3 neurons appear to maintain the same dynamics following a sudden switch in stimulus frequency, adapting neurons can gradually increase their activity in response to an increase in frequency, in essence exhibiting facilitation.

Figure 13: Adapting neurons transiently facilitate after an upward switch in stimulus frequency.

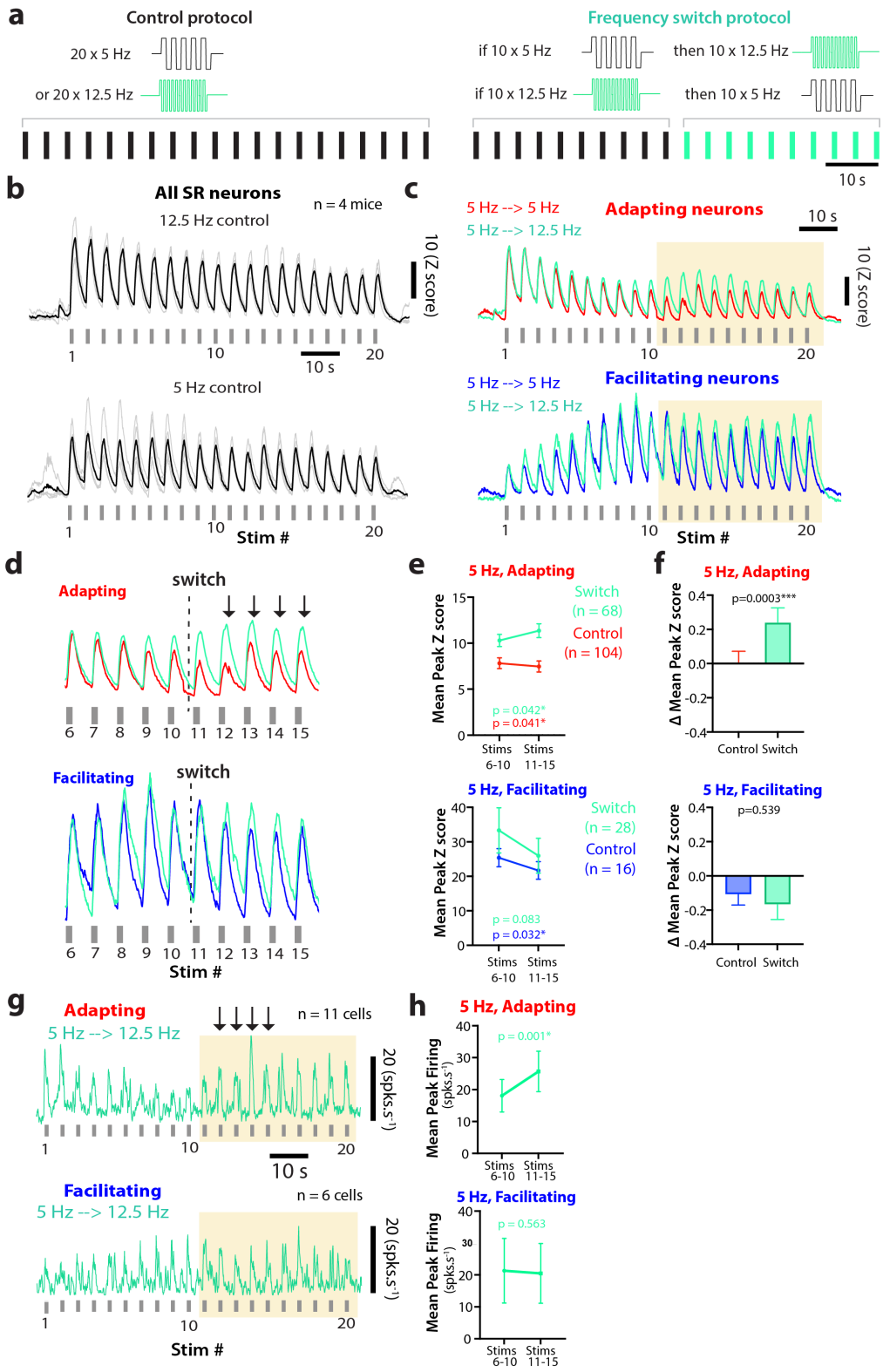

Figure 13: Adapting neurons transiently facilitate after an upward switch in stimulus frequency.

a) Schematic of control (left) and frequency switch (right) whisker stimulation protocols. Each vertical bar represents a single 1 s-long whisker stimulation at 5 or 12.5 Hz (also shown in expanded timeline).

b) MoM traces for animals presented with the 12.5 Hz (top) and 5 Hz (bottom) control protocols. Gray lines represent mean trace of all SR neurons for individual mice and thick black lines represent the MoM trace for all animals.

c) MoM traces of adapting (top) and facilitating (bottom) neurons from the same mice in **b** for the downward frequency switch (left) and upward frequency switch (right) protocols. Control traces (red or blue) and switch traces (green) are scaled to the first response peak.

d) Same traces as in **c** but expanded to highlight stimulations 6-15 (the vertical dashed line indicates the frequency switch).

e) Mean peak Z scores of adapting/facilitating neurons at stims 6-10 and 11-15 for the 5 Hz → 12.5 Hz switch protocol and 5 Hz control protocols. Wilcoxon test.

f) Change in mean peak Z score from stims 6-10 to stims 11-15 in the control 5 Hz control protocol vs. the 5 Hz → 12.5 Hz switch protocol, calculated using the following formula: ((Mean Peak Z score stims 11-15) – (Mean Peak Z score stims 6-10))/(Mean Peak Z score stims 6-10). Mann Whitney test (top, non-normal distribution) and unpaired t-test (bottom). Same cells as in **e**.

g) MoM traces of adapting and facilitating neurons during the upward frequency switch protocol using Neuropixels recordings.

h) Same as in **e**, but for Neuropixels recordings. paired t-test (top) and Wilcoxon test (bottom, non-normal distribution). Same cells as in **g**.

Figure 14: Responses of L2/3 neurons to a downward frequency switch, and control analyses to determine which neurons dynamically change their SA profile to an upward frequency switch.

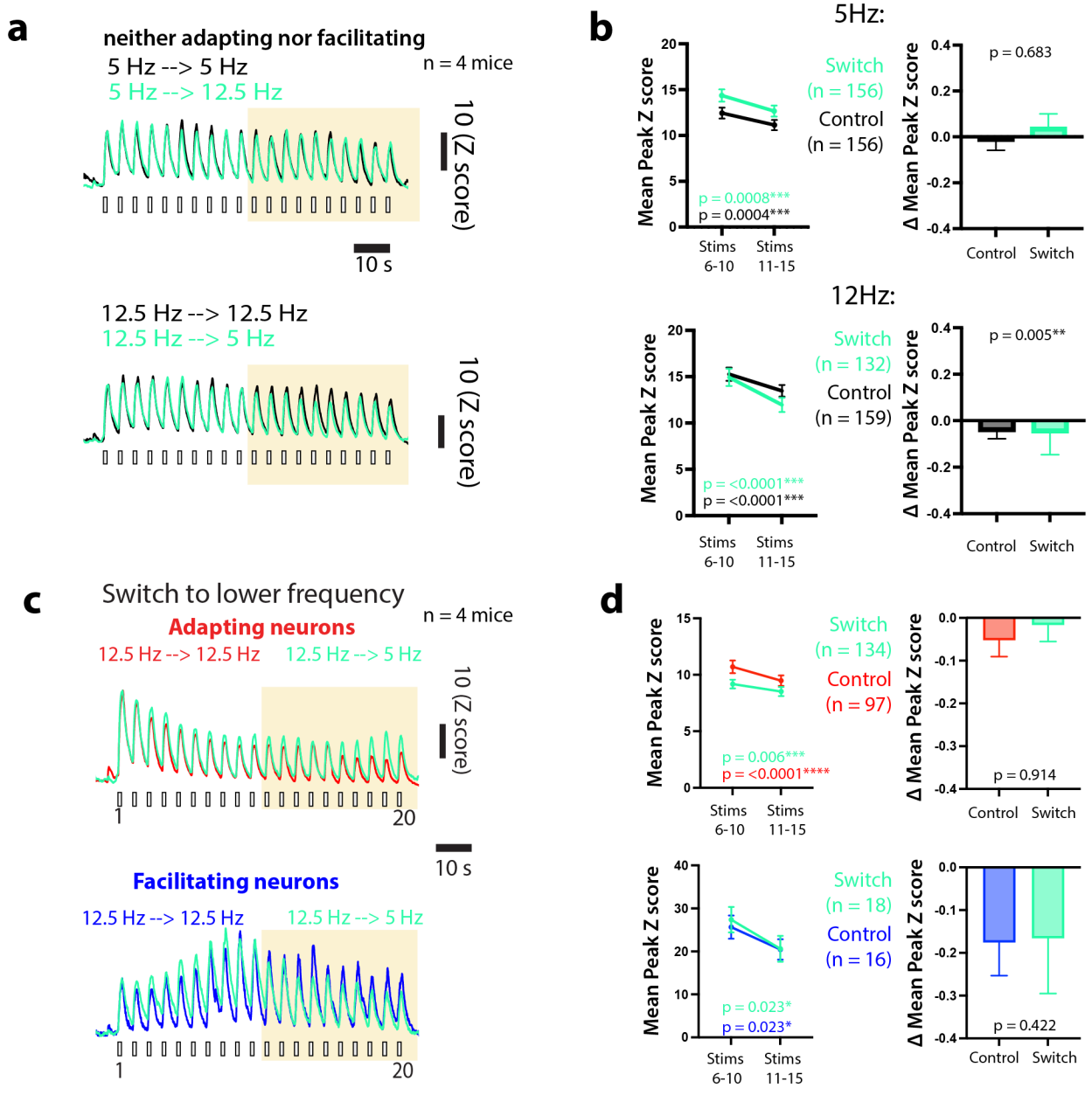

Figure 14: Responses of L2/3 neurons to a downward frequency switch, and control analyses to determine which neurons dynamically change their SA profile to an upward frequency switch.

a) MoM traces of all neurons (n = 4 mice) classified as nonsignificant during upward frequency switch and 5 Hz control whisker stimulation protocols.

b) Same quantification as in Fig. 13e-f, but for nonsignificant neurons. Top, upward frequency switch and 5 Hz whisker stimulation protocols. Bottom, downward frequency switch and 12.5 Hz whisker stimulation protocols. Same cells as in **a**.

c) MoM traces of adapting and facilitating neurons during downward frequency switch and 12.5 Hz control whisker stimulation protocols.

d) Same quantification as in Fig. 13e-f, but in the downward frequency switch and 12.5 Hz control whisker stimulation protocols. No significant differences between control and frequency switch were found for any comparison.

During these experiments, the SA profile of L2/3 neurons (adapting, facilitating etc.) was remarkably dynamic. Most neurons that adapted or facilitated during the control paradigm did not maintain the same response profile during the switch paradigm (**Fig. 15a**). Thus, neurons categorized as adapting in the control paradigm and those categorized as adapting in the frequency-switch paradigm were not necessarily the same neurons. To account for this, we also plotted MoM traces with the same subset of neurons for both the control and switch paradigm, such that the MoM traces were comprised only of cells that adapted or facilitated during the control protocol

(**Fig. 15b**). When plotting the MoM traces using only those cells and quantifying these results, we did not observe an increase in the response peak amplitude for initially adapting cells after the upward frequency switch (**Fig. 15c**). These data suggest that the sensitivity of SR neurons to an upward frequency switch (as observed in **Fig. 13c-f**) depends on how those SR neurons respond during the initial stimulations of the current paradigm.

Figure 15: Instability of response profiles of neurons after control stimulation protocols.

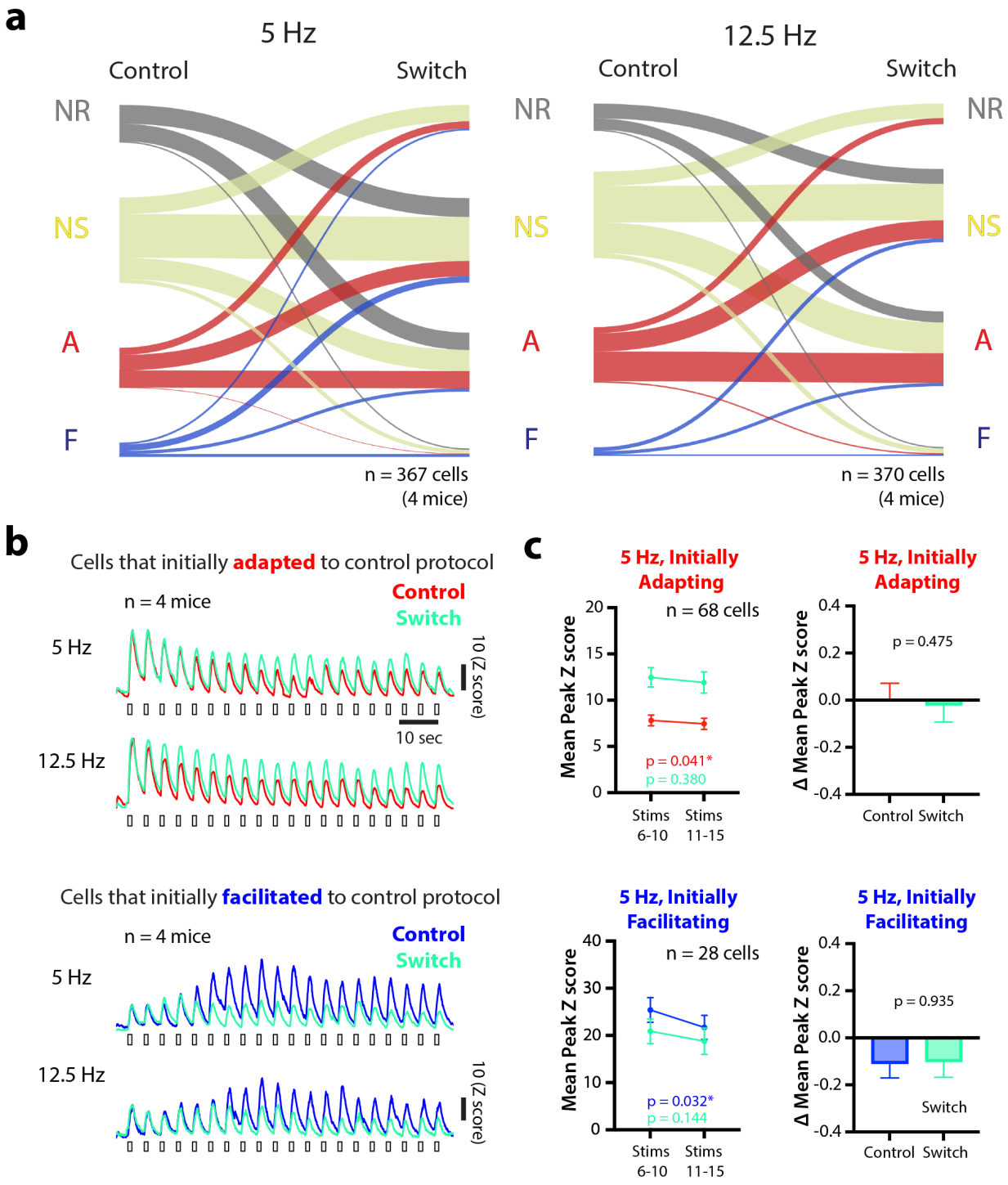

Figure 15. Instability of response profiles of neurons after control stimulation protocols.

a) Sankey diagrams showing transitions in the SA response profiles of the same neurons between control and frequency switch whisker stimulation protocols.

b) MoM traces of SR neurons that were categorized as adapting or facilitating during control and switch protocols. Control and switch traces are scaled to the first whisker stimulation.

c) Same quantification as in Fig. 13e-f but using neurons that are categorized as adapting or facilitating during the 5 Hz control protocol. Top: neurons that adapted during the 5 Hz control protocol, during upward frequency switch and control. Wilcoxon test. Bottom: neurons that facilitated during the 5 Hz control protocol, during upward frequency switch and control (left, Wilcoxon test; right, paired t-test).

METHODS

Experimental animals

As in Chapter 1, we crossed Slc17a7-Cre mice (JAX strain # 023527) to the Ai162 (GCaMP6s) reporter line (JAX strain # 031562) resulting in Cre-dependent expression of GCaMP6s in Vglut1-positive excitatory neurons. All mice were housed in a vivarium with a reverse 12/12 h light/dark cycle and experiments were performed during the dark cycle. Animals were weaned from their dam at postnatal (P) day 21-22 and then group housed with up to five mice per cage.

Cranial window surgery

Cranial windows were implanted as described in Chapter 1.

Intrinsic signal imaging

Intrinsic signal imaging was performed as described in Chapter 1.

2-photon calcium imaging

2PCI was performed in awake mice as described in Chapter 1, but with modifications to the whisker stimulation protocols delivered.

We recorded both spontaneous activity and whisker-evoked activity in S1BF. For L2/3 recordings in Slc17a7-Cre;Ai162 mice, we recorded responses of ~150-200 neuronal somata at 200-280 μm depth above the C2 barrel within a single field of view (FOV) per animal (measuring 512 x 512 pixels, 533.7 x 533.7 μm).

In our first cohort of Slc17a7-Cre;Ai162 mice (n= 8) (**Figs. 5-11**), we first recorded 3 min of spontaneous activity, and then we delivered 2 different whisker stimulation paradigms, in separate movies (with 4-5 min breaks in between each movie), as follows:

- 20 x 5 Hz: stimulus duration 1 s, i.s.i. 3 s
- 20 x 12.5 Hz: stimulus duration 1 s, i.s.i. 3 s

A 20 s baseline period was included in each whisker stimulation movie before initiating whisker deflections. Mice were given 4–5 min breaks between each stimulation paradigm.

In a second cohort of Slc17a7-Cre;Ai162 mice (n = 4) (**Figs. 13-15**), we performed frequency switch experiments, first recording 3 min of spontaneous activity followed by the following whisker stimulation paradigms in separate movies:

- 20 x 5 Hz: stimulus duration 1 s, i.s.i. 3 s (Control)
- 20 x 12.5 Hz: stimulus duration 1 s, i.s.i. 3 s (Control)
- 10 x 5 Hz → 10 x 12.5 Hz (Frequency switch)
- 10 x 12.5 Hz → 10 x 5 Hz (Frequency switch)

These 4 mice were also a part of the cohort of 5 mice from Chapter 1 (**Figs. 2 & 4**).

Neuropixels recordings

Adult mice (P60-90) were anesthetized with isoflurane (5% induction, 1.5-2% maintenance via a nose cone) and placed in a stereotaxic frame. Following skin sterilization with three alternating swabs of 70% ethanol and betadine, an incision was made on the scalp and a titanium horseshoe-shaped headbar was glued to the skull with Metabond adhesive cement. Next, a 2 mm diameter craniotomy was drilled above the cerebellum, just in front of the headbar, and a ground screw was inserted and secured with Metabond. A 1 mm diameter craniotomy was drilled over S1BF (coordinates for now: -1.46 AP, 2.9 ML), through which the shank of a Neuropixels probe (Imec) was carefully inserted at a speed of 10 μm/s using a motorized stereotax (Neurostar). Dental cement was used to secure the probe base to the skull and a protective 3D-printed case was used to encase the probe. Carprofen (5 mg/kg, s.c.) was administered every 24 h for 3 d.

Electrophysiology recordings were performed using a National Instruments PXIe acquisition system and SpikeGLX software (Juavinett et al., 2019; Jun et al., 2017). Probe connectors were attached to a headstage and cable connected to the PXIe system while the mouse was being

habituated to the rig. For Neuropixels recordings, head-fixed mice were allowed to run on a polystyrene ball treadmill. During behavioral habituation, we recorded daily for 10 min to evaluate the stability of spikes (to ensure that firing rates and amplitude were stable across days). Mice showing a loss of >30% units were excluded from further electrophysiological recordings and analysis.

Analysis

Motion correction and segmentation of 2PCI data: Motion correction and segmentation were performed as in Chapter 1.

Spike sorting of Neuropixels data: Action potential spikes were sorted with Kilosort2.5 using default parameters and then manually curated with Phy2. Post-processing with the following quality metrics was used to isolate single units: interspike interval violation <10%, amplitude cutoff and median amplitude >50 μV (Hill et al., 2011).

Stimulus responsiveness: For 2PCI data, stimulus responsive neurons were identified as in Chapter 1.

For Neuropixels recordings, we used a receiver operating characteristic (ROC) approach as has been done previously (Mazuski & O'Keefe, 2022). Firing rates were calculated in 50 ms time bins for each unit, and we calculated the ROC curve for each unit by comparing its firing rate during

each whisker stimulation bout (1 sec) to the firing one second before the stimulation during the interstimulus interval. We determined that a neuron was stimulus responsive if the area under the curve (AUC) exceeded 0.5 and was greater than 97.5% in a null distribution of AUCs. The null distribution of AUCs was generated by shuffling the firing rates and recalculating the AUC over 1000 permutations.

Response reliability: Response reliability was quantified as in Chapter 1.

Adaptation index: To quantify adaptation/facilitation in each SR neuron, an adaptation index (AI) was computed by regressing the response peak magnitude during stimulations 1-15 against stimulation number (i.e., fitting a line to the response peaks for stimulations 1-15 for each cell). Cells with significant negative regression slopes (i.e. a negative slope with a regression p-value of < 0.1) were classified as adapting, while cells with significant positive regression slopes were classified as facilitating. Cells were classified as nonsignificant if their regression slopes were not significant ($p \geq 0.1$). We chose 15 stimulations because in some mice there was motion artifact around stimulations 18-20. In rare cases of motion artifact before stimulation 15, response peak magnitudes during the motion artifact period were extrapolated by calculating the mean of the two response peaks directly before and after the motion artifact period.

We also tested an alternative method of quantifying adaptation, similar to what we had used in a previous publication (He et al., 2017). We calculated the mean response peak magnitude for stimulations 1-5 (Mean, stims 1-5) and for stimulations 10-15 (Mean, stims 11-15), and computed

an AI using the following formula: [(Mean, stims 1-5) – (Mean, stims 11-15)] / [(Mean, stims 1-5) + (Mean, stims 11-15)]. Cutoffs of ±0.4 were set based on the distribution of values (**Fig. 9).**

CHAPTER 3: Instability and drift in SA profiles of S1BF populations across multiple timescales

Our results from Chapter 2 indicate a remarkable diversity in the response profiles of L2/3 neurons—ranging from strongly adapting to strongly facilitating— when mice are exposed to repetitive whisker stimulation. Furthermore, abrupt upward switches in stimulus frequency prompt adapting neurons to transiently facilitate, demonstrating a flexibility in response dynamics that depends on stimulus parameters as well as the current response profile of the neuron (adapting/facilitating). The results from our frequency switch experiments also suggest a marked stochasticity in the SA profile of individual L2/3 neurons, as many neurons that adapted or facilitated during the control stimulation protocol changed their profile during the switch protocol (**Fig. 15a**).

The diversity in response profiles, coupled with their flexibility after frequency switches and their stochasticity between movies led us to wonder how stable the response profiles of individual neurons are across time. In sensory cortex, neurons have been shown to exhibit drift in their response dynamics over time despite behavior remaining stable (Alisha et al., 2023; Deitch et al., 2021; Rule et al., 2019; Schoonover et al., 2021). While studies have begun investigating drift in various aspects of response dynamics in S1BF, (Alisha et al., 2023; Wang et al., 2022), whether population drift applies to SA is not known.

In this chapter, we assess the stability of SA profiles of L2/3 neurons across a single imaging session (i.e., tens of minutes) and longitudinally over 8-9 days. We then extend our longitudinal investigations to L4 to examine whether similar dynamics are observed upstream of L2/3.

RESULTS

The SA profile of individual L2/3 neurons is highly dynamic across tens of minutes, but the population maintains a stable proportion of SR neurons.

Given the heterogenous response profiles of individual neurons within L2/3 of S1BF, and the fact that their SA profile was highly dynamic during the frequency switch experiments, we next asked how stable the population is across a time scale of tens of minutes. We repeated our 5 Hz stimulation protocol (20 bouts of whisker stimulation) six times (rounds R1-R6) every 4-5 min, while longitudinally recording the same L2/3 neurons with 2PCI in 6 mice (**Fig. 16a-b**). While the proportion of neurons responding to whisker stimulation on any given round remained stable on average (**Fig. 16c**, left), the specific neurons that responded to whisker stimulation varied extensively from one round to the next. Across successive rounds of stimulation (within a single imaging session), the cumulative percentage of SR neurons increased significantly (**Fig. 16c**, right). This highlights how individual neurons are stochastic in their responsiveness to whisker stimulation and yet, on average, at the population level, a stable proportion of L2/3 neurons (~20%) is available to respond to whisker stimulation. As one might predict, with ongoing rounds of whisker stimulation, the population became slightly more adapting (**Fig. 16d**) because of a slight decrease in the proportion of facilitating neurons (**Fig. 16e, right**), though these trends were not significant.

L2/3 neurons were seemingly stochastic in their SA profiles to whisker stimulation across different rounds of whisker stimulation, showing clear adaptation or facilitation for one round of whisker stimulation, and changing that identity the next, and sometimes becoming whisker non-responsive (**Fig. 16f-g, Fig. 17a**). Despite this, the overall range of adapting and facilitating response profiles (ordered according to AI values) remained unchanged from R1 to R5 (roughly 40 min apart), albeit in a largely different subset of SR neurons (**Fig. 16g**). Although many SR neurons exhibited highly capricious SA profiles, few cells drastically switched their identity from adapting to facilitating (or vice versa). Instead, many exhibited mild changes in response profile (**Fig. 17b**) (e.g., nonsignificant → adapting/facilitating or vice versa). The change in SA profile from one round of stimulation to the next was not entirely stochastic, as neurons in any category (adapting or facilitating) tended to remain in that category (**Fig. 16g**). Indeed, the correlation between adaptation index values of the same SR neurons on R1 and R3 was higher than on R1 and R5 (**Fig. 16h**) This gradual shift in SA profiles is consistent with population drift, rather than a completely stochastic process. Together, these results indicate that L2/3 maintains a stable proportion of SR neurons across tens of minutes, even though their responsivity and SA profile can change drastically. Although rare neurons will switch between facilitating and adapting response profiles, most do not, and over multiple rounds of whisker stimulation, the population trends slightly toward more adaptation.

Figure 16: The SA profile of individual L2/3 neurons is highly dynamic across different rounds of 20 whisker stimulations over tens of minutes.

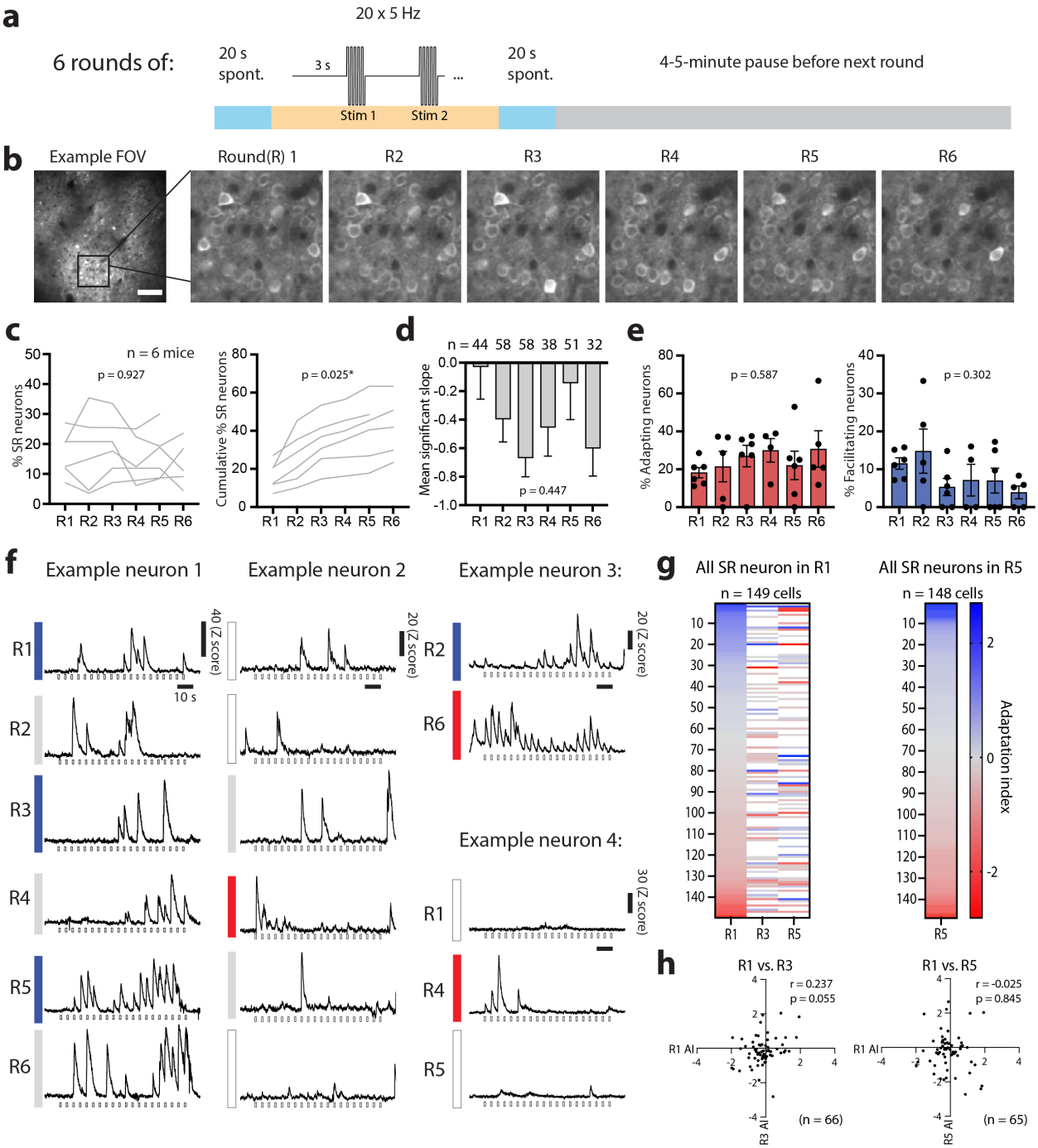

Figure 16. The SA profile of individual L2/3 neurons is highly dynamic across different rounds of 20 whisker stimulations over tens of minutes.

a) Schematic of repeated stimulation protocol within a single imaging session. Mice are exposed to 6 different rounds of the same whisker stimulation protocol (20 stimulation bouts), with a 4-5 min break between each round.

b) Example FOV (GCaMP6s expression in Slc171a-Cre;Ai162 mice) tracked across 6 rounds of whisker stimulation in a single imaging session.

c) Left, percent of L2/3 neurons responding to whisker stimulation on each round. Kruskal-Wallis test. Right, cumulative percent of neurons responding to whisker stimulation with each round of stimulation. Kruskal Wallis test. (n= 908 total neurons imaged across 6 mice).

d) Mean slope value of adaptation index for all neurons with a significant linear regression. Kruskal Wallis test (The number of SR neurons with significant AI slope is indicated for each round). Kruskal-Wallis test.

e) Percent of SR neurons that adapt (left) or facilitate (right) on each stimulation round. Kruskal Wallis test. Kruskal-Wallis test.

f) Traces of example neurons at different rounds of whisker stimulation. Note the stochasticity of responses (with respect to individual bouts of 5 Hz stimulation) and the dynamic changes in their SA profile between different rounds.

g) Left: heatmap of response profiles for all neurons that are SR in R1, sorted by adaptation index during R1. Top right: heatmap of response profiles for all neurons that are SR in R5, sorted by adaptation index during R5.

h) Left: XY plot of the AI values of SR neurons on R1 (x axis) and R3 (y axis). Spearman correlation coefficient and corresponding p-value are displayed. Right: Same, but for R1 (x axis) and R5 (y axis).

Figure 17: Stochasticity of L2/3 neurons during a single imaging session.

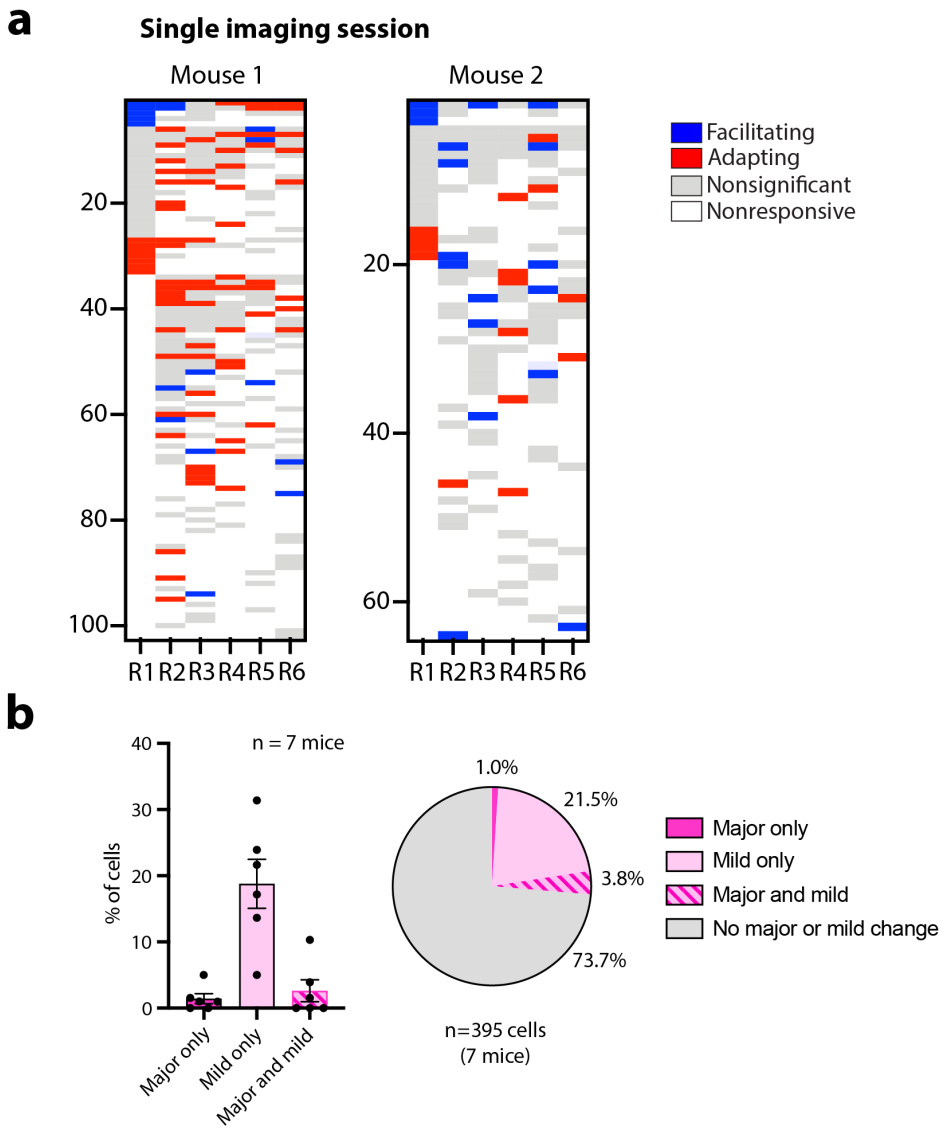

Figure 17. Stochasticity of L2/3 neurons during a single imaging session.

a) Heatmap of response profiles for SR cells in two example mice.

b) Left, percent of SR cells that underwent major or mild changes in response profile across stimulation rounds. Percentages are calculated out of all cells that are at some point SR. Right, same but with cells pooled across all 8 mice.

Representational drift of adapting/facilitating neurons in L2/3 across several days.

Our results above indicate that the response dynamics of individual L2/3 neurons are labile over multiple repetitions across tens of minutes. Thus, the encoding of whisker stimulation exhibits remarkable population drift even within a single imaging session (<1 h). We next investigated whether SA dynamics might change due to sensory experience across days. We conducted 2PCI in the same FOVs in individual mice (n = 8) across 4 separate imaging sessions spanning 8-9 days (**Fig. 18a**), recording L2/3 excitatory neuron responses to the 20-stimulation control protocols at 5 Hz. We identified the same active L2/3 neurons shared between Day 1 and subsequent sessions using the probabilistic cell-tracking method *CellReg* (Sheintuch et al., 2017) (**Fig. 18b**).

We observed remarkably diverse responses of the same identified SR neurons to 20 whisker stimulation bouts across daily imaging sessions (**Fig. 18c**). Cells that responded to only a few bouts of whisker stimulation on one day could respond to most bouts on a different day, and vice versa, similar to what we had observed on different rounds of stimulation across tens of minutes. The

proportion of SR neurons remained stable across days (**Fig. 18d**). We then asked whether sensory experience across days affected SA at the population level. To gain a more nuanced understanding of the SA profile of the L2/3 population across days, we further divided adapting and facilitating neurons into weak and strong subcategories based on their slope value (see Methods). The proportion of SR neurons categorized as nonsignificant remained relatively stable across days (**Fig. 18e**). Unexpectedly, however, we observed a decrease in the proportion of strongly adapting neurons, coupled with an increase in weakly adapting and weakly facilitating neurons (**Fig. 5e**). This resulted in a significant increase in the mean significant AI slope for SR neurons across days from Day 1 to Day 8/9 (**Fig. 18f**). Thus, experiencing the same whisker stimulation protocol repeatedly across several days caused a progressive population-level shift toward a less adapting profile.

When focusing only on a subset of neurons that we successfully tracked longitudinally across multiple days (220/1269 cells that were tracked on Days 1 and 2; 120/917 cells tracked on Days 1 and 8/9), we confirmed that most of them did not maintain the same response profile, though most nonresponsive (86.0%) neurons remained so from Day 1 to Day 8/9 (**Fig. 18g**). When comparing Day 1 to Day 8/9, most tracked SR neurons exhibited a change in response profile, including 17.4 ± 8.0 % of neurons exhibiting a mild change in SA identity (e.g., NS→A, F→NS), and over 50% becoming nonresponsive (**Fig. 18h**, green). Importantly, no neurons exhibited a major change (A→F or F→A) from Day 1 to Day 8/9, and 27.4 ± 3.6% of SR cells maintained their SA identity after 1 week. Across all imaging days, major changes were rare, and ~10% of SR cells tracked on at least 2 days exhibited a mild change (**Fig. 19**).

Figure 18. Experience-dependent decrease in L2/3 population adaptation across days.

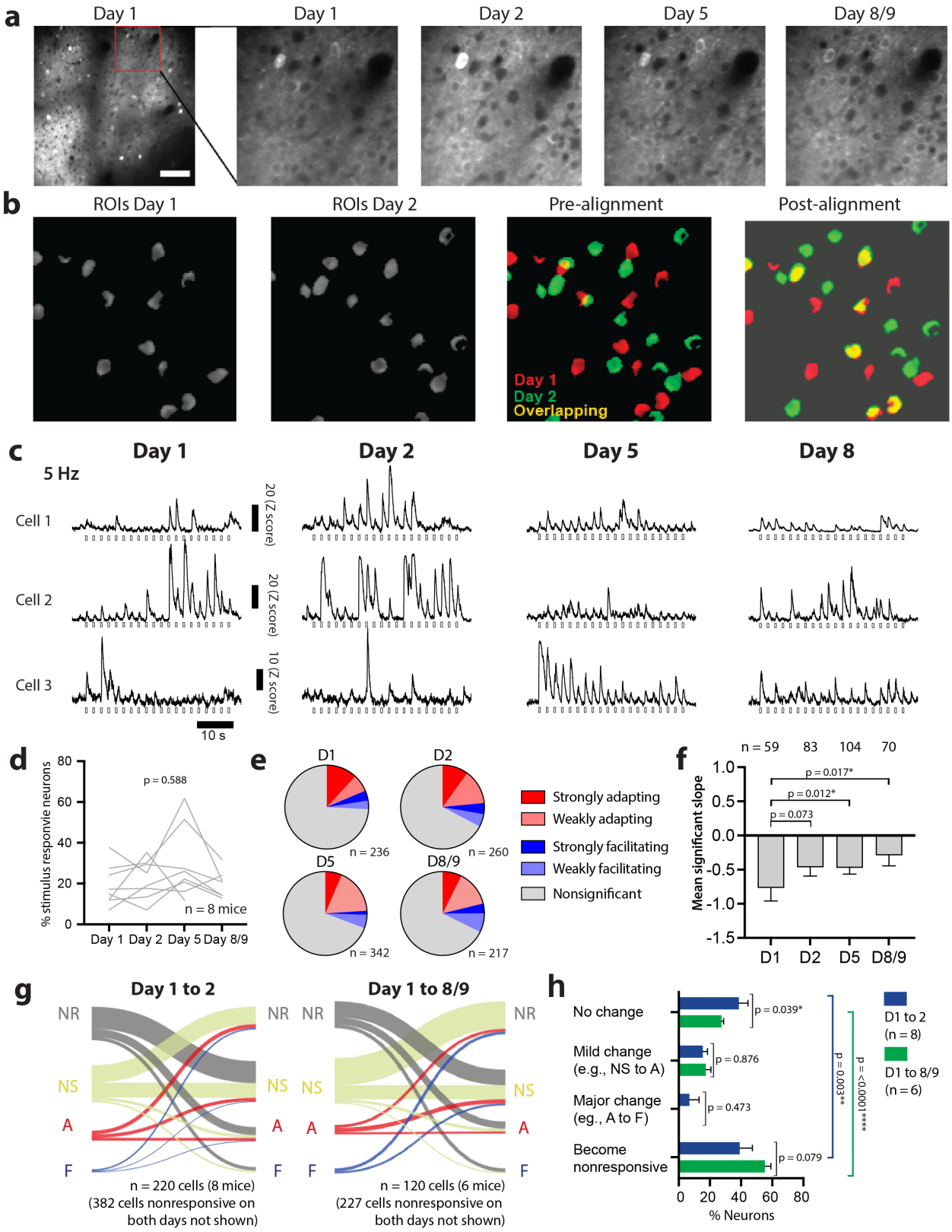

Figure 18. Experience-dependent decrease in L2/3 population adaptation across days.

a) We performed longitudinal 2PCI in the same FOV (left) in L2/3 across 8/9 days. Top left: example FOV from Slc171a-Cre;Ai162 mouse. Top right: enlarged view of a portion of the FOV (red box).

b) CellReg procedure to identify tracked cells across imaging days. Detected ROIs within the red box (top left) on days 1 and 2 of imaging. Using CellReg, masks of active neurons are then overlaid ("Pre-alignment") and aligned ("Post-alignment") to identify SR neurons that are present across multiple days of imaging.

c) Traces of 3 example neurons during 5 Hz whisker stimulation, tracked across all four 2PCI sessions.

d) Percentage of L2/3 neurons responsive to 5 Hz whisker stimulation across days (n = 8 mice). Kruskal-Wallis test.

e) Fraction of cells in each SA profile category across days.

f) Mean slope of SR neurons with a significant linear regression of the AI across days. Mann-Whitney test.

g) Sankey flow diagrams of neurons tracked across two imaging days show dynamic response profiles of neurons from Day 1 to Day 2 and Day 1 to Day 8/9. NR = nonresponsive, NS = nonsignificant, A = adapting, F = facilitating.

h) Percent of longitudinally tracked neurons exhibiting different types of SA response profiles across imaging sessions. Black brackets: Mann-Whitney test. Green and blue brackets: Friedman test with post-hoc Dunn's test.

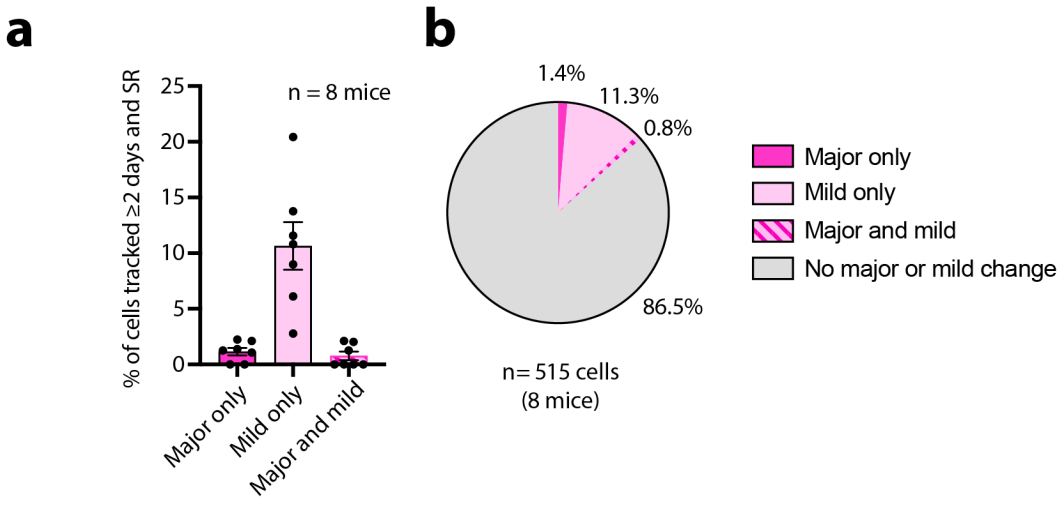

Figure 19: Major and mild changes in response profiles of L2/3 neurons across days.

a) Percent of cells that underwent major or mild changes in response profile across days. Percentage is calculated out of all cells that were tracked at least across two imaging days and responded to whisker stimulation at least once.

b) Same as **a**, but with cells pooled across all 8 mice.

L4 exhibits distinct but similar longitudinal population dynamics compared to L2/3.

The adaptation and facilitation profiles of L2/3 neurons could emerge from local computations in L2/3, or they could be inherited from upstream circuits, such as L4 or the thalamus. L4 is the primary recipient of thalamocortical inputs (Petersen, 2007, 2019) and could inherit a strong adapting response profile from the thalamus. Alternatively, as the superficial layers are the major recipients of projections from other cortical areas (Jones & Wise, 1977; Naskar et al., 2021), L4 could exhibit less adaptation because it is not subject to as much top-down influence as L2/3. To investigate the population dynamics of SA in L4, we repeated this longitudinal imaging protocol in Scnn1a-Cre;GCaMP6s$^{fl/fl}$ mice to characterize the response dynamics of L4 spiny stellate neurons over several days (**Fig. 20a**). Just as in L2/3, the overall response of the L4 population was slightly adapting in individual mice (**Fig. 21a**). L4 neurons tended to respond to fewer bouts of whisker stimulation (**Fig. 20b; Fig. 21b**) than to those in L2/3. The average proportion of SR neurons in L4 was even lower (**Fig. 20c**) than in L2/3, consistent with recent findings (Voelcker et al., 2022).

Longitudinal imaging across 8 days revealed that specific response subcategories of L4 neurons were different from those in L2/3. For example, the L4 population showed a decrease in the proportion of weakly adapting neurons and an increase in the proportion of strongly facilitating neurons (**Fig. 20d**), which we had not observed in L2/3. L4 neurons did show a slight increase in the mean significant slope of the adaptation index (**Fig. 20e**), similar to what we had observed in L2/3. Although this trend was not statistically significant in L4 (there was more variability and a smaller sample size), the overall effect of experience was similar across both layers. Moreover,

just as in L2/3, L4 neurons tracked across multiple days also exhibited substantial drift, changing their response profiles and often becoming nonresponsive (**Fig. 20f-g**). When assessing neurons tracked between Days 1 and 8, the proportion of neurons exhibiting a mild change in response profile was markedly larger compared to Days 1 and 2 (6.7 ± 9.9% between Days 1 and 2 vs. 35 ± 38.4% between Days 1 and 8) (**Fig. 20g**), while this proportion remained relatively stable in L2/3 (14.9 ± 8.6% between Days 1 and 2 vs. 17.4 ± 8.1% between Days 1 and 8/9). When looking across all imaging days and assessing all SR neurons tracked on at least 2 days, mild changes comprised a small fraction of cells (3.1%, **Fig. 21c**). Together, these results suggest that individual L4 neurons exhibit dynamic shifts in their response profiles, and that L4 manifests similar experience-dependent SA plasticity at the population level as L2/3.

Figure 20. SA response dynamics to repetitive whisker stimulation across days in L4 resemble those in L2/3.

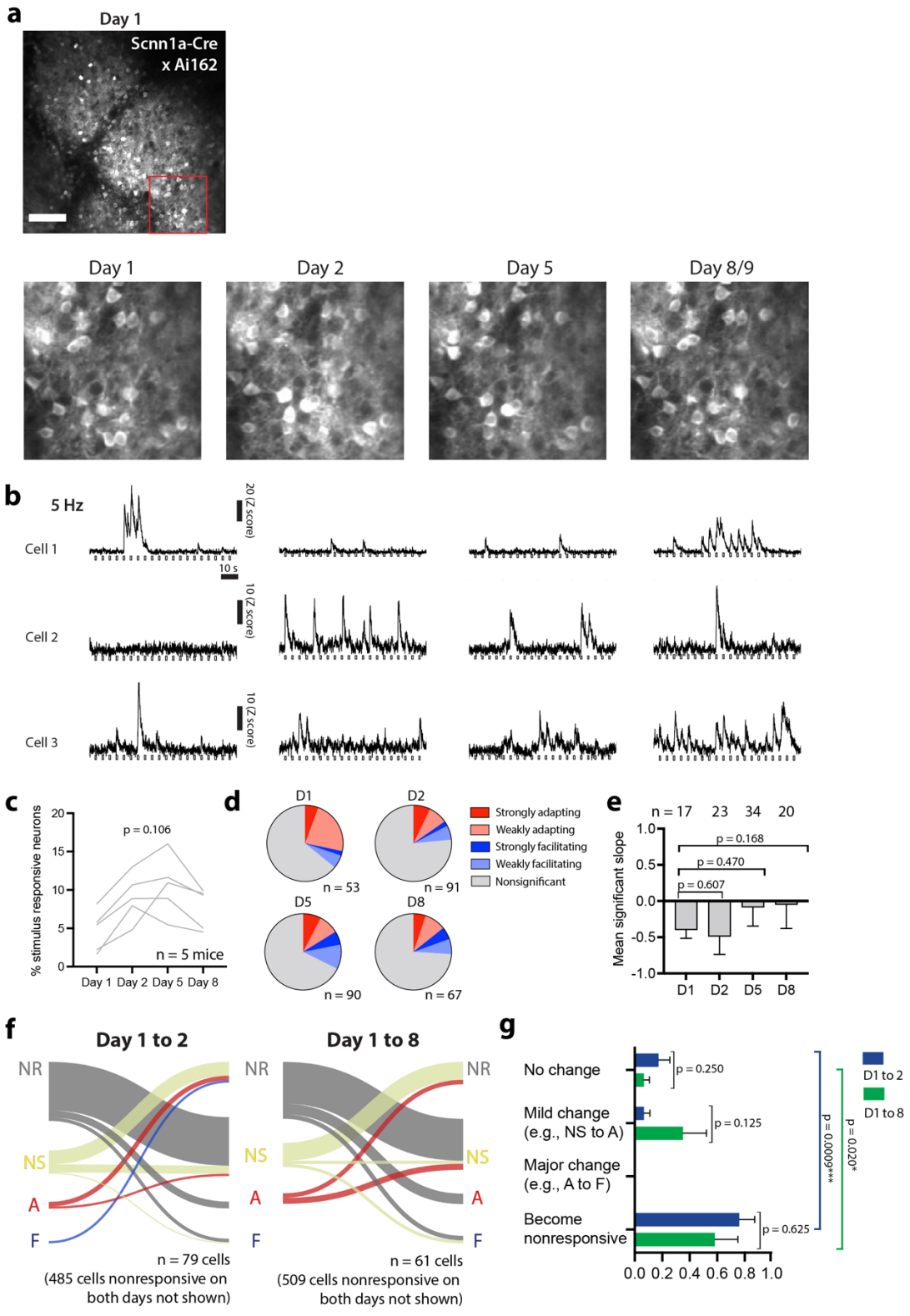

Figure 20. SA response dynamics to repetitive whisker stimulation across days in L4 resemble those in L2/3.

a) Example 2PCI FOV in L4 across days in Scnn1a-Cre;Ai162 mouse. Top, example FOV on Day 1. Bottom, higher magnification view of a portion of the FOV (red box) across days.

b) Traces of 3 example neurons during 5 Hz whisker stimulation, tracked across all four imaging sessions.

c) Percentage of L4 neurons responsive to 5 Hz whisker stimulation across days (n = 5 mice). Kruskal-Wallis test.

d) Fraction of cells in each response profile category.

e) Mean slope of SR neurons with a significant linear regression of the adaptation index across days. Mann-Whitney test.

f) Sankey flow diagrams showing the SA response profiles of L4 neurons across sessions NR = nonresponsive, NS = nonsignificant, A = adapting, F = facilitating.

g) Percent of longitudinally tracked neurons exhibiting certain types of response profile changes between D1 and D2 or D1 and D8 (n = 5 mice). Black brackets: Wilcoxon test. Green and blue brackets: Friedman test with post-hoc Dunn's test.

Figure 21. Response dynamics of L4 during 5 Hz whisker stimulation.

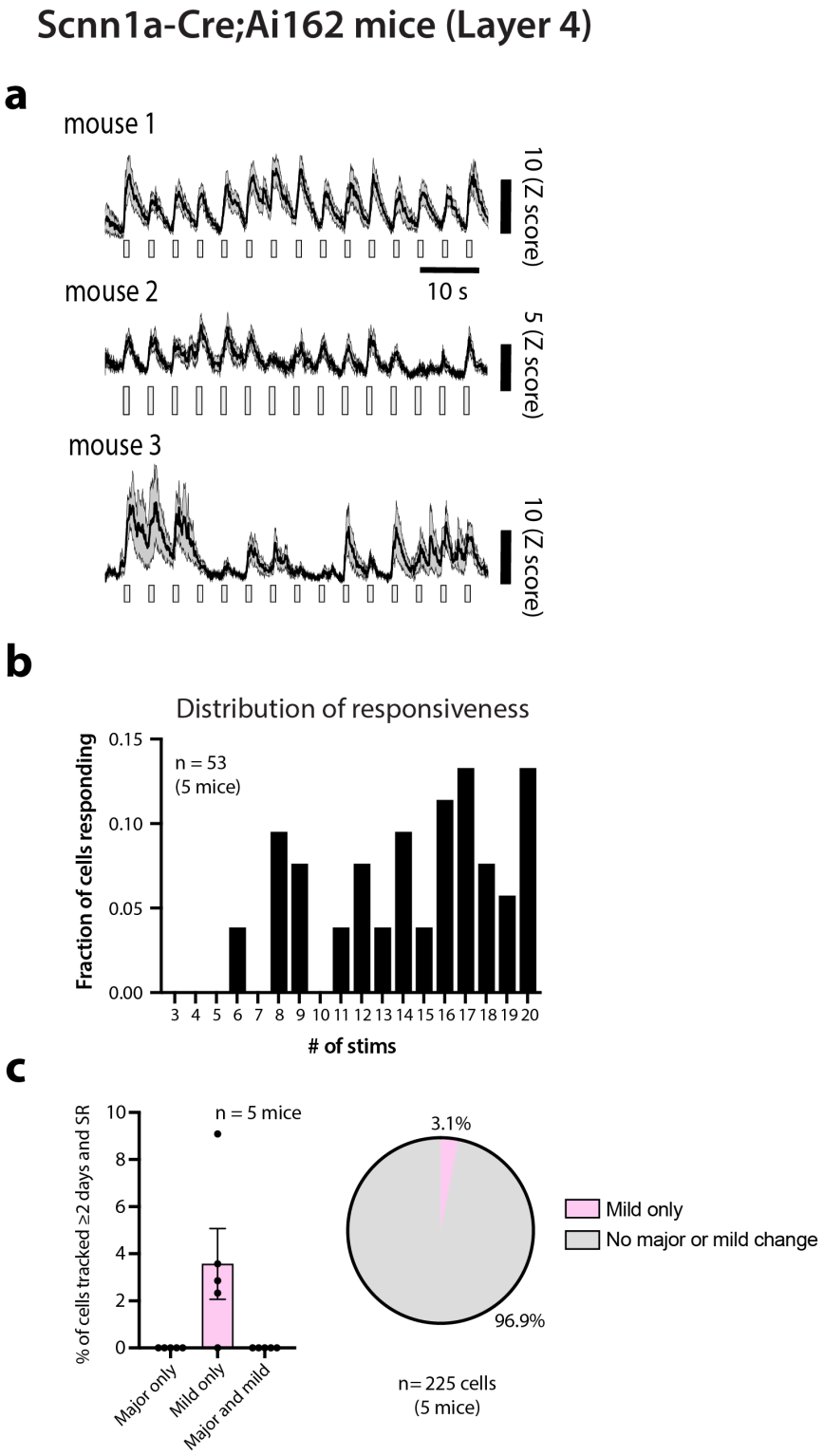

Figure 21. Response dynamics of L4 during 5 Hz whisker stimulation.

a) Mean traces during whisker stimulation of all SR L4 neurons in L4 from 3 example mice on Day 1.

b) Distribution of responsiveness in L4 neurons across mice during stimulation on Day 1.

c) Left, percent of L4 neurons that underwent major or mild changes in response profile across days. Percentage is calculated out of all cells that were tracked at least across two imaging days and responded to whisker stimulation at least once.

METHODS

Experimental animals

As in previous chapters, we used Slc17a7-Cre;Ai162 mice for L2/3 recordings. For L4 recordings, we crossed Scnn1a-Cre mice (JAX strain # 009613) to the Ai162 (GCaMP6s) reporter line (JAX strain # 031562) resulting in Cre-dependent expression of GCaMP6s in L4 spiny stellate neurons.

Cranial window surgery

Cranial windows were implanted as described in Chapter 1.

Intrinsic signal imaging

Intrinsic signal imaging was performed as described in Chapter 1.

2-photon calcium imaging

Habituation and 2-photon microscope details (wavelength, objective used, etc.) were the same as in Chapter 1. For L2/3 recordings, we recorded responses of ~150-200 neuronal somata at 200-280 μm depth within the C2 barrel. For L4 recordings in Scnn1a-Cre;Ai162 mice, we recorded responses of ~300 neuronal somata at 350-400 μm depth within the C2 barrel. FOV size was the same as in L2/3 recordings in previous chapters.

In this chapter, a first cohort of Slc17a7-Cre;Ai162 mice (n= 7) underwent 6 rounds of the 20 x 5 Hz stimulation protocol in a single imaging session, with 4-5 min breaks between rounds (**Figs. 16-17**). 3 of the mice from this cohort were from the first cohort in Chapter 2. As in previous chapters, 3 min of spontaneous activity was recorded before beginning the first round of whisker stimulation.

In this chapter, the first cohort of Slc17a7-Cre;Ai162 mice (n= 8) from Chapter 2 was then imaged over several days and comprised this chapter's second cohort of mice, depicted in **Figs. 18-19**. The

FOV was first identified during the first awake imaging day (Day 1), and then subsequently imaged at +1 d (Day 2), +4 d (Day 5), and +7-8 d (Day 8-9) after the first awake imaging session. On each Imaging Day, we recorded the same movies as in Chapter 2 (**Figs. 5-11**), which were the following:

- 3 min of spontaneous activity
- 20 x 5 Hz: stimulus duration 1 s, i.s.i. 3 s
- 20 x 12.5 Hz: stimulus duration 1 s, i.s.i. 3 s

In a final cohort of Scnn1a-Cre;Ai162 mice (n= 5), we performed the same longitudinal imaging over 8 days but in L4 (**Figs. 20-21**).

Analysis

Motion correction and segmentation of 2PCI data: For L2/3 and L4 movies, motion correction was performed as described in Chapter 1. Segmentation of L2/3 movies was performed as described in Chapter 1.

We segmented L4 movies in Suite2P using default settings. Automated ROI exclusion was performed using a custom classifier built using previous L4 data, followed by a manual refinement step to include or exclude ROIs that had been missed by the classifier.

Stimulus responsiveness: Same as in Chapter 1.

Response reliability: Same as in Chapter 1.

Adaptation index: Adaptation was quantified using the same linear regression approach described in Chapter 2. For **Figs. 18** and **20**, adapting and facilitating cells were divided into strong and weak subcategories. Cells with a slope > 1 were classified as strongly facilitating, while cells with a slope less than -1 were classified as strongly adapting. Cells with a significant slope of ≤ 1 or ≥ -1 were classified as weakly facilitating and weakly adapting, respectively.

Longitudinal imaging analysis: To identify the same ROIs across days in our longitudinal imaging experiments, we employed CellReg (v1.4.9, (Sheintuch et al., 2017)), a probabilistic method for tracking neurons longitudinally in calcium movies. We then calculated the proportion of longitudinally tracked ROIs that maintained or changed their response profile (adapting, facilitating, intermediate, non-responsive) between pairs of imaging sessions (e.g., Day 1 vs. Day 2, Day 1 vs. Day 5, Day 1 vs. Day 8/9). We also assessed the number of ROIs that became non-responsive on the second day in the pair of imaging sessions. **For Fig. 19** and **Fig. 21c**, we tracked the same ROIs across all imaging days (either 3 or 4) and calculated the percentage of cells that exhibited major or mild changes in response profile.

CHAPTER 4: SST interneurons may modulate sensory adaptation at the population level in S1BF

What are the mechanisms responsible for SA at the population level and across multiple days? At the level of individual neurons, both somatic currents and short-term depression of thalamocortical synapses (Chung et al., 2002; Whitmire & Stanley, 2016) have been implicated in adaptation over fast time scales (tens to hundreds of milliseconds). However, GABAergic inhibition could play a role at the longer time scales we recorded (tens of seconds), by gradually reducing the firing of excitatory neurons over time.

Inhibitory interneurons comprise less than a quarter of neurons in rodent S1 (Meyer et al., 2011), but they are densely interconnected with local excitatory neurons (Fino & Yuste, 2011; Packer & Yuste, 2011) and modulate their firing (Moore et al., 2010; Tremblay et al., 2016). Interneurons are comprised of three major subclasses with unique functional and anatomical properties: Somatostatin (SST), parvalbumin (PV) and vasoactive intestinal peptide (VIP) interneurons. SST interneurons, which target the apical dendrites of layer (L) 2/3 excitatory neurons (Naka et al., 2019), are of interest in SA because they exhibit an increase in spiking probability with repetitive stimulation and are sensitive to the firing rate of individual excitatory neurons (Adesnik et al., 2012; Tremblay et al., 2016). In an auditory oddball paradigm, optogenetic suppression of SST interneuron firing leads to an increase in excitatory neuron responses to frequent (redundant) auditory stimuli (Natan et al., 2015), suggesting they specifically inhibit responses to redundant or familiar stimuli. In the visual system, they are necessary for the amplified response of excitatory neurons to deviant stimuli (Hamm & Yuste, 2016).

The diversity in subtypes of interneurons also allows for them to sculpt unique aspects of SA within the circuit. For example, in the auditory system, PV neurons modulate excitatory firing in the same

way before and after adaptation, while SST neurons more strongly inhibit neurons that have strongly adapted (Natan et al., 2017). SST interneurons also form a component of a well characterized disinhibtory circuit in the canonical microcircuit; VIP interneurons, whose dendrites extend into L1, receive top-down inputs from higher-order regions to inhibit SST neurons and in turn disinhibit pyramidal neurons (Fu et al., 2015; S. Lee et al., 2013; Pi et al., 2013). Furthermore, during a single recording session, repetitive whisker stimulation elicits stronger adaptation in inhibitory inputs than excitatory inputs, leading to a net excitatory effect in the network (Heiss et al., 2008). Whether such a phenomenon exists at the time scale of several days remains unclear but worth exploring. Adjustments in the dynamics of inhibitory interneuron subpopulations could also explain the net facilitatory effect we observed with longitudinal imaging over > 1 week.

The ability to recalibrate network activity based on local excitatory dynamics make inhibitory interneurons an ideal candidate for modulating SA. The unique role SST interneurons appear to play in distinguishing between familiar and rare stimuli (Natan et al., 2015), along with their function within the VIP-mediated disinhibitory circuit in S1BF, make them an intriguing potential player in SA of excitatory S1BF neurons. To identify the contributions of SST neurons to SA in S1BF, we employed an all-optical approach by performing calcium imaging in superficial layers of S1BF while simultaneously optogenetically stimulating local SST interneurons.

RESULTS

Characterization of optogenetic stimulation on SA in superficial layers of S1BF

To investigate whether SST interneurons modulate the SA profiles of S1BF neurons, we injected a Flp-dependent red-shifted excitatory opsin virus (AAV-nEF-Coff/Fon-ChRmine-oScarlet), along with one GCaMP6s virus for all neurons (AAV.Syn.GCaMP6s.WPRE.SV40) and one Flp-dependent GCaMP6s virus for SST interneurons (AAV-Ef1a-fDIO-GCaMP6s) into the superficial layer of S1BF in SST-Flp mice (see Methods). Expression of ChRmine (the opsin) was relatively dim and punctate (**Fig. 22**).

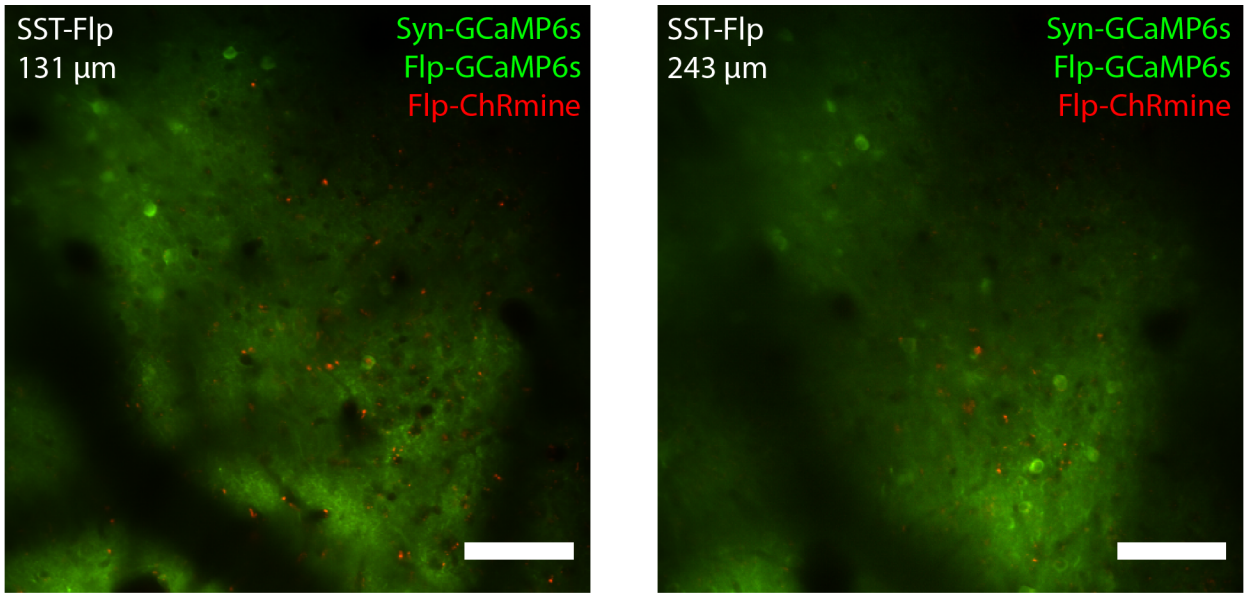

Figure 22. FOVs above the C2 barrel of S1BF exhibiting viral GCaMP6s and ChRmine expression. Left, FOV at approximately 131 µm depth. Right, FOV at approximately 243 µm depth. XY position is the same across both FOVs. Scale bars = 100 µm.

We performed 2PCI over the C2 barrel as in previous chapters, and recorded movies at 4 different depths from L1 ~(95 µm) to L3 (~245 µm). At each depth, we recorded movies during optogenetic stimulation, whisker stimulation, and during paired optogenetic and whisker stimulation (**Fig. 23a**;

see Methods). Optogenetically evoked responses could be observed in the "Opto only" condition: (**Fig. 23b-c**).

Figure 23: Stimulation protocols used and example responses to optogenetic stimulation.

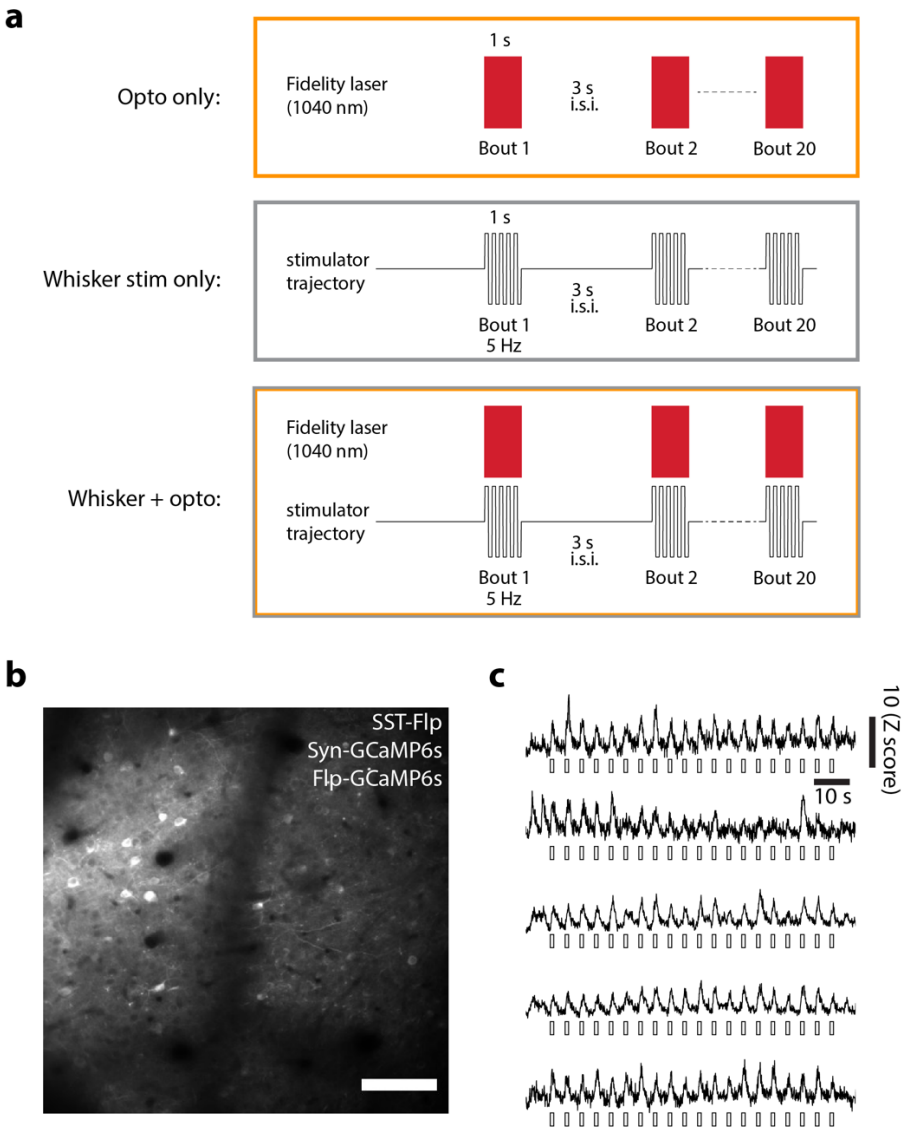

Figure 23. Stimulation protocols used and example responses to optogenetic stimulation.

a) Schematic depicting each stimulation paradigm. Recordings were always performed in this order (with ~2-4 min breaks between protocols)

b) GCaMP6s expression in example FOV at approximately 133 µm depth. Scale bar = 100 µm.

c) Optogenetically evoked responses from individual neurons from FOV in **b**.

A small proportion of cells responded to optogenetic stimulation across depths, and this proportion was smallest at the least superficial depth (**Fig. 24**, orange bars). This low percentage aligns with the relatively low abundance of interneurons compared to excitatory neurons in S1BF (Meyer et al., 2011) Interestingly, despite the particularly small percentage of neurons responsive to optogenetic stimulation at ~245 µm, this was the only depth at which we observed a reduction in responding neurons during whisker stimulation with simultaneous optogenetic stimulation vs. whisker stimulation alone (**Fig. 24**, "237-245 µm"). At all other depths, the fraction of SR neurons remained stable across both whisker stimulation conditions.

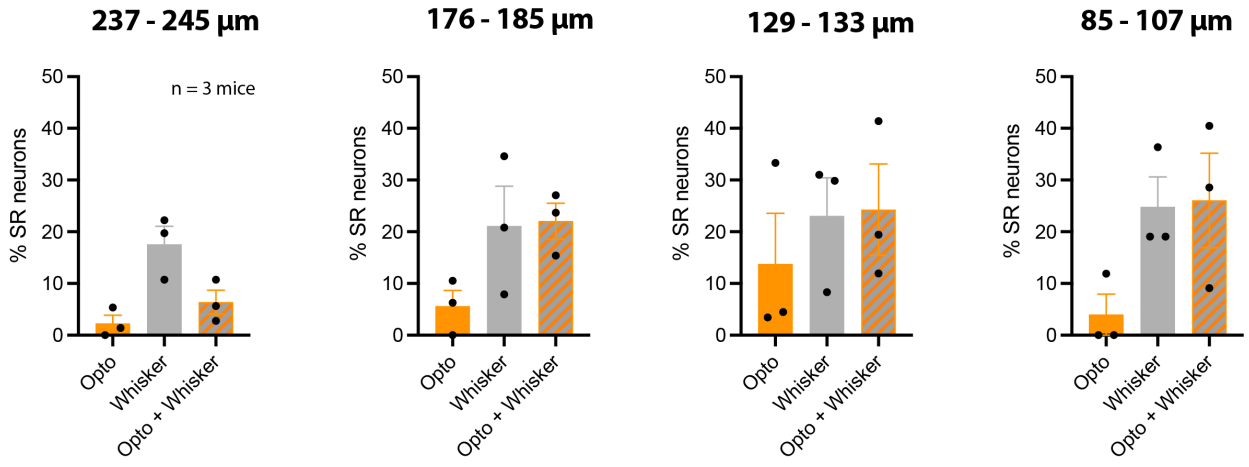

Figure 24. Percentage of neurons responding to different stimulation protocols at different cortical depths.

It is important to note that all forms of SR neurons are included in **Figure 24**; this means that some neurons responding during the Opto + Whisker condition may only be responding to optogenetic activation and not whisker stimulation (i.e., they are not whisker-responsive neurons). Since our aim is to assess the impact of SST activation on the response dynamics of whisker responsive neurons, we excluded any neurons that responded only during the Opto-only protocol from all subsequent analyses in the Whisker and Whisker + Opto conditions (we speculate that those are SST interneurons and refer to them as putative SST cells).

Once these neurons were excluded, we replotted the percentage of SR neurons, and the trends from **Figure 24** remained intact (**Fig. 25**).

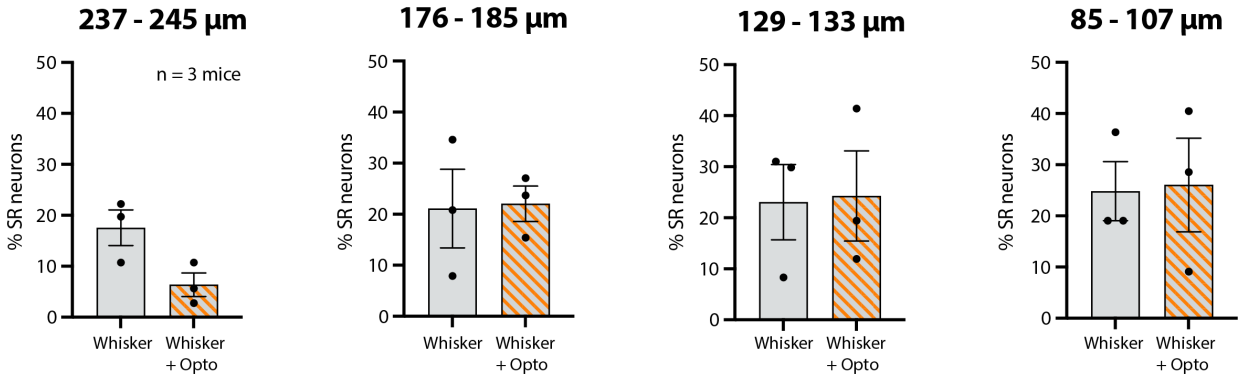

Figure 25. Percentage of SR neurons after exclusion of neurons driven by optogenetic stimulation.

Activation of SST interneurons may increase adaptation and reduce facilitation in superficial layers of S1BF

We then investigated the impact of SST activation on the SA response profiles of SR neurons. Broadly, the mean slope of SR neurons became more negative with optogenetic activation of SSTs, though the ~130 μm depth did not show this trend (**Fig. 26a**). The mean percent of SR neurons adapting to 5 Hz whisker stimulation increased substantially across all recorded depths when whisker stimulation was paired with optogenetic activation of SST neurons (**Fig. 26b**). The fraction of SR neurons facilitating to whisker stimulation was also reduced (**Fig. 26c**), suggesting that activation of SST neurons skews the population away from facilitation and toward a more adapting profile. However, given the small number of mice (n = 3), these findings are preliminary, and future studies will be necessary to definitively characterize the role of SST interneurons (and other interneuron subtypes) in SA in S1BF.

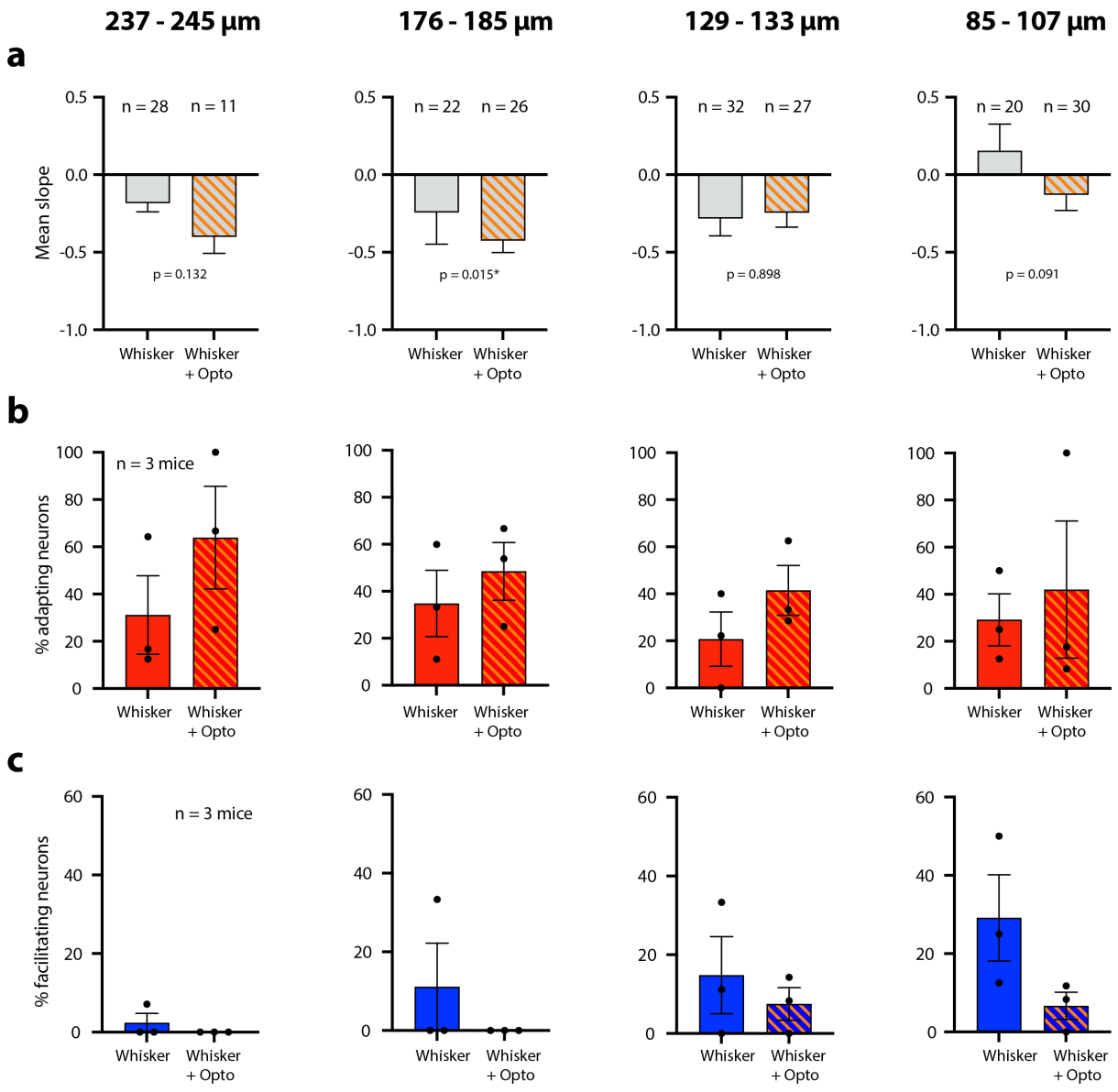

Figure 26. Activation of SST neurons impacts the relative abundance of adapting and facilitating neurons in superficial S1BF.

a) Mean slope of SR neurons across stimulation conditions and cortical depths. Mann Whitney test.

b) Percentage of SR neurons that adapt to whisker stimulation across conditions and cortical depths.

c) Same as **b**, but for facilitating neurons.

METHODS

Experimental animals

For the experiment described in this chapter, we used adult male (n= 2) and female (n= 1) heterozygous SST-Flp mice (Jax # 031629).

AAV injection and cranial window surgery

Cranial window surgery was performed on mice at 3-4 months of age. During the surgery, after performing the craniotomy and prior to placing the coverslip, 3 AAV vectors were injected into the superficial layers of S1BF: 1) Flp-dependent GCaMP6s (pAAV-Ef1a-fDIO-GCaMP6s, Addgene # 105714); 2) Flp-dependent ChRmine (pAAV-nEF-Coff/Fon-ChRmine-oScarlet; Addgene # 137160) (Fenno et al., 2020; Marshel et al., 2019); and 3) Synapsin-GCaMP6s (pAAV.Syn.GCaMP6s.WPRE.SV40; Addgene # 100843) (Chen et al., 2013). This resulted in expression of the red-shifted opsin ChRmine in SST neurons, and pan-neuronal expression of

GCaMP6s, so that the effect of SST activation on the local population could be assessed. Aside from viral injections, cranial window surgery methodology was identical to that described in Chapter 1.

2-photon calcium imaging with simultaneous 2-photon optogenetic stimulation

Imaging and optogenetic stimulation was performed in awake mice. Mice were imaged 2-3 weeks after cranial window surgery, to allow sufficient time for the injected viral constructs to express. During this time, intrinsic signal imaging was performed and mice were habituated to the 2-photon microscope as described in Chapter 1.

For optogenetic stimulation, we used a fixed-wavelength (1,040 nm) 2-photon Fidelity laser (Coherent). For 2-photon calcium imaging, the Chameleon Ultra II Ti:sapphire laser (Coherent) was tuned down to 900 nm to prevent inadvertent excitation of the opsin.

We recorded spontaneous, whisker-evoked, and optogenetically evoked activity in S1BF. For optogenetic stimulation, the shutter gating the Fidelity laser (controlled by MATLAB) was opened for pre-specified intervals. Calcium imaging parameters were identical to those used in Chapters 2 and 3, and whisker stimulation was performed with the same comb as used in Chapters 2 and 3. We recorded responses of ~100-150 neuronal somata above the C2 barrel at 4 different depths covering the superficial layers of S1BF: ~240-245 μm, ~175-185 μm, 120-130 μm, and 85-105 μm.

We first recorded 3 min of spontaneous activity and then delivered the whisker and optogenetic stimulation paradigms in separate movies as follows:

- “Opto”: 20 x optogenetic stimulation: stimulus duration 1 s, i.s.i. 3 s
- “Whisker”: 20 x 5 Hz whisker stimulation: stimulus duration 1 s, i.s.i. 3 s
- “Whisker/Opto”: 20 x 5 Hz whisker stimulation with simultaneous optogenetic stimulation: stimulus duration 1 s, i.s.i. 3 s

Analysis

Movies were motion corrected and segmented using EZcalcium as described in Chapter 1. Following segmentation, ROIs exhibiting calcium transients that were time-locked to bouts of whisker or optogenetic stimulation were identified by visual inspection as in previous chapters. From **Figure 25** onward (**Figs. 25 - 26**), ROIs that responded to optogenetic stimulation alone were excluded from being considered stimulus responsive (SR) in the Whisker and Whisker/Opto conditions. Adaptation index values were computed as described in Chapter 2.

DISCUSSION

SA is a highly conserved neuronal phenomenon present across sensory modalities that involves the progressive adjustment of neuronal activity with repeated exposure to sensory stimuli. Beyond its important roles in sensory discrimination and predictive coding, SA is critical for tuning out repetitive, non-threatening or non-salient, familiar/redundant stimuli across sensory modalities (Barlow, 1961; Brenner et al., 2000; Musall et al., 2017; Ollerenshaw et al., 2014). Most of this evidence has come from studies in single neurons across fast timescales (a few seconds or less). This prompted us to investigate SA at the neuronal and population level, in vivo, and across longer times scales (minutes to days).

Our principal goals were to characterize the temporal profiles of responses to repetitive stimuli across neuronal populations in S1BF and to determine whether these SA profiles were fixed or plastic over timescales of minutes to days. Using 2PCI and Neuropixels recordings in awake mice we characterized SA dynamics in hundreds of excitatory neurons simultaneously in L2/3 and L4 of S1BF. We found that: 1) The mean population response of excitatory cortical neurons to repetitive stimuli is mildly adapting; 2) Individual neurons exhibit a wide array of SA response profiles, ranging from strongly facilitating to strongly adapting; 3) The SA profile of L2/3 neurons to one stimulus can change for different stimulus frequencies (neurons that adapt to bouts of 5 Hz whisker stimulation can exhibit facilitation to 12.5 Hz); 4) S1BF populations show dramatic drift in their responses to whisker stimuli and in SA profile over just a few minutes; 5) Despite this stochasticity, SA in L2/3 and L4 can be shaped by experience across days, such that the population becomes less adapting to a familiar stimulus; and 6) SST interneurons may modulate the balance between adaptation and facilitation in superficial layers of S1BF. Through these findings, we have established that SA indeed occurs with repetitive stimulation at the timescale of tens of seconds in

S1BF, and in contrast to the standard view that SA reflects a hardwired or rigid property of neural responses, our findings suggest that SA is plastic and sculpted by experience.

Potential caveats in the interpretation of our results

Influence of different methods to calculate the magnitude of SA

The method used for classifying SA responses as either adapting/facilitating could also influence our estimates of the relative abundance of adapting and facilitating cells. Encouragingly, we found very similar results when using two different methods to calculate the AI (**Fig. 8** and **Fig. 9**), or two methods for recording neuronal activity (2PCI and Neuropixels) (**Fig. 8** and **Fig. 12**). It is also important to note that in both of our approaches to calculating the AI, we are measuring over the course of 15 whisker stimulation bouts, lasting 60 s in total. This is a considerably longer timescale than those used in previous studies measuring adaptation and facilitation in S1BF (Derdikman, 2006; Garabedian et al., 2003; Kheradpezhouh et al., 2017). Thus, it is possible that different proportions exist at this timescale, and the consistency of our results across two AI methods and two distinct in vivo recording approaches gives us confidence that these proportions are reproducible.

Behavioral state and SA

Finally, the behavioral state of the animal may also dynamically modulate levels of adaptation and facilitation within the population (Phillips et al., 2017). Although we did not systematically track arousal of mice (e.g., monitoring pupil size), videos show that they remain relatively still during passive stimulation, with minimal whisking and intermittent bouts of stepping forelimb movements followed by a return to minimal bodily movement (data not shown). Nevertheless, a more detailed analysis of pupil diameter and orofacial movements, in tandem with 2PCI, would be useful to further characterize the relationship between behavioral state and SA dynamics in the awake animal.

Passive whisker deflections vs. natural whisking

Because we characterized the dynamics of adaptation and facilitation while whiskers were passively deflected, it is possible that the proportion of adapting vs. facilitating cells, or their stability over time, might be different during natural active whisking. Still, the range of stimulation parameters we chose (5-12.5 Hz frequency, 3 s i.s.i., 1 s stimulus duration) falls within the range at which mice spontaneously whisk when exploring their environment (Kleinfeld et al., 2006), and S1BF is indeed required for this form of passive sensation (Miyashita & Feldman, 2013). Two studies from the laboratory of Carl Petersen show that both passive stimulation of the C2 whisker during quiet wakefulness and contacting an object through active whisking recruited robust responses in S1BF (Crochet & Petersen, 2006; Ferezou et al., 2006). Crochet & Petersen also observed that repeated contacts with an object during active whisking did not induce much adaptation; however, this was assessed on a timescale of 1-2 s or less. Future studies characterizing

adaptation and facilitation during periods of active whisking over extended timescales will provide further insight into what these dynamics look like during naturalistic tactile exploratory behavior.

Adaptation and facilitation in S1BF to repetitive whisker stimulation

While SA is generally thought of as a progressive decrease in neuronal responsiveness with repetitive stimulation, prior studies have reported that a minority of neurons show facilitating (or sensitizing) responses. In primary auditory cortex, one study found that ~13% of units exhibited facilitation (Phillips et al., 2017), while another found only 6% (Seay et al., 2020). Similarly, in S1BF, facilitating neurons comprise a small (<10%) fraction of the population (Brecht & Sakmann, 2002; Derdikman, 2006; Ego-Stengel et al., 2005; Kheradpezhouh et al., 2017). In our studies ~6-12% of L2/3 neurons showed significant facilitation to repetitive whisker stimuli, regardless of whether we used 2PCI or Neuropixels recordings. A previous study in S1BF from Derdikman *et al.* reported that input layers like L4 tend to show facilitation while L2/3 shows adaptation (Derdikman, 2006). We observed slightly more adapting neurons in L4, but similar proportions of facilitating neurons in both layers (18.6% adapting in L2/3 vs. 28.3% adapting in L4; 7.2% facilitating in L2/3 vs. 7.5% facilitating in L4). This discrepancy may be due to several methodological differences between our two studies. Electrophysiological recordings from Derdikman et al. were performed under anesthesia, and instead of passive deflection of the whiskers as was done in our study, active whisking was induced artificially by directly stimulating the buccal motor branch of the facial nerve (Derdikman, 2006).

Proportion of whisker responsive neurons in S1BF as a function of stimulation parameters and cortical layer.

In Chapter 1, we find that whisker stimulation bouts with longer durations tend to recruit more SR neurons that shorter stimulation bouts (**Fig. 4a**). The proportion of SR neurons reported in this chapter for 1 s duration/3 s i.s.i. is notably larger than those reported in the other datasets that comprise this dissertation (**Figs. 5c, 12e, 16c, 18d, 24, and 25**). The dataset that comprises most of Chapter 1 (and frequency switch results in Chapter 2) consists of mice who underwent a round whisker trimming in young adulthood (~P45-P60) for a previous experiment, before being used for experiments in this dissertation (once all whiskers had grown back). Repeated whisker trimming from birth to adulthood has been shown to enlarge receptive fields and increase responsiveness in S1BF (Simons & Land, 1987), though a later study suggests that this increased responsiveness occurs largely in L4 rather than L2/3 (S.-H. Lee et al., 2007). In the dataset in question, whiskers were also deflected with an older form of piezoactuator than was used for all other dissertation experiments, and the amplitude of deflection with that piezoactuator was noticeably larger than with the one used for all other experiments. However, previous work from our lab using this older form of piezoactuator reports proportions of SR neurons that align with what we have found in the other datasets of this dissertation (He et al., 2017), suggesting that the elevated proportion of SR neurons observed in the Chapter 1/frequency switch dataset is more likely due to prior whisker trimming than the change in piezoactuator. While this difference in stimulus responsiveness is important to note, we at no point compare results from this dataset (i.e., the studies of stimulus duration/i.s.i. in Chapter 1 and studies of frequency switch in Chapter 2) to

results from other datasets; we only perform comparisons within the dataset itself. Thus, this discrepancy in the percent of SR neurons should not confound any results or conclusions drawn.

Rapid adjustments in SA at the population level to changes in frequency

By recording neuronal responses during a single session, previous studies might have given the impression that individual neurons are always adapting or facilitating, and that they permanently retain such phenotypes. One of the most striking results of this project is that SA response profiles (adapting vs. facilitating) are not a fixed property of neurons. Indeed, S1BF neurons can adapt to one stimulation frequency and then facilitate to another frequency (Chapter 2), or change their SA profile across minutes or days (Chapter 3). Single-session recordings had previously shown that S1BF neurons that facilitate at certain stimulation frequencies do not necessarily respond in the same way to other frequencies (Garabedian et al., 2003). However, our study demonstrates the magnitude and scale of this turnover in response dynamics for several repetitions of the same stimulation protocol in a single-day imaging session, and we are the first to demonstrate a shift towards facilitation across days. The results of Chapters 2 and 3 support a novel model of SA in which neuronal responses are dynamic and experience can reshape population SA dynamics across days.

<u>Adapting neurons appear uniquely poised to adjust population SA, but not through an oddball response</u>

We also report that an abrupt change in stimulus parameters is not encoded equally across all SR neurons, as only neurons that had adapted to 5 Hz showed a change in activity to a sudden switch to 12.5 Hz. Thus, adapting neurons may be best poised to represent changes in tactile stimuli as a mouse navigates its environment, which is consistent with the notion that SA is useful for detecting deviant stimuli (Musall et al., 2017).

Importantly, the behavior of adapting neurons after the frequency switch did not resemble a classic "oddball response" (Hamm & Yuste, 2016; Natan et al., 2015) because it emerged gradually over subsequent stimuli at the higher frequency. This suggests that adapting neurons may adjust their activity over time through evidence accumulation. This gradual readjustment in firing magnitude may reflect an important balance that the network must maintain between readjusting neuronal activity in a timely and efficient manner, but not too quickly so as to avoid incorrectly recalibrating neuronal responsiveness when a change in the parameters (e.g., frequency) of forthcoming stimuli has not actually occurred (Wark et al., 2009).

Recent work in the auditory system may also help explain the absence of an oddball response in our frequency switch experiments. In an elegant review of rapid SA, Whitmire & Stanley describe a model for stimulus-specific sensory adaptation (SSA) and the "oddball response" it evokes in the auditory system, in which a postsynaptic neuron receives input from several differentially tuned presynaptic neuronal populations (Whitmire & Stanley, 2016). With repeated presentations of the adapting (standard) stimulus, presynaptic neurons tuned to the adapting stimulus will depress—resulting in a depressed response in the postsynaptic neuron—but presynaptic neurons tuned to the oddball (deviant) stimulus will not depress during these presentations. Thus, when the deviant

stimulus is finally presented, this will drive the presynaptic neurons tuned to the deviant stimulus, resulting in an increase in the response of the postsynaptic neuron to the deviant stimulus relative to the standard. Importantly, the authors note that within this framework, SSA cannot occur if the adapting and deviant stimuli drive responses in largely overlapping populations. This model has been supported by recent work in the inferior colliculus showing a robust oddball response when varying frequency (which drives distinct populations of presynaptic neurons) but not when varying intensity (which does not drive distinct presynaptic populations) (Duque et al., 2016; Whitmire & Stanley, 2016). While S1BF neurons exhibit tuning to certain stimulus parameters such as direction of whisker deflection (Andermann & Moore, 2006; Bruno et al., 2003), our stimulation frequencies (5 Hz and 12.5 Hz) did not appear to recruit distinct subpopulations of neurons in L2/3 (not shown). Furthermore, our results in Chapter 3 show that across multiple rounds of the same whisker stimulation protocol, different neurons respond each time (**Fig. 16c**). This suggests that S1BF does not maintain a specific subpopulation of cells tuned to a given stimulation frequency, which could explain why we do not observe an oddball response but instead a gradual increase in response magnitude, likely due to other mechanisms.

Frequency-specific changes in SA dynamics

In our frequency switch experiments, we also observed that adapting neurons were sensitive to increases—but not decreases—in frequency. This aligns with work from Adibi and colleagues demonstrating that adaptation to one stimulus amplitude shifts a neuron's response function (i.e., input-output relation, see Introduction) rightward, such that subsequent stimuli with an amplitude lower than the adapting stimulus elicit a weak response, but stimuli with higher amplitudes strongly recruit neuronal responses (Adibi et al., 2013). This aligns with our data showing an

increase in adapting neurons that is specific to upward switches in frequency. In a recent review, Adibi & Lampl propose a purpose for this phenomenon that is unique to the tactile modality (Adibi & Lampl, 2021), arguing that tactile stimuli with higher intensities than what the animal experiences at baseline possess the most relevance for behavior.

Experience-dependent changes in SA across days

After several days of whisker stimulation, excitatory populations in L2/3 gradually became significantly less adapting, which seems counterintuitive considering the stimuli were familiar to the animal (non-threatening and not particularly salient behaviorally). Because this did not occur after multiple rounds of stimulation within a single imaging session, we surmise that, over longer timescales of days, recurrent familiar stimuli occurring infrequently (one daily session) gain some salience for the mice that is encoded in the network as facilitation.

This experience plasticity of SA dynamics was similar between L2/3 and L4. Future studies that examine the role of facilitation— perhaps using optogenetics to artificially modulate neuronal activity over time— or rewards to provide behavioral salience, should explore the role of this phenomenon in perception and stimulus representation.

Are these dynamics changes in the response profiles of SR neurons a form of representational drift?

Representational drift describes the shift in neuronal representations of otherwise stable behavior that can occur over times scales of days or longer (Rule et al., 2019). This form of drift has been observed in the encoding of spatial maps by different populations of place cells in hippocampal CA1 over days (Ziv et al., 2013). In another study of CA1 ensembles but during an olfactory working memory task, the temporal sequence of active populations after task learning was shown to drift over days, even though the new pattern also accurately encodes the temporal sequence of working memory (Taxidis et al., 2020).

We observed similar drift-like phenomena in our experiments: individual neuronal responses in S1BF could change from adapting to facilitating (and vice versa) across multiple rounds of whisker stimulation. When comparing one round to the next, the composition of facilitating and adapting ensembles degraded, but importantly, when SR neurons were re-ordered based on their SA profile on the last round of stimulation, the percentage of adapting and facilitating neurons remained stable at the population level (**Fig. 16g**). Given the importance of SA as a property of cortical sensory neurons and its contribution to encoding important aspects of the stimulus (e.g., salience), we surmise that the change in SA dynamics we observe is a genuine example of representational drift. While population drift has previously been observed for whisker tuning of L2/3 neurons in S1BF (Wang et al., 2022) and touch responsiveness (Alisha et al., 2023), to our knowledge, we are the first to demonstrate population drift for SA profiles of neocortical neurons (**Fig. 16-18**).

Mechanisms of SA

Until now, the primary mechanisms identified for SA in S1BF have been intrinsic (e.g., spike frequency adaptation) or synaptic (e.g., the depression of thalamocortical synapses), and they have largely been proposed as explanations for SA of individual neurons, without regard for the overall population. Normalization, a process in which the activity of one neuron is modulated by the activity of the surrounding population (Carandini & Heeger, 2011) has been proposed as a mechanism by which population-level SA could occur (Adibi & Lampl, 2021; Weber et al., 2019; Whitmire & Stanley, 2016), though this phenomenon has not been extensively explored in the somatosensory system. In the auditory system, studies from Natan and colleagues have elegantly delineated distinct roles for PV and SST interneurons in adaptation (Natan et al., 2015, 2017), with SST interneurons being particularly important for distinguishing between frequent and rare stimuli by modulating adaptation specifically to frequent tones (Natan et al., 2015). Given these intriguing findings and the important role GABAergic interneurons play in modulating cortical firing at the network level (Moore et al., 2010; Tremblay et al., 2016), we set out to explore SST interneurons as a candidate network mechanism for SA.

In a final set of experiments, we began to probe the mechanistic underpinnings of population SA by optogenetically manipulating the activity of SST interneurons. While our findings are preliminary, they suggest that SST interneurons may help maintain the balance of adaptation and facilitation in S1BF, as optogenetic activation of SSTs both increased adaptation and decreased facilitation (**Fig. 26**). In addition to increasing the sample size to confirm the validity of these results, it would be informative to manipulate SST activity longitudinally to assess whether SST interneurons are required for the experience-dependent reduction in adaptation to take place as we have observed in Chapter 3 (**Fig. 18e-f**).

Future directions

Exposure to repetitive sensory stimuli over timescales of tens of seconds likely engages higher-order brain regions to access prior knowledge or expectations regarding the statistics of forthcoming stimuli. Under a predictive coding framework, higher-order areas send predictive signals to primary sensory areas via feedback projections to induce or lessen SA, depending on the stimulus (Rao & Ballard, 1999; Weber et al., 2019). Anatomical studies have identified reciprocal connections between neurons in L2/3 of S1BF and secondary somatosensory cortex and vibrissal primary motor cortex (Aronoff et al., 2010; Mao et al., 2011; Naskar et al., 2021; Petreanu et al., 2009). Elucidating the impact of top-down feedback projections on population SA will be an important next step in understanding how repeated exposure to sensory stimuli shapes neuronal activity at the population level.

In addition to top-down mechanisms, there are several other avenues one could pursue to build upon this characterization of population SA in S1BF. Optogenetics provides a powerful tool with which one could dissect the relative contributions of adaptation and facilitation to population dynamics and behavior—future studies using optogenetics to actively modulate the response profiles of cells and "mimic" adaptation/facilitation (similarly to work published by Musall et al., 2014) could provide valuable insights into the functions of each of these response profiles in sensory processing. Related to this, formulating behavioral tasks that require adaptation would allow us to better understand how SA ultimately impacts sensory perception in the intact animal.

Finally, studies in humans as well as animal models have shown alterations of SA in autism spectrum disorders and Fragile X syndrome, which may underlie sensory hypersensitivity symptoms that can occur with these conditions (Ethridge et al., 2016; Green et al., 2015; He et al., 2017; Kourdougli et al., 2023; Miller et al., 1999; Puts et al., 2014; Tommerdahl et al., 2007). Examining these population SA dynamics in mouse models of these conditions may thus provide insight into the circuit dynamics that underlie tactile hypersensitivity.

In conclusion, our study revealed remarkably complex dynamics of SA across populations of S1BF neurons, which were shaped by experience over days. This experience-dependent plasticity of SA profiles has profound implications regarding the primary function of sensory adaptation. Specifically, if SA primarily reflects predictive coding (tuning out an expected stimulus), it is not clear why it would undergo an experience-dependent shift towards facilitation across days. In contrast, if SA contributes to the formation of representations that capture the temporal structure of repeating stimuli, one might expect the observed shift towards facilitation. Future work examining candidate mechanisms underlying population SA, as well as the distinct functions of facilitation and adaptation in sensory perception, will provide valuable insights about how SA ultimately impacts behavior. Further insights into the population dynamics of SA may also prove useful for research related to neurological and psychiatric conditions in which altered SA may underlie sensory hypersensitivity or chronic pain symptoms.

APPENDIX: STATISTICAL METHODS

Results were plotted using Prism 9 and MATLAB and tested for statistical significance using Prism 9. Central tendencies are reported as mean plus or minus standard error of the mean (S.E.M.). Means were either calculated as an average of mice or as an average of cells pooled across all mice. Tests for normality were always completed before performing statistical tests. For any exclusions of outlier values, the ROUT method (Q = 1%) was used. All statistical tests are reported in figure legends, and corresponding p-values are reported in figures.

REFERENCES

Adesnik, H., Bruns, W., Taniguchi, H., Huang, Z. J., & Scanziani, M. (2012). A neural circuit for spatial summation in visual cortex. *Nature*, *490*(7419), 226–231. https://doi.org/10.1038/nature11526

Adibi, M. (2019). Whisker-Mediated Touch System in Rodents: From Neuron to Behavior. *Frontiers in Systems Neuroscience*, *13*, 40. https://doi.org/10.3389/fnsys.2019.00040

Adibi, M., & Lampl, I. (2021). Sensory Adaptation in the Whisker-Mediated Tactile System: Physiology, Theory, and Function. *Frontiers in Neuroscience*, *15*, 770011. https://doi.org/10.3389/fnins.2021.770011

Adibi, M., McDonald, J. S., Clifford, C. W. G., & Arabzadeh, E. (2013). Adaptation improves neural coding efficiency despite increasing correlations in variability. *The Journal of Neuroscience: The Official Journal of the Society for Neuroscience*, *33*(5), 2108–2120. https://doi.org/10.1523/JNEUROSCI.3449-12.2013

Ahissar, E., Sosnik, R., & Haidarliu, S. (2000). Transformation from temporal to rate coding in a somatosensory thalamocortical pathway. *Nature*, *406*(6793), 302–306. https://doi.org/10.1038/35018568

Alisha, A., Bettina, V., & Simon, P. (2023). *Representational drift in barrel cortex is receptive field dependent* [Preprint]. Neuroscience. https://doi.org/10.1101/2023.10.20.563381

Andermann, M. L., & Moore, C. I. (2006). A somatotopic map of vibrissa motion direction within a barrel column. *Nature Neuroscience*, *9*(4), 543–551. https://doi.org/10.1038/nn1671

Aronoff, R., Matyas, F., Mateo, C., Ciron, C., Schneider, B., & Petersen, C. C. H. (2010). Long-range connectivity of mouse primary somatosensory barrel cortex. *The European Journal of Neuroscience*, *31*(12), 2221–2233. https://doi.org/10.1111/j.1460-9568.2010.07264.x

Aschner, A., Solomon, S. G., Landy, M. S., Heeger, D. J., & Kohn, A. (2018). Temporal Contingencies Determine Whether Adaptation Strengthens or Weakens Normalization. *The Journal of Neuroscience: The Official Journal of the Society for Neuroscience*, *38*(47), 10129–10142. https://doi.org/10.1523/JNEUROSCI.1131-18.2018

Azouz, R., & Gray, C. M. (2000). Dynamic spike threshold reveals a mechanism for synaptic coincidence detection in cortical neurons *in vivo*. *Proceedings of the National Academy of Sciences*, *97*(14), 8110–8115. https://doi.org/10.1073/pnas.130200797

Baranek, G. T., Foster, L. G., & Berkson, G. (1997). Tactile defensiveness and stereotyped behaviors. *The American Journal of Occupational Therapy: Official Publication of the American Occupational Therapy Association*, *51*(2), 91–95. https://doi.org/10.5014/ajot.51.2.91

Barlow, H. B. (1961). Possible Principles Underlying the Transformations of Sensory Messages. *Sensory Communication*, 216–234.

Bastos, G., Holmes, J. T., Ross, J. M., Rader, A. M., Gallimore, C. G., Wargo, J. A., Peterka, D. S., & Hamm, J. P. (2023). Top-down input modulates visual context processing through an interneuron-specific circuit. *Cell Reports*, *42*(9), 113133. https://doi.org/10.1016/j.celrep.2023.113133

Benda, J., & Herz, A. V. M. (2003). A Universal Model for Spike-Frequency Adaptation. *Neural Computation*, *15*(11), 2523–2564. https://doi.org/10.1162/089976603322385063

Benucci, A., Saleem, A. B., & Carandini, M. (2013). Adaptation maintains population homeostasis in primary visual cortex. *Nature Neuroscience*, *16*(6), 724–729. https://doi.org/10.1038/nn.3382

Berglund, U., & Berglund, B. (1970). Adaptation and Recovery in Vibrotactile Perception. *Perceptual and Motor Skills*, *30*(3), 843–853. https://doi.org/10.2466/pms.1970.30.3.843

Bhattacharjee, A., & Kaczmarek, L. (2005). For K channels, Na is the new Ca. *Trends in Neurosciences*, *28*(8), 422–428. https://doi.org/10.1016/j.tins.2005.06.003

Brecht, M., & Sakmann, B. (2002). -Dynamic representation of whisker deflection by synaptic potentials in spiny stellate and pyramidal cells in the barrels and septa of layer 4 rat somatosensory cortex. *The Journal of Physiology*, *543*(1), 49–70. https://doi.org/10.1113/jphysiol.2002.018465

Brenner, N., Bialek, W., & de Ruyter van Steveninck, R. (2000). Adaptive rescaling maximizes information transmission. *Neuron*, *26*(3), 695–702. https://doi.org/10.1016/s0896-6273(00)81205-2

Bruno, R. M., Khatri, V., Land, P. W., & Simons, D. J. (2003). Thalamocortical Angular Tuning Domains within Individual Barrels of Rat Somatosensory Cortex. *The Journal of Neuroscience*, *23*(29), 9565–9574. https://doi.org/10.1523/JNEUROSCI.23-29-09565.2003

Cantu, D. A., Wang, B., Gongwer, M. W., He, C. X., Goel, A., Suresh, A., Kourdougli, N., Arroyo, E. D., Zeiger, W., & Portera-Cailliau, C. (2020). EZcalcium: Open-Source Toolbox for Analysis of Calcium Imaging Data. *Frontiers in Neural Circuits*, *14*, 25. https://doi.org/10.3389/fncir.2020.00025

Carandini, M., & Heeger, D. J. (2011). Normalization as a canonical neural computation. *Nature Reviews. Neuroscience*, *13*(1), 51–62. https://doi.org/10.1038/nrn3136

Carvell, G. E., & Simons, D. J. (1990). Biometric analyses of vibrissal tactile discrimination in the rat. *The Journal of Neuroscience: The Official Journal of the Society for Neuroscience*, *10*(8), 2638–2648. https://doi.org/10.1523/JNEUROSCI.10-08-02638.1990

Castro-Alamancos, M. A. (2004). Absence of rapid sensory adaptation in neocortex during information processing states. *Neuron*, *41*(3), 455–464. https://doi.org/10.1016/s0896-6273(03)00853-5

Castro-Alamancos, M. A., & Gulati, T. (2014). Neuromodulators Produce Distinct Activated States in Neocortex. *The Journal of Neuroscience*, *34*(37), 12353–12367. https://doi.org/10.1523/JNEUROSCI.1858-14.2014

Chander, D., & Chichilnisky, E. J. (2001). Adaptation to Temporal Contrast in Primate and Salamander Retina. *The Journal of Neuroscience*, *21*(24), 9904–9916. https://doi.org/10.1523/JNEUROSCI.21-24-09904.2001

Chen, T.-W., Wardill, T. J., Sun, Y., Pulver, S. R., Renninger, S. L., Baohan, A., Schreiter, E. R., Kerr, R. A., Orger, M. B., Jayaraman, V., Looger, L. L., Svoboda, K., & Kim, D. S. (2013). Ultrasensitive fluorescent proteins for imaging neuronal activity. *Nature*, *499*(7458), 295–300. https://doi.org/10.1038/nature12354

Chung, S., Li, X., & Nelson, S. B. (2002). Short-term depression at thalamocortical synapses contributes to rapid adaptation of cortical sensory responses in vivo. *Neuron*, *34*(3), 437–446. https://doi.org/10.1016/s0896-6273(02)00659-1

Clancy, K. B., Schnepel, P., Rao, A. T., & Feldman, D. E. (2015). Structure of a single whisker representation in layer 2 of mouse somatosensory cortex. *The Journal of Neuroscience: The Official Journal of the Society for Neuroscience*, *35*(9), 3946–3958. https://doi.org/10.1523/JNEUROSCI.3887-14.2015

Colins Rodriguez, A., Loft, M. S. E., Schiessl, I., Maravall, M., & Petersen, R. (2022). *Sensory adaptation in the barrel cortex during active sensation in the awake, behaving mouse* [Preprint]. Neuroscience. https://doi.org/10.1101/2022.07.07.499259

Constantinople, C. M., & Bruno, R. M. (2011). Effects and Mechanisms of Wakefulness on Local Cortical Networks. *Neuron*, *69*(6), 1061–1068. https://doi.org/10.1016/j.neuron.2011.02.040

Crochet, S., & Petersen, C. C. H. (2006). Correlating whisker behavior with membrane potential in barrel cortex of awake mice. *Nature Neuroscience*, *9*(5), 608–610. https://doi.org/10.1038/nn1690

Daigle, T. L., Madisen, L., Hage, T. A., Valley, M. T., Knoblich, U., Larsen, R. S., Takeno, M. M., Huang, L., Gu, H., Larsen, R., Mills, M., Bosma-Moody, A., Siverts, L. A., Walker, M., Graybuck, L. T., Yao, Z., Fong, O., Nguyen, T. N., Garren, E., … Zeng, H. (2018). A Suite of Transgenic Driver and Reporter Mouse Lines with Enhanced Brain-Cell-Type Targeting and Functionality. *Cell*, *174*(2), 465-480.e22. https://doi.org/10.1016/j.cell.2018.06.035

Deitch, D., Rubin, A., & Ziv, Y. (2021). Representational drift in the mouse visual cortex. *Current Biology*, *31*(19), 4327-4339.e6. https://doi.org/10.1016/j.cub.2021.07.062

Derdikman, D. (2006). Layer-Specific Touch-Dependent Facilitation and Depression in the Somatosensory Cortex during Active Whisking. *Journal of Neuroscience*, *26*(37), 9538–9547. https://doi.org/10.1523/JNEUROSCI.0918-06.2006

Deschênes, M., Timofeeva, E., Lavallée, P., & Dufresne, C. (2005). The vibrissal system as a model of thalamic operations. In *Progress in Brain Research* (Vol. 149, pp. 31–40). Elsevier. https://doi.org/10.1016/S0079-6123(05)49003-2

Dhruv, N. T., Tailby, C., Sokol, S. H., & Lennie, P. (2011). Multiple adaptable mechanisms early in the primate visual pathway. *The Journal of Neuroscience: The Official Journal of the Society for Neuroscience*, *31*(42), 15016–15025. https://doi.org/10.1523/JNEUROSCI.0890-11.2011

Diamond, M. E., Von Heimendahl, M., Knutsen, P. M., Kleinfeld, D., & Ahissar, E. (2008). "Where" and "what" in the whisker sensorimotor system. *Nature Reviews Neuroscience*, *9*(8), 601–612. https://doi.org/10.1038/nrn2411

Douglas, R. J., & Martin, K. A. (1991). A functional microcircuit for cat visual cortex. *The Journal of Physiology*, *440*, 735–769. https://doi.org/10.1113/jphysiol.1991.sp018733

Dragoi, V., Sharma, J., & Sur, M. (2000). Adaptation-induced plasticity of orientation tuning in adult visual cortex. *Neuron*, *28*(1), 287–298. https://doi.org/10.1016/s0896-6273(00)00103-3

Duque, D., Wang, X., Nieto-Diego, J., Krumbholz, K., & Malmierca, M. S. (2016). Neurons in the inferior colliculus of the rat show stimulus-specific adaptation for frequency, but not for intensity. *Scientific Reports*, *6*(1), 24114. https://doi.org/10.1038/srep24114

Ego-Stengel, V., Mello E Souza, T., Jacob, V., & Shulz, D. E. (2005). Spatiotemporal Characteristics of Neuronal Sensory Integration in the Barrel Cortex of the Rat. *Journal of Neurophysiology*, *93*(3), 1450–1467. https://doi.org/10.1152/jn.00912.2004

Erchova, I. A., Lebedev, M. A., & Diamond, M. E. (2002). Somatosensory cortical neuronal population activity across states of anaesthesia. *European Journal of Neuroscience*, *15*(4), 744–752. https://doi.org/10.1046/j.0953-816x.2002.01898.x

Ethridge, L. E., White, S. P., Mosconi, M. W., Wang, J., Byerly, M. J., & Sweeney, J. A. (2016). Reduced habituation of auditory evoked potentials indicate cortical hyper-excitability in Fragile X Syndrome. *Translational Psychiatry*, *6*(4), e787. https://doi.org/10.1038/tp.2016.48

Fairhall, A. L., Lewen, G. D., Bialek, W., & De Ruyter Van Steveninck, R. R. (2001). Efficiency and ambiguity in an adaptive neural code. *Nature*, *412*(6849), 787–792. https://doi.org/10.1038/35090500

Feldmeyer, D. (2012). Excitatory neuronal connectivity in the barrel cortex. *Frontiers in Neuroanatomy*, *6*. https://doi.org/10.3389/fnana.2012.00024

Feldmeyer, D., Brecht, M., Helmchen, F., Petersen, C. C. H., Poulet, J. F. A., Staiger, J. F., Luhmann, H. J., & Schwarz, C. (2013). Barrel cortex function. *Progress in Neurobiology*, *103*, 3–27. https://doi.org/10.1016/j.pneurobio.2012.11.002

Fenno, L. E., Ramakrishnan, C., Kim, Y. S., Evans, K. E., Lo, M., Vesuna, S., Inoue, M., Cheung, K. Y. M., Yuen, E., Pichamoorthy, N., Hong, A. S. O., & Deisseroth, K. (2020). Comprehensive Dual- and Triple-Feature Intersectional Single-Vector Delivery of Diverse Functional Payloads to Cells of Behaving Mammals. *Neuron*, *107*(5), 836-853.e11. https://doi.org/10.1016/j.neuron.2020.06.003

Ferezou, I., Bolea, S., & Petersen, C. C. H. (2006). Visualizing the Cortical Representation of Whisker Touch: Voltage-Sensitive Dye Imaging in Freely Moving Mice. *Neuron*, *50*(4), 617–629. https://doi.org/10.1016/j.neuron.2006.03.043

Fino, E., & Yuste, R. (2011). Dense inhibitory connectivity in neocortex. *Neuron*, *69*(6), 1188–1203. https://doi.org/10.1016/j.neuron.2011.02.025

Fu, Y., Kaneko, M., Tang, Y., Alvarez-Buylla, A., & Stryker, M. P. (2015). A cortical disinhibitory circuit for enhancing adult plasticity. *eLife*, *4*, e05558. https://doi.org/10.7554/eLife.05558

Ganmor, E., Katz, Y., & Lampl, I. (2010). Intensity-dependent adaptation of cortical and thalamic neurons is controlled by brainstem circuits of the sensory pathway. *Neuron*, *66*(2), 273–286. https://doi.org/10.1016/j.neuron.2010.03.032

Garabedian, C. E., Jones, S. R., Merzenich, M. M., Dale, A., & Moore, C. I. (2003). Band-Pass Response Properties of Rat SI Neurons. *Journal of Neurophysiology*, *90*(3), 1379–1391. https://doi.org/10.1152/jn.01158.2002

Gill, N. K., & Francis, N. A. (2023). *Repetition plasticity in primary auditory cortex occurs across long timescales for spectrotemporally randomized pure-tones* [Preprint]. Neuroscience. https://doi.org/10.1101/2023.04.26.538446

Gjorgjieva, J., Mease, R. A., Moody, W. J., & Fairhall, A. L. (2014). Intrinsic Neuronal Properties Switch the Mode of Information Transmission in Networks. *PLoS Computational Biology*, *10*(12), e1003962. https://doi.org/10.1371/journal.pcbi.1003962

Goble, A. K., & Hollins, M. (1993). Vibrotactile adaptation enhances amplitude discrimination. *The Journal of the Acoustical Society of America*, *93*(1), 418–424. https://doi.org/10.1121/1.405621

Goble, A. K., & Hollins, M. (1994). Vibrotactile adaptation enhances frequency discrimination. *The Journal of the Acoustical Society of America*, *96*(2 Pt 1), 771–780. https://doi.org/10.1121/1.410314

Green, S. A., Hernandez, L., Tottenham, N., Krasileva, K., Bookheimer, S. Y., & Dapretto, M. (2015). Neurobiology of Sensory Overresponsivity in Youth With Autism Spectrum Disorders. *JAMA Psychiatry*, *72*(8), 778–786. https://doi.org/10.1001/jamapsychiatry.2015.0737

Grienberger, C., Giovannucci, A., Zeiger, W., & Portera-Cailliau, C. (2022). Two-photon calcium imaging of neuronal activity. *Nature Reviews Methods Primers*, *2*(1), 67. https://doi.org/10.1038/s43586-022-00147-1

Grinvald, A., Lieke, E., Frostig, R. D., Gilbert, C. D., & Wiesel, T. N. (1986). Functional architecture of cortex revealed by optical imaging of intrinsic signals. *Nature*, *324*(6095), 361–364. https://doi.org/10.1038/324361a0

Haider, B., Häusser, M., & Carandini, M. (2013). Inhibition dominates sensory responses in the awake cortex. *Nature*, *493*(7430), 97–100. https://doi.org/10.1038/nature11665

Hamm, J. P., Shymkiv, Y., Han, S., Yang, W., & Yuste, R. (2021). Cortical ensembles selective for context. *Proceedings of the National Academy of Sciences of the United States of America*, *118*(14), e2026179118. https://doi.org/10.1073/pnas.2026179118

Hamm, J. P., & Yuste, R. (2016). Somatostatin Interneurons Control a Key Component of Mismatch Negativity in Mouse Visual Cortex. *Cell Reports*, *16*(3), 597–604. https://doi.org/10.1016/j.celrep.2016.06.037

Han, S., & Helmchen, F. (2024). Behavior-relevant top-down cross-modal predictions in mouse neocortex. *Nature Neuroscience*, *27*(2), 298–308. https://doi.org/10.1038/s41593-023-01534-x

Harris, J. A., Hirokawa, K. E., Sorensen, S. A., Gu, H., Mills, M., Ng, L. L., Bohn, P., Mortrud, M., Ouellette, B., Kidney, J., Smith, K. A., Dang, C., Sunkin, S., Bernard, A., Oh, S. W., Madisen, L., & Zeng, H. (2014). Anatomical characterization of Cre driver mice for neural circuit mapping and manipulation. *Frontiers in Neural Circuits*, *8*, 76. https://doi.org/10.3389/fncir.2014.00076

Harris, K. D., & Thiele, A. (2011). Cortical state and attention. *Nature Reviews Neuroscience*, *12*(9), 509–523. https://doi.org/10.1038/nrn3084

He, C. X., Cantu, D. A., Mantri, S. S., Zeiger, W. A., Goel, A., & Portera-Cailliau, C. (2017). Tactile Defensiveness and Impaired Adaptation of Neuronal Activity in the Fmr1 Knock-Out Mouse Model of Autism. *The Journal of Neuroscience: The Official Journal of the Society for Neuroscience*, *37*(27), 6475–6487. https://doi.org/10.1523/JNEUROSCI.0651-17.2017

Heiss, J. E., Katz, Y., Ganmor, E., & Lampl, I. (2008). Shift in the balance between excitation and inhibition during sensory adaptation of S1 neurons. *The Journal of Neuroscience: The Official Journal of the Society for Neuroscience*, *28*(49), 13320–13330. https://doi.org/10.1523/JNEUROSCI.2646-08.2008

Hill, D. N., Mehta, S. B., & Kleinfeld, D. (2011). Quality metrics to accompany spike sorting of extracellular signals. *The Journal of Neuroscience: The Official Journal of the Society for Neuroscience*, *31*(24), 8699–8705. https://doi.org/10.1523/JNEUROSCI.0971-11.2011

Holtmaat, A., Bonhoeffer, T., Chow, D. K., Chuckowree, J., De Paola, V., Hofer, S. B., Hübener, M., Keck, T., Knott, G., Lee, W.-C. A., Mostany, R., Mrsic-Flogel, T. D., Nedivi, E., Portera-Cailliau, C., Svoboda, K., Trachtenberg, J. T., & Wilbrecht, L. (2009). Long-term, high-resolution imaging in the mouse neocortex through a chronic cranial window. *Nature Protocols*, *4*(8), 1128–1144. https://doi.org/10.1038/nprot.2009.89

Jones, E. G., & Wise, S. P. (1977). Size, laminar and columnar distribution of efferent cells in the sensory-motor cortex of monkeys. *Journal of Comparative Neurology*, *175*(4), 391–437. https://doi.org/10.1002/cne.901750403

Juavinett, A. L., Bekheet, G., & Churchland, A. K. (2019). Chronically implanted Neuropixels probes enable high-yield recordings in freely moving mice. *eLife*, *8*, e47188. https://doi.org/10.7554/eLife.47188

Jun, J. J., Steinmetz, N. A., Siegle, J. H., Denman, D. J., Bauza, M., Barbarits, B., Lee, A. K., Anastassiou, C. A., Andrei, A., Aydın, Ç., Barbic, M., Blanche, T. J., Bonin, V., Couto, J., Dutta, B., Gratiy, S. L., Gutnisky, D. A., Häusser, M., Karsh, B., … Harris, T. D. (2017). Fully integrated silicon probes for high-density recording of neural activity. *Nature*, *551*(7679), 232–236. https://doi.org/10.1038/nature24636

Kastner, D. B., & Baccus, S. A. (2011). Coordinated dynamic encoding in the retina using opposing forms of plasticity. *Nature Neuroscience*, *14*(10), 1317–1322. https://doi.org/10.1038/nn.2906

Keller, G. B., & Mrsic-Flogel, T. D. (2018). Predictive Processing: A Canonical Cortical Computation. *Neuron*, *100*(2), 424–435. https://doi.org/10.1016/j.neuron.2018.10.003

Khatri, V., Hartings, J. A., & Simons, D. J. (2004). Adaptation in thalamic barreloid and cortical barrel neurons to periodic whisker deflections varying in frequency and velocity. *Journal of Neurophysiology*, *92*(6), 3244–3254. https://doi.org/10.1152/jn.00257.2004

Kheradpezhouh, E., Adibi, M., & Arabzadeh, E. (2017). Response dynamics of rat barrel cortex neurons to repeated sensory stimulation. *Scientific Reports*, *7*(1), 11445. https://doi.org/10.1038/s41598-017-11477-6

Kim, K. J., & Rieke, F. (2001). Temporal Contrast Adaptation in the Input and Output Signals of Salamander Retinal Ganglion Cells. *The Journal of Neuroscience*, *21*(1), 287–299. https://doi.org/10.1523/JNEUROSCI.21-01-00287.2001

Kleinfeld, D., Ahissar, E., & Diamond, M. E. (2006). Active sensation: Insights from the rodent vibrissa sensorimotor system. *Current Opinion in Neurobiology*, *16*(4), 435–444. https://doi.org/10.1016/j.conb.2006.06.009

Kourdougli, N., Suresh, A., Liu, B., Juarez, P., Lin, A., Chung, D. T., Graven Sams, A., Gandal, M. J., Martínez-Cerdeño, V., Buonomano, D. V., Hall, B. J., Mombereau, C., & Portera-Cailliau, C. (2023). Improvement of sensory deficits in fragile X mice by increasing cortical interneuron activity after the critical period. *Neuron*, *111*(18), 2863-2880.e6. https://doi.org/10.1016/j.neuron.2023.06.009

La Camera, G., Rauch, A., Thurbon, D., Lüscher, H.-R., Senn, W., & Fusi, S. (2006). Multiple Time Scales of Temporal Response in Pyramidal and Fast Spiking Cortical Neurons. *Journal of Neurophysiology*, *96*(6), 3448–3464. https://doi.org/10.1152/jn.00453.2006

Latimer, K. W., Barbera, D., Sokoletsky, M., Awwad, B., Katz, Y., Nelken, I., Lampl, I., Fairhall, A. L., & Priebe, N. J. (2019). Multiple Timescales Account for Adaptive Responses across Sensory Cortices. *The Journal of Neuroscience: The Official Journal of the Society*

for Neuroscience, *39*(50), 10019–10033. https://doi.org/10.1523/JNEUROSCI.1642-19.2019

Laughlin, S. (1981). A Simple Coding Procedure Enhances a Neuron's Information Capacity. *Zeitschrift Für Naturforschung C*, *36*(9–10), 910–912. https://doi.org/10.1515/znc-1981-9-1040

Lee, H., Tanabe, S., Wang, S., & Hudetz, A. G. (2021). Differential Effect of Anesthesia on Visual Cortex Neurons with Diverse Population Coupling. *Neuroscience*, *458*, 108–119. https://doi.org/10.1016/j.neuroscience.2020.11.043

Lee, S., Kruglikov, I., Huang, Z. J., Fishell, G., & Rudy, B. (2013). A disinhibitory circuit mediates motor integration in the somatosensory cortex. *Nature Neuroscience*, *16*(11), 1662–1670. https://doi.org/10.1038/nn.3544

Lee, S.-H., Land, P. W., & Simons, D. J. (2007). Layer- and Cell-Type-Specific Effects of Neonatal Whisker-Trimming in Adult Rat Barrel Cortex. *Journal of Neurophysiology*, *97*(6), 4380–4385. https://doi.org/10.1152/jn.01217.2006

Lundstrom, B. N., Higgs, M. H., Spain, W. J., & Fairhall, A. L. (2008). Fractional differentiation by neocortical pyramidal neurons. *Nature Neuroscience*, *11*(11), 1335–1342. https://doi.org/10.1038/nn.2212

Mao, T., Kusefoglu, D., Hooks, B. M., Huber, D., Petreanu, L., & Svoboda, K. (2011). Long-range neuronal circuits underlying the interaction between sensory and motor cortex. *Neuron*, *72*(1), 111–123. https://doi.org/10.1016/j.neuron.2011.07.029

Maravall, M., Petersen, R. S., Fairhall, A. L., Arabzadeh, E., & Diamond, M. E. (2007). Shifts in coding properties and maintenance of information transmission during adaptation in barrel cortex. *PLoS Biology*, *5*(2), e19. https://doi.org/10.1371/journal.pbio.0050019

Marco, E. J., Hinkley, L. B. N., Hill, S. S., & Nagarajan, S. S. (2011). Sensory processing in autism: A review of neurophysiologic findings. *Pediatric Research*, *69*(5 Pt 2), 48R-54R. https://doi.org/10.1203/PDR.0b013e3182130c54

Marshel, J. H., Kim, Y. S., Machado, T. A., Quirin, S., Benson, B., Kadmon, J., Raja, C., Chibukhchyan, A., Ramakrishnan, C., Inoue, M., Shane, J. C., McKnight, D. J., Yoshizawa, S., Kato, H. E., Ganguli, S., & Deisseroth, K. (2019). Cortical layer–specific critical dynamics triggering perception. *Science*, *365*(6453), eaaw5202. https://doi.org/10.1126/science.aaw5202

Martin-Cortecero, J., & Nuñez, A. (2014). Tactile response adaptation to whisker stimulation in the lemniscal somatosensory pathway of rats. *Brain Research*, *1591*, 27–37. https://doi.org/10.1016/j.brainres.2014.10.002

Mazuski, C., & O'Keefe, J. (2022). Representation of ethological events by basolateral amygdala neurons. *Cell Reports*, *39*(10), 110921. https://doi.org/10.1016/j.celrep.2022.110921

Mégevand, P., Troncoso, E., Quairiaux, C., Muller, D., Michel, C. M., & Kiss, J. Z. (2009). Long-term plasticity in mouse sensorimotor circuits after rhythmic whisker stimulation. *The Journal of Neuroscience: The Official Journal of the Society for Neuroscience*, *29*(16), 5326–5335. https://doi.org/10.1523/JNEUROSCI.5965-08.2009

Meyer, H. S., Schwarz, D., Wimmer, V. C., Schmitt, A. C., Kerr, J. N. D., Sakmann, B., & Helmstaedter, M. (2011). Inhibitory interneurons in a cortical column form hot zones of inhibition in layers 2 and 5A. *Proceedings of the National Academy of Sciences of the United States of America*, *108*(40), 16807–16812. https://doi.org/10.1073/pnas.1113648108

Miller, L. J., McIntosh, D. N., McGrath, J., Shyu, V., Lampe, M., Taylor, A. K., Tassone, F., Neitzel, K., Stackhouse, T., & Hagerman, R. J. (1999). Electrodermal responses to sensory stimuli in individuals with fragile X syndrome: A preliminary report. *American Journal of Medical Genetics*, *83*(4), 268–279.

Miyashita, T., & Feldman, D. E. (2013). Behavioral Detection of Passive Whisker Stimuli Requires Somatosensory Cortex. *Cerebral Cortex*, *23*(7), 1655–1662. https://doi.org/10.1093/cercor/bhs155

Mohar, B., Katz, Y., & Lampl, I. (2013). Opposite Adaptive Processing of Stimulus Intensity in Two Major Nuclei of the Somatosensory Brainstem. *The Journal of Neuroscience*, *33*(39), 15394–15400. https://doi.org/10.1523/JNEUROSCI.1886-13.2013

Moore, C. I., Carlen, M., Knoblich, U., & Cardin, J. A. (2010). Neocortical interneurons: From diversity, strength. *Cell*, *142*(2), 189–193. https://doi.org/10.1016/j.cell.2010.07.005

Mostany, R., & Portera-Cailliau, C. (2008). A craniotomy surgery procedure for chronic brain imaging. *Journal of Visualized Experiments: JoVE*, *12*, 680. https://doi.org/10.3791/680

Musall, S., Haiss, F., Weber, B., & von der Behrens, W. (2017). Deviant Processing in the Primary Somatosensory Cortex. *Cerebral Cortex (New York, N.Y.: 1991)*, *27*(1), 863–876. https://doi.org/10.1093/cercor/bhv283

Musall, S., von der Behrens, W., Mayrhofer, J. M., Weber, B., Helmchen, F., & Haiss, F. (2014). Tactile frequency discrimination is enhanced by circumventing neocortical adaptation. *Nature Neuroscience*, *17*(11), 1567–1573. https://doi.org/10.1038/nn.3821

Naka, A., Veit, J., Shababo, B., Chance, R. K., Risso, D., Stafford, D., Snyder, B., Egladyous, A., Chu, D., Sridharan, S., Mossing, D. P., Paninski, L., Ngai, J., & Adesnik, H. (2019).

Complementary networks of cortical somatostatin interneurons enforce layer specific control. *eLife*, *8*, e43696. https://doi.org/10.7554/eLife.43696

Naskar, S., Qi, J., Pereira, F., Gerfen, C. R., & Lee, S. (2021). Cell-type-specific recruitment of GABAergic interneurons in the primary somatosensory cortex by long-range inputs. *Cell Reports*, *34*(8), 108774. https://doi.org/10.1016/j.celrep.2021.108774

Natan, R. G., Briguglio, J. J., Mwilambwe-Tshilobo, L., Jones, S. I., Aizenberg, M., Goldberg, E. M., & Geffen, M. N. (2015). Complementary control of sensory adaptation by two types of cortical interneurons. *eLife*, *4*, e09868. https://doi.org/10.7554/eLife.09868

Natan, R. G., Rao, W., & Geffen, M. N. (2017). Cortical Interneurons Differentially Shape Frequency Tuning following Adaptation. *Cell Reports*, *21*(4), 878–890. https://doi.org/10.1016/j.celrep.2017.10.012

Ollerenshaw, D. R., Zheng, H. J. V., Millard, D. C., Wang, Q., & Stanley, G. B. (2014). The adaptive trade-off between detection and discrimination in cortical representations and behavior. *Neuron*, *81*(5), 1152–1164. https://doi.org/10.1016/j.neuron.2014.01.025

Packer, A. M., & Yuste, R. (2011). Dense, unspecific connectivity of neocortical parvalbumin-positive interneurons: A canonical microcircuit for inhibition? *The Journal of Neuroscience: The Official Journal of the Society for Neuroscience*, *31*(37), 13260–13271. https://doi.org/10.1523/JNEUROSCI.3131-11.2011

Petersen, C. C. H. (2007). The Functional Organization of the Barrel Cortex. *Neuron*, *56*(2), 339–355. https://doi.org/10.1016/j.neuron.2007.09.017

Petersen, C. C. H. (2019). Sensorimotor processing in the rodent barrel cortex. *Nature Reviews Neuroscience*, *20*(9), 533–546. https://doi.org/10.1038/s41583-019-0200-y

Petreanu, L., Mao, T., Sternson, S. M., & Svoboda, K. (2009). The subcellular organization of neocortical excitatory connections. *Nature*, *457*(7233), 1142–1145. https://doi.org/10.1038/nature07709

Phillips, E. A. K., Schreiner, C. E., & Hasenstaub, A. R. (2017). Diverse effects of stimulus history in waking mouse auditory cortex. *Journal of Neurophysiology*, *118*(2), 1376–1393. https://doi.org/10.1152/jn.00094.2017

Pi, H.-J., Hangya, B., Kvitsiani, D., Sanders, J. I., Huang, Z. J., & Kepecs, A. (2013). Cortical interneurons that specialize in disinhibitory control. *Nature*, *503*(7477), 521–524. https://doi.org/10.1038/nature12676

Pozzorini, C., Naud, R., Mensi, S., & Gerstner, W. (2013). Temporal whitening by power-law adaptation in neocortical neurons. *Nature Neuroscience*, *16*(7), 942–948. https://doi.org/10.1038/nn.3431

Puts, N. A. J., Wodka, E. L., Tommerdahl, M., Mostofsky, S. H., & Edden, R. A. E. (2014). Impaired tactile processing in children with autism spectrum disorder. *Journal of Neurophysiology*, *111*(9), 1803–1811. https://doi.org/10.1152/jn.00890.2013

Rao, R. P., & Ballard, D. H. (1999). Predictive coding in the visual cortex: A functional interpretation of some extra-classical receptive-field effects. *Nature Neuroscience*, *2*(1), 79–87. https://doi.org/10.1038/4580

Rule, M. E., O'Leary, T., & Harvey, C. D. (2019). Causes and consequences of representational drift. *Current Opinion in Neurobiology*, *58*, 141–147. https://doi.org/10.1016/j.conb.2019.08.005

Sanchez-Vives, M. V., Nowak, L. G., & McCormick, D. A. (2000). Cellular Mechanisms of Long-Lasting Adaptation in Visual Cortical Neurons *In Vitro*. *The Journal of*

Neuroscience, *20*(11), 4286–4299. https://doi.org/10.1523/JNEUROSCI.20-11-04286.2000

Schoonover, C. E., Ohashi, S. N., Axel, R., & Fink, A. J. P. (2021). Representational drift in primary olfactory cortex. *Nature*, *594*(7864), 541–546. https://doi.org/10.1038/s41586-021-03628-7

Seay, M. J., Natan, R. G., Geffen, M. N., & Buonomano, D. V. (2020). Differential Short-Term Plasticity of PV and SST Neurons Accounts for Adaptation and Facilitation of Cortical Neurons to Auditory Tones. *The Journal of Neuroscience: The Official Journal of the Society for Neuroscience*, *40*(48), 9224–9235. https://doi.org/10.1523/JNEUROSCI.0686-20.2020

Sheintuch, L., Rubin, A., Brande-Eilat, N., Geva, N., Sadeh, N., Pinchasof, O., & Ziv, Y. (2017). Tracking the Same Neurons across Multiple Days in Ca2+ Imaging Data. *Cell Reports*, *21*(4), 1102–1115. https://doi.org/10.1016/j.celrep.2017.10.013

Simons, D. J., & Land, P. W. (1987). Early experience of tactile stimulation influences organization of somatic sensory cortex. *Nature*, *326*(6114), 694–697. https://doi.org/10.1038/326694a0

Smirnakis, S. M., Berry, M. J., Warland, D. K., Bialek, W., & Meister, M. (1997). Adaptation of retinal processing to image contrast and spatial scale. *Nature*, *386*(6620), 69–73. https://doi.org/10.1038/386069a0

Staiger, J. F., & Petersen, C. C. H. (2021). Neuronal Circuits in Barrel Cortex for Whisker Sensory Perception. *Physiological Reviews*, *101*(1), 353–415. https://doi.org/10.1152/physrev.00019.2019

Syka, J., Šuta, D., & Popelář, J. (2005). Responses to species-specific vocalizations in the auditory cortex of awake and anesthetized guinea pigs. *Hearing Research*, *206*(1–2), 177–184. https://doi.org/10.1016/j.heares.2005.01.013

Tannan, V., Whitsel, B. L., & Tommerdahl, M. A. (2006). Vibrotactile adaptation enhances spatial localization. *Brain Research*, *1102*(1), 109–116. https://doi.org/10.1016/j.brainres.2006.05.037

Taxidis, J., Pnevmatikakis, E. A., Dorian, C. C., Mylavarapu, A. L., Arora, J. S., Samadian, K. D., Hoffberg, E. A., & Golshani, P. (2020). Differential Emergence and Stability of Sensory and Temporal Representations in Context-Specific Hippocampal Sequences. *Neuron*, *108*(5), 984-998.e9. https://doi.org/10.1016/j.neuron.2020.08.028

Tian, L., Hires, S. A., Mao, T., Huber, D., Chiappe, M. E., Chalasani, S. H., Petreanu, L., Akerboom, J., McKinney, S. A., Schreiter, E. R., Bargmann, C. I., Jayaraman, V., Svoboda, K., & Looger, L. L. (2009). Imaging neural activity in worms, flies and mice with improved GCaMP calcium indicators. *Nature Methods*, *6*(12), 875–881. https://doi.org/10.1038/nmeth.1398

Tommerdahl, M., Tannan, V., Cascio, C. J., Baranek, G. T., & Whitsel, B. L. (2007). Vibrotactile adaptation fails to enhance spatial localization in adults with autism. *Brain Research*, *1154*, 116–123. https://doi.org/10.1016/j.brainres.2007.04.032

Tremblay, R., Lee, S., & Rudy, B. (2016). GABAergic Interneurons in the Neocortex: From Cellular Properties to Circuits. *Neuron*, *91*(2), 260–292. https://doi.org/10.1016/j.neuron.2016.06.033

Ulanovsky, N., Las, L., & Nelken, I. (2003). Processing of low-probability sounds by cortical neurons. *Nature Neuroscience*, *6*(4), 391–398. https://doi.org/10.1038/nn1032

Voelcker, B., Pancholi, R., & Peron, S. (2022). Transformation of primary sensory cortical representations from layer 4 to layer 2. *Nature Communications*, *13*(1), 5484. https://doi.org/10.1038/s41467-022-33249-1

Wang, H. C., LeMessurier, A. M., & Feldman, D. E. (2022). Tuning instability of non-columnar neurons in the salt-and-pepper whisker map in somatosensory cortex. *Nature Communications*, *13*(1), 6611. https://doi.org/10.1038/s41467-022-34261-1

Wark, B., Fairhall, A., & Rieke, F. (2009). Timescales of inference in visual adaptation. *Neuron*, *61*(5), 750–761. https://doi.org/10.1016/j.neuron.2009.01.019

Weber, A. I., Krishnamurthy, K., & Fairhall, A. L. (2019). Coding Principles in Adaptation. *Annual Review of Vision Science*, *5*, 427–449. https://doi.org/10.1146/annurev-vision-091718-014818

Whitmire, C. J., & Stanley, G. B. (2016). Rapid Sensory Adaptation Redux: A Circuit Perspective. *Neuron*, *92*(2), 298–315. https://doi.org/10.1016/j.neuron.2016.09.046

Whitmire, C. J., Waiblinger, C., Schwarz, C., & Stanley, G. B. (2016). Information Coding through Adaptive Gating of Synchronized Thalamic Bursting. *Cell Reports*, *14*(4), 795–807. https://doi.org/10.1016/j.celrep.2015.12.068

Wiggins, L. D., Robins, D. L., Bakeman, R., & Adamson, L. B. (2009). Brief report: Sensory abnormalities as distinguishing symptoms of autism spectrum disorders in young children. *Journal of Autism and Developmental Disorders*, *39*(7), 1087–1091. https://doi.org/10.1007/s10803-009-0711-x

Wilent, W. B., & Contreras, D. (2005). Dynamics of excitation and inhibition underlying stimulus selectivity in rat somatosensory cortex. *Nature Neuroscience*, *8*(10), 1364–1370. https://doi.org/10.1038/nn1545

Woolsey, T. A., & Van Der Loos, H. (1970). The structural organization of layer IV in the somatosensory region (S I) of mouse cerebral cortex. *Brain Research*, *17*(2), 205–242. https://doi.org/10.1016/0006-8993(70)90079-X

Wright, N. C., Borden, P. Y., Liew, Y. J., Bolus, M. F., Stoy, W. M., Forest, C. R., & Stanley, G. B. (2021). Rapid Cortical Adaptation and the Role of Thalamic Synchrony during Wakefulness. *The Journal of Neuroscience: The Official Journal of the Society for Neuroscience*, *41*(25), 5421–5439. https://doi.org/10.1523/JNEUROSCI.3018-20.2021

Yang, H., Kwon, S. E., Severson, K. S., & O'Connor, D. H. (2016). Origins of choice-related activity in mouse somatosensory cortex. *Nature Neuroscience*, *19*(1), 127–134. https://doi.org/10.1038/nn.4183

Zeiger, W. A., Marosi, M., Saggi, S., Noble, N., Samad, I., & Portera-Cailliau, C. (2021). Barrel cortex plasticity after photothrombotic stroke involves potentiating responses of pre-existing circuits but not functional remapping to new circuits. *Nature Communications*, *12*(1), 3972. https://doi.org/10.1038/s41467-021-24211-8

Ziv, Y., Burns, L. D., Cocker, E. D., Hamel, E. O., Ghosh, K. K., Kitch, L. J., Gamal, A. E., & Schnitzer, M. J. (2013). Long-term dynamics of CA1 hippocampal place codes. *Nature Neuroscience*, *16*(3), 264–266. https://doi.org/10.1038/nn.3329